Chapter 10
Elementary Car-Following Models

Progress is the realization of Utopias.
Oscar Wilde

Abstract Microscopic models describe traffic flow dynamics in terms of single vehicles. The mathematical formulations include car-following models, the topic of this and the next two chapters, and cellular automata, which are described in Chap. 13. This chapter begins with a discussion of general principles that apply to all microscopic models of traffic flow, such as the microscopic steady-state equilibrium, the micro-macro transition to the fundamental diagram, and heterogeneous traffic. The next sections discuss Newell's car-following model and the Optimal Velocity Model (and variants thereof) as the generic examples of simple car-following models.

10.1 General Remarks

Car following models are the most important representatives of microscopic traffic flow models (cf. Sect. 10.6). They describe traffic dynamics from the perspective of individual *driver-vehicle units*.[1] In a strict sense, car-following models describe the driver's behavior only in the presence of interactions with other vehicles while free traffic flow is described by a separate model. In a more general sense, car-following

[1] This technical term expresses the fact that the driving behavior depends not only on the driver but also on the acceleration and braking capabilities of the vehicle.

M. Treiber and A. Kesting, *Traffic Flow Dynamics*,
DOI: 10.1007/978-3-642-32460-4_10,

models include all traffic situations such as car-following situations, free traffic, and also stationary traffic. In this case we say that the microscopic models is complete:

> A car-following model is *complete* if it is able to describe all situations including acceleration and cruising in free traffic, following other vehicles in stationary and non-stationary situations, and approaching slow or standing vehicles, and red traffic lights.

Depending on the actions modeled, one distinguishes between *acceleration models* models for longitudinal movement, *lane-changing models* for lateral movement, and *decision models* for other discrete-choice situations such as entering a priority road. The latter two classes will be described in Chap. 14. Furthermore, more complex and realistic models describe the complex and often subtle interactions between acceleration and discrete-choice situations such as acceleration to the prevailing speed on the target lane in preparation of a lane change. This implies that the longitudinal and transversal dynamics can no longer be separated but must be part of a single complex model. Such models often form the simulation core of commercial traffic simulation software.

The first car-following models were proposed more than fifty years ago by Reuschel (1950), and Pipes (1953). These two models already contained one essential element of modern microscopic modeling: The minimum bumper-to-bumper distance to the leading vehicle (also known as the "safety distance") should be proportional to the speed. This can be expressed equivalently by requiring that the time gap should not be below a fixed *safe time gap*. We emphasize that, for obvious reasons, the relevant spatial or temporal distances are the net, i.e., rear-bumper-to-front-bumper, distances. In contrast, the commonly used term *time headway* generally refers to the time interval between the passage times of the front bumpers of two consecutive vehicles, i.e., including the *occupancy time interval* needed for a vehicle to move forward its own length. Unfortunately, this distinction (which is essential for vehicular traffic) is often ignored.[2] To avoid confusion and in order to be consistent with Sect. 2.2, we will refer to "gaps" if net quantities are meant and define gaps and headways as follows (the modifiers in parentheses will be omitted if the meaning is clear from the context):

> distance headway = (distance) gap + length of the leading vehicle,
> (time) headway = time gap + occupancy time interval of the leading vehicle.

[2] This has essentially historic reasons. The term "time headway" originates from rail transport indicating the succession time interval between two trains. Since this interval is measured in terms of minutes or hours, a distinction between gross and net quantities is irrelevant, in this context.

In this chapter, we will describe *minimal models* for the longitudinal dynamics that do not describe realistic driving behavior. Particularly, they yield unrealistic acceleration values. Nevertheless, they capture many essential features at a qualitative level and can be implemented and simulated easily (sometimes even allowing an analytical solution). Therefore, they are suited to introduce the essential concepts. Real applications require more refined models which will be presented in the subsequent chapters.

Regarding the classification of Sect. 6.2, the minimal models, as well as the cellular automata treated in Chap. 13, belong to the class of *heuristic models*. In contrast, the strategy-based models of the Chaps. 11 and 12 can be considered as *first-principles* models.

Examples of minimal models include the first ever car-following models of Reuschel and Pipes in which the speed is varied instantaneously as a function of the actual distance to the leading vehicle. Another class of minimal models are the *General Motors* (GM) based car-following models in which the acceleration depends on the speed difference and the distance gap according to a power law while the driver's own speed is not considered as an influencing factor. These models are not complete since they cannot describe either free traffic or approaches to standing obstacles. In this chapter, we will therefore focus on other models.

10.2 Mathematical Description

Each driver-vehicle combination α is described by the state variables location $x_\alpha(t)$ (position of the front bumper along the arc length of the road, increasing in driving direction), and speed $v_\alpha(t)$[3] as a function of the time t, and by the attribute "vehicle length" l_α. Depending on the model, additional state variables are required, for example, the acceleration $\dot{v}_\alpha = \mathrm{d}v/\mathrm{d}t$, or binary activation-state variables for brake lights or indicators. We define the vehicle index α such that vehicles pass a stationary observer (or detector) in ascending order, i.e., the first vehicle has the lowest index (cf. Fig. 10.1). Notice that this implies that the vehicles are numbered in *descending* order with respect to their location x.[4]

From the vehicle locations and lengths, we obtain the (bumper-to-bumper) *distance gaps*

$$s_\alpha = x_{\alpha-1} - l_{\alpha-1} - x_\alpha = x_l - l_l - x_\alpha \tag{10.1}$$

[3] To distinguish the vehicle speed in microscopic models from the local speed in macroscopic models, we denote the speed of individual vehicles in lowercase (in analogy to the notation for single-vehicle data). Generally, the relation $V = \langle v_\alpha \rangle$ applies.

[4] There is no generally accepted convention for the vehicle numbering in the literature. The converse numbering scheme (ascending in space, descending in time) is used as well, particularly in the literature of traffic engineers.

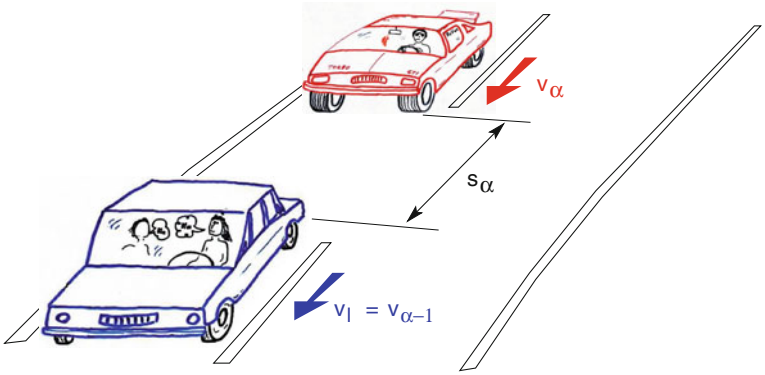

Fig. 10.1 Defining the state variables of car-following models

which (together with the vehicle speeds) constitute the main input of the microscopic models. For ease of notation, we sometimes denote the index $\alpha - 1$ of the leading vehicle with the symbol l (see Fig. 10.1).

The minimal models (and many of the more realistic models of the subsequent chapters) describe the response of the driver as a function of the gap s_α to the lead vehicle, the driver's speed v_α, and the speed v_l of the leader. In *continuous-time models*, the driver's response is directly given in terms of an *acceleration function* $a_{\text{mic}}(s, v, v_l)$ leading to a set of *coupled ordinary differential equations* of the form

$$\dot{x}_\alpha(t) = \frac{\mathrm{d}x_\alpha(t)}{\mathrm{d}t} = v_\alpha(t), \tag{10.2}$$

$$\dot{v}_\alpha(t) = \frac{\mathrm{d}v_\alpha(t)}{\mathrm{d}t} = a_{\text{mic}}(s_\alpha, v_\alpha, v_l) = \tilde{a}_{\text{mic}}(s_\alpha, v_\alpha, \Delta v_\alpha). \tag{10.3}$$

In most acceleration functions, the speed v_l of the leader enters only in form of the speed difference (approaching rate)[5]

$$\Delta v_\alpha = v_\alpha - v_{\alpha-1} = v_\alpha - v_l. \tag{10.4}$$

The corresponding models can be formulated more concisely in terms of the alternative acceleration function

$$\tilde{a}_{\text{mic}}(s, v, \Delta v) = a_{\text{mic}}(s, v, v - \Delta v). \tag{10.5}$$

Taking the time derivative of Eq. (10.1), one can reformulate Eq. (10.2) by

$$\dot{s}_\alpha(t) = \frac{\mathrm{d}s_\alpha(t)}{\mathrm{d}t} = v_l(t) - v_\alpha(t) = -\Delta v_\alpha(t). \tag{10.6}$$

[5] Again, there is no common consensus about the definition. Sometimes, the speed difference is defined as $v_l - v$, i.e., as the negative approaching rate.

The set of Eqs. (10.3) and (10.6) can be considered as the generic formulation of most time-continuous car-following models. In this formulation, the coupling between the gap s_α and the speed v_α as well as the coupling between the speed v_α and the speed v_l of the leader becomes explicit.

There are also *discrete-time* car-following models, where time is not modeled as a continuous variable but discretized into finite and generally constant time steps. Instead of differential equations, one obtains *iterated coupled maps* of the general form

$$v_\alpha(t + \Delta t) = v_{\text{mic}}\left(s_\alpha(t), v_\alpha(t), v_l(t)\right), \tag{10.7}$$

$$x_\alpha(t + \Delta t) = x_\alpha(t) + \frac{v_\alpha(t) + v_\alpha(t + \Delta t)}{2}\,\Delta t. \tag{10.8}$$

The driver's response is no longer modeled by an acceleration function but by a *speed function* $v_{\text{mic}}(s, v, v_l)$ indicating the speed that will be reached at the end of the next time step.

Compared to continuous models, discrete-time car-following models are generally less realistic and less flexible but require less computing power for their numerical integration. Most discrete-time car-following models have been proposed at times where computing was more expensive. Nowadays, hundreds of thousand vehicles can be simulated with time-continuous models on a PC in real-time, so this numerical advantage becomes less relevant. Most commercial traffic simulation software uses time-continuous models.

We emphasize that the Eqs. (10.2) and (10.6) represent kinematic facts that are valid *a priori*—in analogy to the continuity equations of the macroscopic models. Therefore, a specific time-continuous model is uniquely characterized by its acceleration function a_{mic}. Similarly, a specific discrete-time model is completely characterized by its speed function v_{mic}. When simulating heterogeneous traffic consisting of a variety of driving styles and vehicle classes (such as cars and trucks), each driver-vehicle combination is described by different acceleration functions $a^\alpha_{\text{mic}}(s, v, v_l)$ or speed functions $v^\alpha_{\text{mic}}(s, v, v_l)$, respectively.

Numerical integration. In general, time-continuous models cannot be solved analytically and an integration scheme is necessary for an approximate numerical solution of the system of Eqs. (10.3) and (10.6). For traffic flow applications, only explicit update schemes with a fixed time step are practical. Furthermore, the performance of the standard fourth order *Runge-Kutta scheme* is generally inferior to simpler lower-order update methods.[6]

[6] For typical single-lane simulations, the mixed first-order-second-order scheme (10.9), (10.10) is more efficient by a factor of about two compared to the Runge-Kutta scheme, and by a factor of about three with respect to the simple first-order *Euler update*, Eq. (10.9) combined with the positional update $x_\alpha(t + \Delta t) = x_\alpha(t) + v(t)\Delta t$. For multi-lane simulations, the difference is less pronounced. Ignoring bookkeeping costs, numerical efficiency is defined by the inverse of the number of evaluations of the acceleration function for obtaining a numerical solution with given accuracy.

While this may seem surprising at first sight, it can be understood when considering the standard principles of numerical mathematics: Higher-order schemes are guaranteed to be more effective than lower-order schemes only if the exact solution is sufficiently smooth *and* the update time is sufficiently small: Specifically, the standard Runge-Kutta scheme has its nominal consistency order of four only if the acceleration function is at least three times continuously differentiable with respect to all independent variables and with respect to time. While this is satisfied for single-lane simulations of some car-following models, it always breaks down for multi-lane simulations: When lane changes occur, the acceleration function of the subject vehicle (active lane change) and the old and new followers is not even continuous in time. In this case, the accuracy of higher-order schemes may even be *worse* than that of lower-order schemes for the same time step. Furthermore, the proposed scheme (10.9), (10.10) has an intuitive meaning in the context of car-following models: It corresponds to drivers that act only at the beginning of each time step but do nothing in between (see Sect. 12.2 for details).

Assuming a constant update time step Δt, a simple but efficient explicit update method is given by the "ballistic" assumption of constant accelerations during each time step,

$$v_\alpha(t+\Delta t) = v_\alpha(t) + a_{\text{mic}}\left(s_\alpha(t), v_\alpha(t), v_l(t)\right)\Delta t, \tag{10.9}$$

$$x_\alpha(t+\Delta t) = x_\alpha(t) + \frac{v_\alpha(t) + v_\alpha(t+\Delta t)}{2}\,\Delta t. \tag{10.10}$$

Consequently, the combination of a continuous-time model with the ballistic update scheme (10.9), (10.10) is *mathematically* equivalent to discrete-time models if one sets

$$a_{\text{mic}}(s, v, v_l) = \frac{v_{\text{mic}}(s, v, v_l) - v}{\Delta t}. \tag{10.11}$$

However, there is a *conceptual* difference: For discrete-time models, the time step Δt plays the role of a model parameter typically describing the reaction time, the time headway, or the speed adaptation time. For time-continuous models, the update time Δt is an auxiliary variable of the approximate numerical solution which preferably should be small as the true solution is obtained in the limit $\Delta t \to 0$ (at least if the numerical method is consistent and stable).

10.3 Steady State Equilibrium and the Fundamental Diagram

Since the driver-vehicle units of microscopic models are equivalent to *driven particles* of physical systems, there is no equilibrium in the strict sense. Instead, there is a stationary state where the forces and the entering and exiting energy fluxes are

balanced. Strictly physically, this can be interpreted in terms of a balance of the forces (the sum of friction, wind drag, and engine driving force equates to zero) or energy fluxes (engine power equals change in potential and kinetic energy plus energy dissipation rate by friction and wind drag). More relevant for traffic flow, however, is the concept of balancing the *social forces*: The desire to go ahead generates a positive (accelerating) social force while the interactions with other vehicles generally lead to negative social forces in order to avoid critical situations and crashes.[7] In any case, such a balanced state is denoted as *steady-state equilibrium*. For microscopic models, a consistent description of the steady-state equilibrium requires identical driver-vehicle units on a homogeneous road.[8] Technically, this implies that the model parameters are the same for all drivers and vehicles, i.e., the acceleration or speed functions characterizing the respective model do not depend on the vehicle index, $a^{\alpha}_{\text{mic}}(s, v, v_l) = a_{\text{mic}}(s, v, v_l)$, and $v^{\alpha}_{\text{mic}}(s, v, v_l) = v_{\text{mic}}(s, v, v_l)$, respectively. From the modeling point of view, the steady-state equilibrium is characterized by the following two conditions:

- *Homogeneous traffic*: All vehicles drive at the same speed ($v_\alpha = v$) and keep the same gap behind their respective leaders ($s_\alpha = s$).
- *No accelerations*: $\dot{v}_\alpha = 0$ or $v_\alpha(t + \Delta t) = v_\alpha(t)$ for all vehicles α.

For time-continuous models with acceleration functions of the form a_{mic} or $\tilde{a}_{\text{mic}}$ this implies

$$a_{\text{mic}}(s, v, v) = 0, \quad \text{or} \quad \tilde{a}_{\text{mic}}(s, v, 0) = 0, \tag{10.12}$$

respectively, while the condition

$$v_{\text{mic}}(s, v, v) = v \tag{10.13}$$

is valid for discrete-time models with the speed function (10.7). Depending on the model, the microscopic steady-state relations (10.12) or (10.13) can be solved for

- the equilibrium speed $v_e(s)$ as a function of the gap (microscopic fundamental diagram, see below),
- the equilibrium gap $s_e(v)$ for a given speed.

Microscopic fundamental diagram. The Eqs. (10.12) and (10.13) allow for a one-dimensional manifold of possible steady states that can be parameterized by the

[7] The physical interpretation of forces becomes more relevant when simulating driven particles where the available driving power is a major limiting factor. Examples include trucks going up a steep hill, bicycle traffic, inline skating, and cross-country-skiing mass events.

[8] One can conceive of microscopic models having no unique steady state even in this case. Such models "without a fundamental diagram" have been postulated by some researchers. However, they are controversial (see the KKW model in Sect. 13.3.2 for an example).

distance gap s and described by the equilibrium speed function $v_e(s)$ which is also termed the *microscopic fundamental diagram*.[9]

Transition to macroscopic relations. In order to obtain a *micro–macro relation* between the distance gap s and the density ρ we directly apply the definition of the density as number of vehicles per road length. For a given vehicle length l, we obtain

$$s_\alpha = s = \frac{1}{\rho} - l. \tag{10.14}$$

Furthermore, the steady-state equilibrium implies that the speed of all vehicles is the same and equal to the macroscopic speed

$$V(x,t) = \langle v_\alpha(t) \rangle = v_e(s). \tag{10.15}$$

With these relations, we can derive the macroscopic steady-state speed-density diagram and the macroscopic fundamental diagram:

$$V_e(\rho) = v_e\left(\frac{1}{\rho} - l\right), \quad Q_e(\rho) = \rho v_e\left(\frac{1}{\rho} - l\right). \tag{10.16}$$

10.4 Heterogeneous Traffic

Microscopic models play out their advantages when describing different drivers and vehicles, i.e., *heterogeneous traffic*. Including different drivers and vehicles is crucial when modeling the effects of active traffic management such as variable message signs, speed limits, or ramp metering, or when simulating traffic-related effects of new driver-assistance systems as discussed in Chap. 21 of this book. Heterogeneous traffic can be microscopically modeled in two ways:

1. All driver-vehicle units are described by the same model using different parameter values. The heterogeneity can be applied on the level of vehicle classes (e.g., different parameters for cars and trucks), individually (distributed parameters), or both (different parameter distributions for cars and trucks). The last combined approach has the advantage that it automatically leads to realistic correlations between the parameters.[10]
2. Different driver-vehicle classes can also be described with different *models*. This allows us to directly represent qualitatively different driving characteristics between, e.g., cars and trucks or between human driving and semi-automated driving with the help of adaptive cruise control (ACC) systems.

[9] Not to be confused with the data related microscopic flow-density diagram, i.e., a scatter plot of the points $(1/d_\alpha, 1/\Delta t_\alpha)$ that can be derived from single-vehicle detector data, see Chap. 3.

[10] For example, trucks tend to drive more slowly than cars and they tend to accelerate more slowly as well. Thus, speed and acceleration parameters are positively correlated.

We emphasize that simulating heterogeneous traffic is only sensible in the context of multi-lane traffic models. Otherwise, a single long queue will eventually form behind the slowest vehicle, which is unrealistic. Finally, when parameterizing heterogeneous traffic, it is favorable if the model parameters have an intuitive meaning (such as that of the models presented in Chap. 11).

10.5 Fact Sheet of Dynamical Model Characteristics

In order to compare the properties of the different microscopic models introduced in this chapter and the following Chaps. 11 and 12, we will provide, for each model, simulation results for two example scenarios in form of a *fact sheet*. We consider these characteristics for the different microscopic models as one of the core elements of this book. Using the simulation tool on the book's website[11] the reader can interactively reproduce the characteristics, and can also produce new simulation results by changing the model parameters (see Fig. 10.2 for a screenshot).

In the following, we will describe the simulation scenarios with the help of Fig. 10.3 displaying the essential characteristics of a given model in terms of a *fact sheet*. The model itself (the Optimal Velocity Model) will be discussed in Sect. 10.6 below.

10.5.1 Highway Scenario

The left column of Fig. 10.3 shows the simulation of a highway with an on-ramp during rush-hour conditions. In order to display the "pure" characteristics of the acceleration models, we simulate a single freeway lane. Lane changes (see Chap. 14 for details) take place in the 1km long merging zone of the on-ramp centered at $x = 0$, only. The traffic demand during the rush hour is modeled by prescribing a time-varying inflow at the upstream end of the simulated main-road section with a peak value of 2,200 vehicles per hour.[12] The on-ramp inflow of 550 vehicles/h is assumed to be constant. Furthermore, "free" boundary conditions are assumed at the downstream end of the road: As soon as a vehicle crosses the downstream boundary, it is taken out of the system. The next vehicle behaves as though there is an empty road of infinite length until it leaves the system as well.

Due to the high traffic demand, traffic breaks down near the merging zone around $x = 0$ at about $t = 10$ min. Fig. 10.3a depicts the spatiotemporal evolution of

[11] see: www.traffic-flow-dynamics.org

[12] The speed of the entering vehicles must be given as well. However, since the speed will reach equilibrium during the first few hundred meters, its initial value is irrelevant as long as it allows the vehicles to be inserted at the rate prescribed by the flow. Specifically, we determine the gap at insertion time and set the speed to the equilibrium speed given by the microscopic fundamental diagram for this gap.

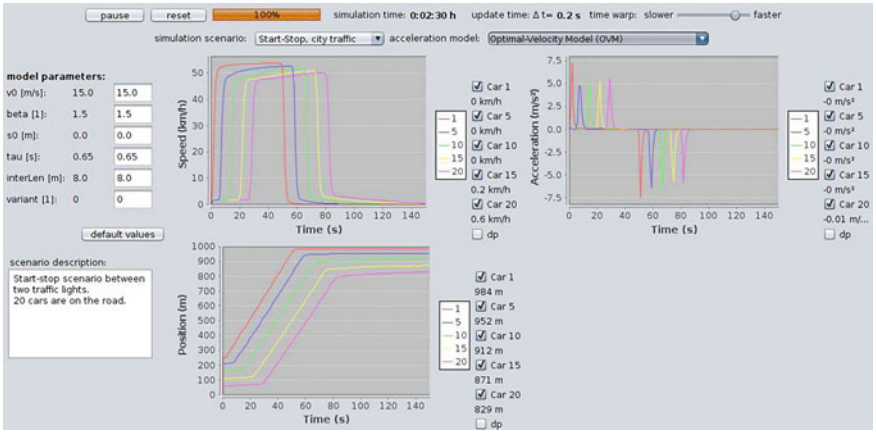

Fig. 10.2 Screenshot of the interactive simulation tool on the book's website. Shown is the city scenario for the Optimal Velocity Model simulated with the standard parameters

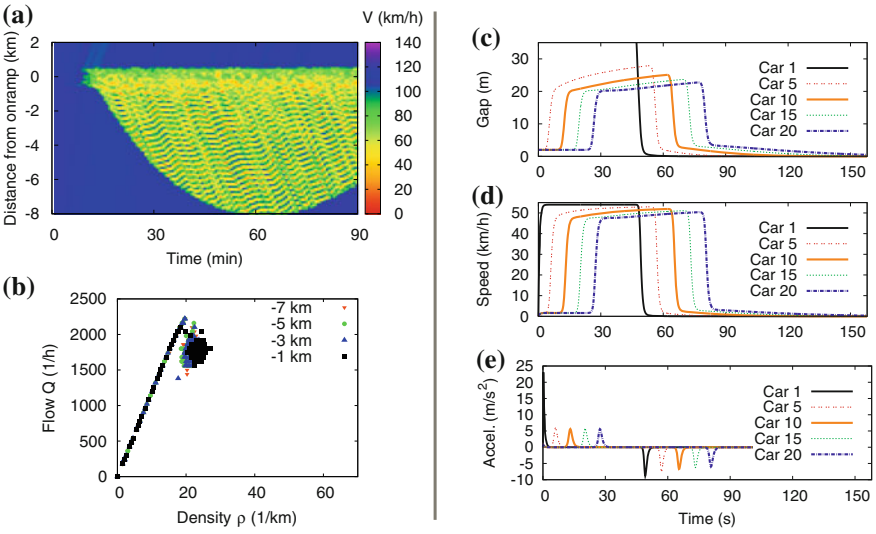

Fig. 10.3 Fact sheet of the Optimal Velocity Model with the OV function (10.21) and model parameters according to Table 10.1. The *left column* displays results of the highway scenario with an on-ramp: **a** Local speed, and **b** flow-density data of virtual detectors. The *right column* depicts the city start–stop scenario where vehicles move from one traffic-light controlled intersection to the next. See Sect. 10.5 for a detailed description of the simulation scenarios

the congestion following the traffic breakdown by plotting the *macroscopic local speed* $V(x,t)$. The local speed is derived from the set $\{x_\alpha(t)\}$ of simulated trajectories by a linear interpolation over space at fixed time according to

$$V(x,t) = \frac{x - x_\alpha(t)}{x_{\alpha-1}(t) - x_\alpha(t)} v_{\alpha-1}(t) + \frac{x_{\alpha-1}(t) - x}{x_{\alpha-1}(t) - x_\alpha(t)} v_\alpha(t). \tag{10.17}$$

For a given spatiotemporal point (x,t), the vehicle index α is determined such that $x_\alpha(t) \leq x < x_{\alpha-1}(t)$. This plot shows that the congested region caused by the traffic breakdown grows for $t < 60$ min. Later on, it shrinks due to the decreasing demand. The following aspects of the simulated traffic dynamics can be compared with real-world traffic:

- Driving in free traffic.
- Braking characteristics when approaching the upstream jam front (in real traffic flow, the deceleration profile is smooth and the deceleration rarely exceeds 2 m/s^2).
- Acceleration characteristics when exiting the stationary downstream jam front near the on-ramp bottleneck (again, the real acceleration is smooth and the accelerations generally do not exceed 2 m/s^2).
- Capacity of the *activated* bottleneck, i.e., the flow downstream of the bottleneck after breakdown (observed values are of the order of 2,000 vehicles/h per lane).
- Stability of traffic flow in free and congested conditions (free traffic should be stable and congested traffic unstable with respect to oscillations and stop-and-go traffic, see Chap. 15 for details).

Finally, the simulated spatiotemporal dynamics of regions with traffic oscillations can be compared with following observed facts (see Sect. 18.3 for details): All oscillations and waves of a congested area propagate upstream at the same velocity (-20 to -15 km/h, depending only weakly on the country and the traffic composition). Furthermore, the wavelength of contiguous stop-and-go waves varies between 1 and 3 km, and the wave amplitude grows during the upstream propagation. Finally, the decelerations and accelerations of the vehicles entering and leaving the waves rarely exceed 2 m/s^2.

Figure 10.3b shows flow-density data at several locations. To enable a direct comparison with real data, we simulate the data capturing process as well by means of *virtual detectors* positioned at several locations. To this end, we create *virtual single-vehicle data* by recording the passing times and speeds of each vehicle trajectory when it passes one of the detectors. Furthermore, we generate aggregated virtual data by determining, for each one-minute aggregation interval, the number of passing vehicles (or, equivalently, the traffic flow), and the arithmetic mean speed according to Sect. 3.2. Finally, flow and density is calculated and plotted as in the Sects. 3.3.1 and 4.4, respectively. Following characteristics can be compared with real observations (for example, that displayed in Sect. 4.4):

- The free branch of the flow-density data shows comparatively little scattering and a negative curvature near capacity.

- The congested flow-density data shows wide scattering.[13]
- In many cases, real flow-density data are distributed according to an inverse-λ shape corresponding to a capacity drop of typically 10–20 % and associated hysteresis effects.

10.5.2 City Scenario

The right column of the fact sheet 10.3 shows a typical inner-city situation with intersections and traffic lights. The simulation is initialized by a queue of 20 vehicles waiting behind a red traffic light which turns green at $t = 0$. During the simulation, the vehicle queue moves in single file to the next red traffic light 740 m further downstream. Red traffic lights are simulated by a standing virtual vehicle of zero length positioned at the stopping line which is removed when the light turns green. Following driving characteristics can be compared with reality:

- Starting phase: The acceleration ranges between 1 and 2.5 m/s^2 and smoothly decreases to zero as cruising speed is approached. The first vehicle takes 3–4 s to pass the stopping line of the traffic light. Afterwards, the cars pass at a rate of one vehicle every 1.5–2 s.
- Cruising phase: In this phase, all vehicles should travel at close to the desired speed. The vehicles should move as a platoon with time gaps of the order of 1–2 s corresponding to distance gaps of about 15–30 m.
- Approaching phase: All vehicles should decelerate smoothly such that the values for the *jerk*

$$J = \left|\frac{\mathrm{d}\dot{v}}{\mathrm{d}t}\right| = \left|\frac{\mathrm{d}^2 v}{\mathrm{d}t^2}\right| \tag{10.18}$$

  remain below 2 m/s^3. The braking decelerations themselves generally do not exceed 2 m/s^2 and the braking becomes less pronounced for vehicles more at the back of the platoon.

10.6 Optimal Velocity Model

The *Optimal Velocity Model* (OVM) is a time-continuous model whose acceleration function is of the form $a_{\mathrm{mic}}(s, v)$, i.e., the speed difference exogenous variable is missing. The acceleration equation is given by

[13] We point to the fact that this difference is partly caused by the way of presentation. When plotting flow-density, speed-density or speed-flow diagrams from the same data, only the flow-density data show a distinct discrepancy of the amount of scattering on the free and congested branches, see Fig. 4.12.

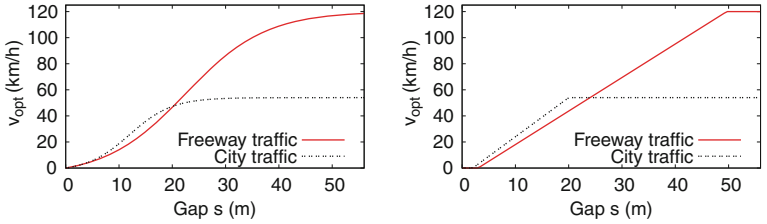

Fig. 10.4 Optimal velocity functions (10.21) (*left*) and (10.22) (*right*) for the parameter values of Table 10.1

$$\boxed{\dot{v} = \frac{v_{\text{opt}}(s) - v}{\tau} \quad \text{Optimal Velocity Model.}} \tag{10.19}$$

This equation describes the adaption of the actual speed $v = v_\alpha$ to the *optimal velocity* $v_{\text{opt}}(s)$ on a time scale given by the *adaptation time* τ. Comparing the acceleration equation (10.19) with the steady-state condition (10.12) it becomes evident that the optimal velocity (OV) function[14] $v_{\text{opt}}(s)$ is equivalent to the microscopic fundamental diagram $v_e(s)$. It should obey the plausibility conditions

$$v'_{\text{opt}}(s) \geq 0, \quad v_{\text{opt}}(0) = 0, \quad \lim_{s\to\infty} v_{\text{opt}}(s) = v_0, \tag{10.20}$$

but is arbitrary, otherwise. Thus, the acceleration equation (10.19) defines a whole class of models whose members are distinguished by their respective optimal velocity functions. The OV function originally proposed by Bando et al.,

$$v_{\text{opt}}(s) = v_0 \frac{\tanh\left(\frac{s}{\Delta s} - \beta\right) + \tanh\beta}{1 + \tanh\beta}, \tag{10.21}$$

uses a hyperbolic tangent.[15] Besides the parameter τ which is relevant for all optimal velocity models,[16] the OVM of Bando et al. has three additional parameters, the desired speed v_0, the transition width Δs, and the form factor β (see Fig. 10.4 and Table 10.1).

A more intuitive OV function can be derived by characterizing free traffic by the desired speed v_0, congested traffic by the time gap T in car-following mode under stationary conditions, and standing traffic by the minimum gap s_0. In analogy to the Section-Based Model of Sect. 8.5, we obtain

[14] Strictly speaking, this is an "optimal speed function". In order to be consistent with the literature (and the model name), we will nevertheless stick to velocity instead of speed, in this context.

[15] We have adapted the notation with respect to the original publication such that $v_0 = v_{\text{opt}}(0)$ strictly has the meaning of the desired speed if no other vehicles are present.

[16] Sometimes, τ is replaced by the sensitivity parameter $a = 1/\tau$.

Table 10.1 Parameter of two variants of the Optimal Velocity Model (OVM)

Parameter	Typical value highway	Typical value city traffic
Adaptation time τ	0.65 s	0.65 s
Desired speed v_0	120 km/h	54 km/h
Transition width Δs [v_{opt} according to Eq. (10.21)]	15 m	8 m
Form factor β [v_{opt} according to Eq. (10.21)]	1.5	1.5
Time gap T [v_{opt} according to Eq. (10.22)]	1.4 s	1.2 s
Minimum distance gap s_0 [v_{opt} according to Eq. (10.22)]	3 m	2 m

$$v_{\text{opt}}(s) = \max\left[0,\ \min\left(v_0, \frac{s - s_0}{T}\right)\right]. \tag{10.22}$$

This relation is the microscopic equivalent to the triangular fundamental diagrams of the macroscopic Section-Based and Cell-Transmission Models (cf. Fig. 10.4). The simulation results are similar to that of the hyperbolic tangent OV function. Again, typical parameter values are given in Table 10.1.

Model properties. For the simulations of the model fact sheet in Fig. 10.3, we have assumed a speed adaptation time $\tau = 0.65$ s. Obviously this is an unrealistically low value since typical time scales for reaching a desired speed are of the order of 10 s. As a consequence, the periods of the stop-and-go waves (about 1–2 min) are too low. Furthermore, in the simulation of the city scenario, the accelerations and decelerations of the vehicle platoon (up to 22 m/s^2 and down to -10 m/s^2, respectively) differ from real accelerations by a factor of about ten.[17] However, when increasing the adaptation time τ by only 5 %, the simulations eventually lead to negative distance gaps s_α corresponding to *accidents*. On the other hand, when decreasing τ by 5 %, we obtain absolute string stability even for congested freeway traffic. While this agrees with the theoretical stability limits (see Chap. 15) it is at variance with the observations. We conclude that the simulation outcome is qualitatively correct. However:

- On a quantitative level, the OVM results are unrealistic.
- On a qualitative level, the simulation outcome has a strong dependency on the fine tuning of the model parameters, i.e., the OVM is not *robust*.

These deficiencies are mainly due to the fact that the OVM acceleration function does not contain the speed difference as exogenous variable, i.e., the simulated driver reaction depends only on the gap but is the same whether the leading vehicle is slower or faster than the subject vehicle. This corresponds to an extremely short-sighted driving style.

[17] In reality, accelerations above 4 m/s^2 (corresponding to 7 s for accelerating from zero to 100 km/h) and below -9 m/s^2 (corresponding to an emergency braking maneuver on a dry road) are physically impossible. Furthermore, everyday accelerations (which the simulations should reproduce) generally are only a fraction of the accelerations at these limits.

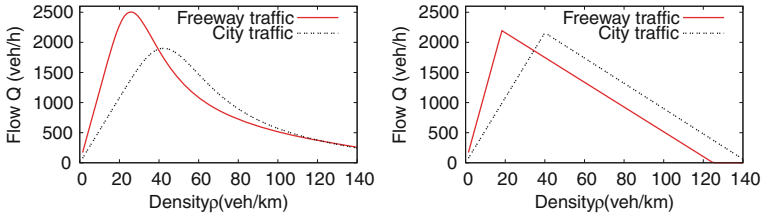

Fig. 10.5 Fundamental diagrams of the OVM for the OV functions (10.21) (*left*) and (10.22) (*right*) for the parameter values of Table 10.1

Steady-state equilibrium. As already mentioned, the steady-state condition (10.12) for the OVM leads to $v_e(s) = v_{\text{opt}}(s)$, i.e., the microscopic fundamental diagram Fig. 10.4 is given by the OV function. The macroscopic fundamental diagram (Fig. 10.5) is obtained from the microscopic one using Eq. (10.16). In particular, the OV function (10.22) results in the triangular macroscopic fundamental diagram

$$Q_e(\rho) = \min\left(v_0\rho, \frac{1-\rho(l+s_0)}{T}\right).$$

10.7 Full Velocity Difference Model

By extending the OVM with an additional linear stimulus for the speed difference, one obtains the *Full Velocity Difference Model* (FVDM):

$$\boxed{\dot{v} = \frac{v_{\text{opt}}(s) - v}{\tau} - \gamma\,\Delta v \quad \text{Full Velocity Difference Model.}} \tag{10.23}$$

As in the OVM, the steady-state equilibrium is directly given by the optimal velocity function v_{opt}. When assuming suitable values for the speed difference sensitivity γ of the order of $0.6\,\text{s}^{-1}$, the FVDM remains accident-free for speed adaptation times of the order of several seconds. Furthermore, the fact sheet (Fig. 10.6) shows that the waves in the congested region of the freeway scenario are more realistic than that of the OVM, although the wavelengths remain too short. Furthermore, the accelerations remain in a realistic range.

However, in contrast to the OVM, the Full Velocity Difference Model is not *complete* in the sense defined at the beginning of Sect. 10.1, i.e., it is not able to describe all traffic situations. The reason is that the term $\gamma\,\Delta v$ describing the sensitivity to speed difference in Eq. (10.23) does not depend on the gap. Consequently, a slow vehicle (or a red traffic light corresponding to a standing virtual vehicle) leads to a significant decelerating contribution even if it is miles away. Thus, simulated vehicles do not reach their desired speed even on a long road with no other vehicles.

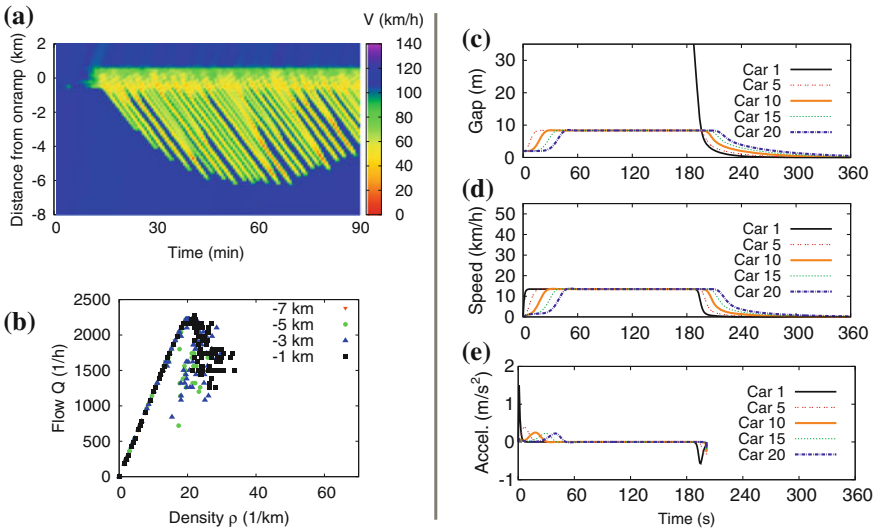

Fig. 10.6 Fact sheet of the Full Velocity Difference Models (FVDM), Eq. (10.23), with the OV function (10.21), the sensitivity $\gamma = 0.6\,\mathrm{s}^{-1}$, and the speed adaptation time $\tau = 5\,\mathrm{s}$. The vehicle length and the parameters v_0, β and Δs of the OV function are given by Table 10.1. The simulation scenarios are discussed in detail in Sect. 10.5

In fact, the maximum speed in the city scenario of the model fact Sheet of Fig. 10.6 is less than 15 km/h (see Problem 10.4 for a quantitative analysis).

Improved Full Velocity Difference Model. In the following, we show how a model developer would proceed to resolve this problem. Obviously, the sensitivity to speed differences must decrease with the gap s and tend to zero as $s \to \infty$. This can be realized by replacing the contribution $-\gamma\,\Delta v$ of Eq. (10.23) by a multiplicative term $-\tilde{\gamma}\,\Delta v/s$. However, now the sensitivity diverges for $s \to 0$ which is unrealistic. Furthermore, $\tilde{\gamma}$ has a different unit compared to γ (and, consequently, a different numerical value) which should be avoided if possible.[18] The arguably simplest approach to resolve these new problems consists in applying the inverse proportionality only if the gap is larger than the interaction length $v_0 T$. Hence, the resulting acceleration equation of the new "complete" variant of the FVDM is given by

$$\dot{v} = \frac{v_{\mathrm{opt}}(s) - v}{\tau} - \frac{\gamma\ \Delta v}{\max[1, s/(v_0 T)]}. \tag{10.24}$$

Figure 10.7 displays the city scenario for this model variant. It turns out that model (10.24) is able to realistically simulate the cruising phase, in contrast to the

[18] Three principles for improving existing models are the following: (i) Introduce as few new parameters as possible (ideally zero), (ii) do not change the meaning of existing parameters, (iii) keep it as simple as possible, but not simpler.

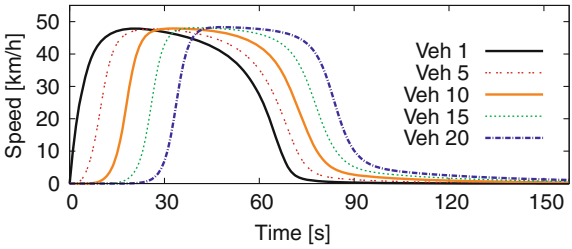

Fig. 10.7 The city scenario of Fig. 10.6 for the "complete" Full Velocity Difference Model (10.24) with the OV function (10.21). The model parameters are the same as in the original simulation

original model (10.23), and produces realistic accelerations, in contrast to the OVM. However, the robustness problem is not resolved.[19]

10.8 Newell's Car-Following Model

Newell's car-following model is the arguably simplest representative of time-discrete models of the type (10.7). Its speed function is directly given by the optimal speed function (10.22) corresponding to the triangular fundamental diagram (10.22) with $s_0 = 0$,

$$\boxed{v(t+T) = v_{\text{opt}}(s(t)), \quad v_{\text{opt}}(s) = \min\left(v_0, \frac{s}{T}\right) \quad \text{Newell's Model.}} \tag{10.25}$$

When restricting to the car-following regime, Newell's model has two parameters: The time gap or reaction time T, and the (effective) vehicle length l_{eff}. Since in this regime the kinematic wave velocity is constant and given by

$$w = c_{\text{cong}} = -l_{\text{eff}}/T,$$

the set of model parameters can alternatively be expressed by $\{T, w\}$ or by $\{l_{\text{eff}}, w\}$. The standard value for the time gap is $T = 1$ s while the wave speed should be within the observed range $w \in [-20\,\text{km/h}, -15\,\text{km/h}]$ corresponding to a plausible effective vehicle length l_{eff} of about 5 m. The minimum condition of the optimal velocity function makes the model complete by defining a free-flow regime and introducing the desired speed v_0 as a third model parameter. It is straightforward to generalize Newell's model by replacing Eq. (10.22) with other microscopic fundamental diagrams.

Newell's model can also be considered as a continuous-in-time model with a time delay assuming that the drivers have a constant *reaction time* $T_r = T$. In this interpretation, Eq. (10.25) has the mathematical form of a *delay-differential equation*

[19] The reader can verify this by simulating the improved FVDM on the book's website www.traffic-flow-dynamics.org and changing the sensitivity γ.

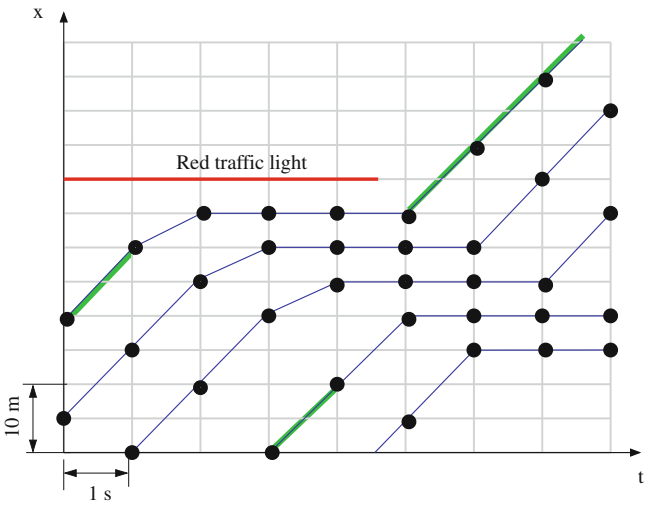

Fig. 10.8 Trajectory plot of the OVM with the triangular fundamental diagram ($l_{\text{eff}} = 5\,\text{m}$, $v_0 = 10\,\text{m/s}$, $T = \tau = 1\,\text{s}$) with an update time $\Delta t = 1\,\text{s}$, and using Eq. (10.26) for the positional update. Shown are vehicles approaching a traffic light (*red line*) turning *green* at $t = 4.5\,\text{s}$ (*end of the line*). The vehicle trajectories correspond to free traffic if drawn *green*, and to bound traffic, otherwise

which will be discussed in Chap. 12 in more detail. This model has several interesting properties which we now investigate further.

Relation to the Optimal Velocity Model. According to Eq. (10.11), Newell's model is mathematically equivalent to the OVM (10.19) in the car-following regime (bound traffic) if one sets $\tau = T$ and updates the OVM speed according to the explicit integration scheme (10.9) and the vehicle positions by the simple *Euler scheme*[20]

$$x_\alpha(t + \Delta t) = x_\alpha(t) + v_\alpha(t + \Delta t)\,\Delta t. \tag{10.26}$$

As a consequence, the parameter T of Newell's model has the additional meaning of a speed adaptation time τ.

Figure 10.8 shows that this equivalence only applies for the triangular fundamental diagram and only in the bound traffic regime, i.e., for gaps s satisfying $v_e(s) < v_0$ or $s < s_0 + v_0 T$. Otherwise, discretization errors are present.

Generally, the OVM is updated with time steps significantly smaller than the adaptation time. However, this does not invalidate the reasoning above, at least, qualitatively. In any case, the steady-state equilibria of the two models are equivalent.

[20] We emphasize that the usual second-order "ballistic" update scheme (10.8) may not be applied, here.

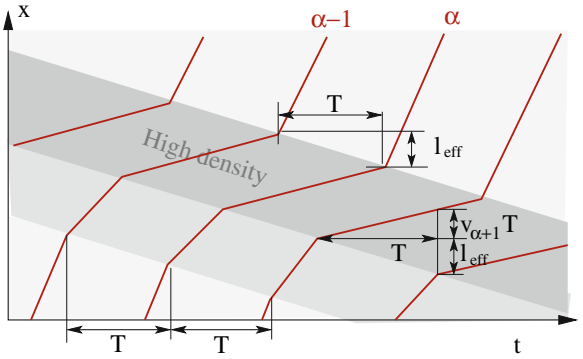

Fig. 10.9 Relation between Newell's model and the Section-Based Model: The *shaded regions* represent the evolution of the macroscopic local density. The gradient $v_e(\rho) = (1/\rho - l_{\text{eff}})/T$ corresponds to the local speed

Relation to the macroscopic Section-Based Model. When disaggregating the solutions of the Section-Based Model (8.2) with the function (8.11) by generating trajectories from the density and speed fields of congested traffic using the macro-micro relation (8.23), these trajectories are simultaneously solutions of Newell's model (as illustrated by Fig. 10.9).

Interpretation from the driver's point of view. The trajectories corresponding to the solution of Newell's model for congested traffic shown in Fig. 10.9 are given by the recursive relations

$$\begin{aligned} x_\alpha(t+T) &= x_{\alpha-1}(t) + wT = x_{\alpha-1}(t) - l_{\text{eff}}, \\ v_\alpha(t+T) &= v_{\alpha-1}(t). \end{aligned} \tag{10.27}$$

This means that the trajectory of the follower is completely determined by the trajectory of the leading vehicle.

> In Newell's car-following model, the position of a vehicle following another vehicle at time $t + T$ is given by the position of the leader at time t minus the (effective) vehicle length l_{eff}. As a corollary, the speed profile of a vehicle *exactly* reproduces that of its leader with a time delay T.

The different meanings of the parameter T. From the above considerations we conclude that the parameter T of Newell's model can be interpreted in four different ways:

1. As the *reaction time* when interpreting Eq. (10.25) as a time-delay differential equation or when considering the trajectories (10.27).

2. As the *time gap* of the microscopic fundamental diagram (10.22).
3. As the *speed adaptation time* following from the equivalence between Newell's model and the OVM combined with speed update rule (10.9).
4. And as the *numerical update time* $T = \Delta t$ when interpreting Eq. (10.25) as a discrete-time model.

The interpretation in terms of a reaction time or a time gap can only be applied for congested traffic. In contrast, the interpretation as a speed adaptation time or a numerical update time is generally valid.

Relation to the macroscopic Payne's model. Besides illustrating another interesting property of Newell's model, this paragraph shows how to derive macroscopic from microscopic traffic flow models by the micro–macro relations between the vehicle speed and the local speed field and between distance and local density, respectively, and by first-order Taylor expansions.

Left-hand side of Newell's model equation. In deriving a macroscopic equivalent of $v_\alpha(t+T)$, we start with the expression (10.17) for the macroscopic local speed. For points (x,t) lying on the trajectory of vehicle α, we have

$$v_\alpha(t) = V(x_\alpha(t), t) = V(x,t). \tag{10.28}$$

Furthermore, the change in position and speed during one update time step $\Delta t = T$ is expressed in terms of local macroscopic fields by a Taylor expansion up to first order,

$$\begin{aligned} v_\alpha(t+T) &= V(x_\alpha + v_\alpha T, t+T) \\ &= V(x_\alpha, t) + \frac{\partial V(x,t)}{\partial x} v_\alpha T + \frac{\partial V(x,t)}{\partial t} t \\ &= V(x,t) + \left(V(x,t)\frac{\partial V}{\partial x} + \frac{\partial V}{\partial t} \right) T. \end{aligned} \tag{10.29}$$

Right-hand side of Newell's car-following model equation. First, we apply the micro–macro relation between the optimal velocity function and the macroscopic speed-density relation, $v_{\text{opt}}(s) = v_e(s) = V_e(\rho)$. In a second step, the local density ρ in the argument is determined such that the approximation error is minimal. Since $d_\alpha = s_\alpha + l_{\alpha-1} = 1/\rho$ denotes the distance *between* the vehicles α and $\alpha - 1$, we evaluate ρ at the intermediate location $x_\alpha + d_\alpha/2 = x + d_\alpha/2$ (Fig. 10.10) and consistently express everything up to first order by macroscopic local quantities,

$$\begin{aligned} v_{\text{opt}}(s_\alpha(t)) &= V_e\left(\rho\left(x + d_\alpha/2, t\right)\right) \\ &= V_e(\rho(x,t)) + V_e'(\rho)\frac{\partial \rho}{\partial x}\frac{d_\alpha}{2} \\ &= V_e(\rho(x,t)) + \frac{V_e'(\rho)}{2\rho}\frac{\partial \rho}{\partial x}. \end{aligned} \tag{10.30}$$

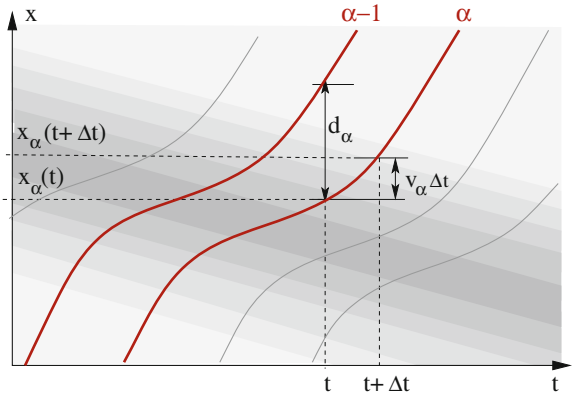

Fig. 10.10 Illustration of the derivation of Payne's model from the (*generalized*) Newell's model. Shown are the trajectories $x_\alpha(t)$ and $x_{\alpha-1}(t)$ of the subject and leading vehicles, respectively, and the associated local density (*shaded*). The error of the micro–macro transition is minimal when defining the local density at as $x_\alpha + d_\alpha/2$ as the inverse of the distance Δx_α

In the second line we have applied the first-order Taylor expansion, and the chain rule. In the third line, we have expressed $d_\alpha/2$ by $\frac{1}{2\rho(x,t)}$.[21] Equating (10.29) with Eq. (10.30) leads to

$$\frac{\partial V}{\partial t} + V\frac{\partial V}{\partial x} = \frac{V_e(\rho) - V}{T} + \frac{V_e'(\rho)}{2\rho T}\frac{\partial \rho}{\partial x}. \tag{10.31}$$

When identifying $T = \tau$ this corresponds to Payne's model (9.18). We conclude that Newell's model and its extensions to other fundamental diagrams are always *approximatively* equivalent to Payne's model. Simultaneously, Newell's model is exactly equivalent to the Section-Based Model if restricting conditions apply (traffic in the car-following regime, triangular fundamental diagram).

Relation of Newell's model with anticipation to the FVDM. In order to compensate for at least part of the reaction time delay described by Newell's model, a driver would try to predict the distance gap (the only exogenous stimulus of Newell's model) by a certain time interval T_a into the future. Using the rate of change $\dot{s} = -\Delta v$ for an estimate of the gap at this time, $\hat{s}(t + T_a) = s(t) - T_a \Delta v$, this results in the *generalized Newell's model*

$$v(t + T) = v_{\text{opt}}\left(s(t) - T_a \Delta v\right) \approx v_{\text{opt}}(s(t)) - v_{\text{opt}}'(s) T_a \Delta v. \tag{10.32}$$

According to Eq. (10.11) this is equivalent to a time-continuous model given by

$$\frac{\mathrm{d}v}{\mathrm{d}t} = \frac{v_{\text{opt}}(s) - v}{T} - \frac{T_a v_{\text{opt}}'(s)}{T}\,\Delta v.$$

[21] The displacement d_α appears only in terms that are already of first order. Therefore, we only need the zeroth order relation $d_\alpha(t) = 1/\rho(x,t)$.

This corresponds to a Full Velocity Difference Model with a gap dependent sensitivity $\gamma(s) = T_a v'_{\mathrm{opt}}(s)/T$. From the OV plausibility conditions (10.20) it follows that $\lim_{s\to\infty} v'_{\mathrm{opt}}(s) = 0$, i.e., the sensitivity tends to zero when the gap becomes sufficiently large (for the triangular fundamental diagram it is exactly zero for $s > s_0 + v_0 T$). This means, the resulting FVDM-like model is complete, similarly to the "improved" FVDM presented in Sect. 10.7.

Problems

10.1 Dynamics of a single vehicle approaching a red traffic light
A single car in city-traffic conditions can be described by the following time-continuous acceleration model:

$$\frac{\mathrm{d}v}{\mathrm{d}t} = \begin{cases} \frac{v_0 - v}{\tau} & \text{if } \Delta v \le \sqrt{2b(s - s_0)}, \\ -b & \text{otherwise.} \end{cases}$$

Here, s denotes the distance to the next car or the next traffic light (whichever is nearer), and Δv is the approaching rate. A red traffic light is modeled by a virtual standing vehicle of zero dimension at the stopping line which is removed when the light turns green.

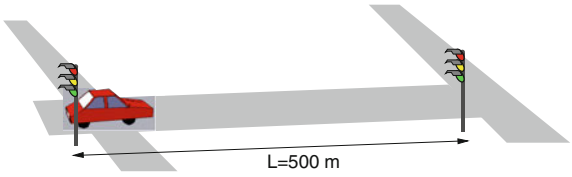

1. What is the meaning of the model parameters v_0, τ, s_0, and b? Describe the qualitative acceleration profile after the initially standing car starts moving, and the deceleration profile when approaching a red traffic light. Which essential human property is not taken care of by this model?
2. The first traffic light turns green at $t = 0$ s. Calculate the speed and the acceleration as a function of time for general model parameters assuming that the second traffic light is always green.
3. Consider now a situation where the subject car is approaching a red traffic light with cruising speed $v_0 = 50$ km/h assuming $s_0 = 2$ m and $b = 2$ m/s^2. At which distance to the traffic light does the driver initiate his or her braking maneuver? What is the braking deceleration and the final distance of the standing car to the stopping line?
4. Calculate the trajectory and the speed profile of the car during the complete start-stop cycle for a distance of 500 m between the stopping lines of the two traffic lights assuming $\tau = 5$ s and values for the other model parameters as above.

Hint: There are two phases: The acceleration phase eventually going into cruising mode, and the braking phase. As an essential step, you have to determine the location and the time where the braking maneuver begins. You can assume that the car has already reached its cruising speed at this time.

10.2 OVM acceleration on an empty road
Consider a single vehicle on an empty road whose acceleration is described by the *Optimal Velocity Model*

$$\frac{\mathrm{d}v}{\mathrm{d}t} = \frac{v_0 - v}{\tau}$$

assuming the initial conditions $x(0) = 0$, and $v(0) = 0$. (i) At which time does the vehicle reach its maximum acceleration? What is its value? (ii) Determine the parameter τ if the desired speed is given by 120 km/h and the maximum acceleration by 2 m/s^2. (iii) At which time does the vehicle reach a speed of 100 km/h?

10.3 Optimal Velocity Model on a ring road
Consider a closed ring road with identical vehicles. Initially ($t = 0$ s), all vehicles are motionless and evenly positioned with a gap of 20 m between each other. Calculate the speed profile of all vehicles for the OVM with the optimal velocity function (10.22) assuming $\tau = 1$ s, $v_0 = 72$ km/h, $s_0 = 2$ m, and $T = 1.8$ s.

10.4 Full Velocity Difference Model
When modeling the city scenario of the fact sheet with the FVDM (Fig. 10.6), neither vehicle reaches, or at least approaches, its cruising speed $v_0 = 54$ km/h although the distance between the traffic light would allow for the cruising speed. In order to find the underlying mechanism for this, calculate the stationary speed if there is a red traffic light (modeled by a standing virtual vehicle) at an arbitrarily large distance (i) for general parameters, (ii) for the values $v_0 = 54$ km/h, $\tau = 5$ s, and $\gamma = 0.6\,\mathrm{s}^{-1}$. Compare the result with the right column of Fig. 10.6.

10.5 A simple model for emergency braking maneuvers
Critical situations requiring emergency braking maneuvers can be described by following microscopic model:

$$\frac{\mathrm{d}v}{\mathrm{d}t} = \begin{cases} 0 & \text{if } t < T_r, \\ -b_{\max} & \text{otherwise.} \end{cases}$$

1. Give an intuitive meaning of the parameters T_r and $b_{\max}$.
2. Calculate the braking distance and the overall stopping distance for initial speeds of 50 and 70 km/h assuming $b_{\max} = 8$ m/s^2 and $T_r = 1$ s.
   Hint: The overall stopping distance is composed of the *braking distance*, i.e., the vehicle displacement during the actual braking phase, and the *reaction distance* the vehicle travels during the reaction time of the driver.
3. Imagine a situation where a child suddenly runs into the road from a hidden position behind a vehicle. A driver driving according to the above model just

manages to stop if his or her initial speed is 50 km/h. At what speed would this driver collide with the child if the initial speed is 70 km/h and the situation is otherwise unchanged?

Further Reading

- Reuschel, A.: Fahrzeugbewegungen in der Kolonne. Österreichisches Ingenieur-Archiv **4** (1950) 193–215
- Pipes, L.A.: An operational analysis of traffic dynamics. Journal of Applied Physics **24** (1953) 274–281
- Chandler, R.E., Herman, R., Montrol, E.W.: Traffic dynamics: Studies in car-following. Operation Research **6** (1958) 165–184
- Gazis, D.C., Herman, R., Rothery, R.W.: Nonlinear follow-the-leader models of traffic flow. Operation Research **9** (1961) 545–567
- Bando, M., Hasebe, K., Nakayama, A., Shibata, A., Sugiyama, Y.: Dynamical model of traffic congestion and numerical simulation. Physical Review E **51** (1995) 1035–1042
- Jiang, R., Wu, Q., Zhu, Z.: Full velocity difference model for a car-following theory. Physical Review E **64** (2001) 017101
- Newell, G.F.: A simplified car-following theory: a lower order model. Transportation Research Part B: Methodological **36** (2002) 195–205

Chapter 11
Car-Following Models Based on Driving Strategies

Ideas are like children: you always love your own the most.
Lothar Schmidt

Abstract The models introduced in this chapter are derived from assumptions about real driving behavior such as keeping a "safe distance" from the leading vehicle, driving at a desired speed, or preferring accelerations to be within a comfortable range. Additionally, kinematical aspects are taken into account, such as the quadratic relation between braking distance and speed. We introduce two examples: The simplified Gipps model, and the Intelligent Driver Model. Both models use the same input variables as the sensors of *adaptive cruise control* (ACC) systems, and produce a similar driving behavior. Characteristics that are specific to the human nature, like erroneous judgement, reaction time, and multi-anticipation, are discussed in the next chapter.

11.1 Model Criteria

The models introduced in this chapter are formally identical to the minimal models presented in the previous chapter. They are defined by an acceleration function a_{mic} (see Eq. (10.3)) or a speed function v_{mic} (see Eq. (10.7)). In contrast to the minimal models, the acceleration or speed functions encoding the driving behavior should at least model the following aspects:

1. The acceleration is a strictly decreasing function of the speed. Moreover, the vehicle accelerates towards a *desired speed* v_0 if not constrained by other vehicles or obstacles:

$$\frac{\partial a_{\mathrm{mic}}(s, v, v_l)}{\partial v} < 0, \quad \lim_{s\to\infty} a_{\mathrm{mic}}(s, v_0, v_l) = 0 \quad \text{for all } v_l. \tag{11.1}$$

M. Treiber and A. Kesting, *Traffic Flow Dynamics*,
DOI: 10.1007/978-3-642-32460-4_11, © Springer-Verlag Berlin Heidelberg 2013

2. The acceleration is an increasing function of the distance s to the leading vehicle:

$$\frac{\partial a_{\text{mic}}(s, v, v_l)}{\partial s} \geq 0, \quad \lim_{s\to\infty} \frac{\partial a_{\text{mic}}(s, v, v_l)}{\partial s} = 0 \quad \text{for all } v_l. \tag{11.2}$$

The inequality becomes an equality if other vehicles or obstacles (including "virtual" obstacles such as the stopping line at a red traffic light) are outside the interaction range and therefore do not influence the driving behavior. This defines the *free-flow acceleration*

$$a_{\text{free}}(v) = \lim_{s\to\infty} a_{\text{mic}}(s, v, v_l) = \geq a_{\text{mic}}(s, v, v_l). \tag{11.3}$$

3. The acceleration is an increasing function of the speed of the leading vehicle. Together with requirement (1), this also means that the acceleration decreases (the deceleration increases) with the speed of approach to the lead vehicle (or obstacle):

$$\frac{\partial \tilde{a}_{\text{mic}}(s, v, \Delta v)}{\partial \Delta v} \leq 0 \text{ or } \frac{\partial a_{\text{mic}}(s, v, v_l)}{\partial v_l} \geq 0, \quad \lim_{s\to\infty} \frac{\partial a_{\text{mic}}(s, v, v_l)}{\partial v_l} = 0. \tag{11.4}$$

Again, the equality holds if other vehicles (or obstacles) are outside the interaction range.

4. A minimum gap (bumper-to-bumper distance) s_0 to the leading vehicle is maintained (also during a standstill). However, there is no backwards movement if the gap has become smaller than s_0 by past events:

$$a_{\text{mic}}(s, 0, v_l) = 0 \quad \text{for all } v_l \geq 0, \quad s \leq s_0. \tag{11.5}$$

By virtue of relation (10.11), these requirements (or *plausibility conditions*) for the acceleration function naturally imply conditions for the speed function v_{mic} of models formulated in terms of coupled maps.

A car-following model meeting these requirements is *complete* in the sense that it can consistently describe all situations that may arise in single-lane traffic. Particularly, it follows that (i) all vehicle interactions are of finite reach, (ii) following vehicles are not "dragged along",

$$a_{\text{mic}}(s, v, v_l) \leq a_{\text{mic}}(\infty, v, v_l') = a_{\text{free}}(v) \quad \text{for all} \quad s, v, v_l, \text{ and } v_l', \tag{11.6}$$

and (iii) an equilibrium speed $v_e(s)$ exists, which has the properties already postulated for the optimal-speed function (10.20):

$$v_e'(s) \geq 0, \quad v_e(0) = 0, \quad \lim_{s\to\infty} v_e(s) = v_0. \tag{11.7}$$

This means that the model possesses a unique steady-state flow-density relation, i.e., a fundamental diagram.[1]

These conditions are necessary but not sufficient. For example, when in the car-following regime (steady-state congested traffic), the time gap to the leader has to remain within reasonable bounds (say, between 0.5 and 3 s). Furthermore, the acceleration has to be constrained to a "comfortable" range (e.g., ± 2 m/s^2), or at least, to physically possible values. Particularly, when approaching the leading vehicle, the quadratic relation between braking distance and speed has to be taken into account. Finally, any car-following model should allow instabilities and thus the emergence of "stop-and-go" traffic waves, but should not produce accidents, i.e., negative bumper-to-bumper gaps $s < 0$.[2]

Which of the car-following models introduced in Chap. 10 satisfy the conditions (11.1)–(11.5)?

11.2 Gipps' Model

Gipps' model presented here is a modified version of the one described in his original publication. It is simplified, but conceptually unchanged. Although it produces an unrealistic acceleration profile, this model is probably the simplest complete and accident-free model that leads to accelerations within a realistic range.

11.2.1 Safe Speed

Accidents are prevented in the model by introducing a "safe speed" $v_{\text{safe}}(s, v_l)$, which depends on the distance to and speed of the leading vehicle. It is based on the following assumptions:

1. Braking maneuvers are always executed with constant deceleration b. There is no distinction between comfortable and (physically possible) maximum deceleration.
2. There is a constant "reaction time" Δt.

[1] If one were to weaken condition (11.1) to $\partial a_{\text{mic}}/\partial v \leq 0$, it is possible to formulate models that do *not* have a fundamental diagram. Such models are proposed in the context of B. Kerner's *three-phase theory*.

[2] Traffic-flow models are meant to describe *normal* conditions, while accidents are almost always caused by *exceptional* driving mistakes that are not part of normal driving behavior and thus not part of the intended scope of the model.

3. Even if the leading vehicle suddenly decelerates to a complete stop (worst case scenario), the distance gap to the leading vehicle should not become smaller than a minimum gap s_0.[3]

Condition 1 implies that the *braking distance* that the leading vehicle needs to come to a complete stop is given by

$$\Delta x_l = \frac{v_l^2}{2b}.$$

From condition 2 it follows that, in order to come to a complete stop, the driver of the considered vehicle needs not only his or her braking distance $v^2/(2b)$, but also an additional *reaction distance* $v\,\Delta t$ travelled during the reaction time.[4] Consequently, the *stopping distance* is given by

$$\Delta x = v\Delta t + \frac{v^2}{2b}. \tag{11.8}$$

Finally, condition 3 is satisfied if the gap s exceeds the required minimum final value s_0 by the difference $\Delta x - \Delta x_l$ between the stopping distance of the considered vehicle and the breaking distance of the leader:

$$s \geq s_0 + v\Delta t + \frac{v^2}{2b} - \frac{v_l^2}{2b}. \tag{11.9}$$

The speed v for which the equal sign holds (the highest possible speed) defines the "safe speed"

$$v_{\text{safe}}(s, v_l) = -b\Delta t + \sqrt{b^2\Delta t^2 + v_l^2 + 2b(s - s_0)}. \tag{11.10}$$

11.2.2 Model Equation

The simplified Gipps' model is defined as an iterated map with the "safe speed" (11.10) as its main component:

$$\boxed{v(t + \Delta t) = \min\left[v + a\Delta t, v_0, v_{\text{safe}}(s, v_l)\right] \quad \text{Gipps' model.}} \tag{11.11}$$

This model equation reflects the following properties:

- The simulation update time step is equal to the reaction time Δt.

[3] This condition is not present in the original paper, but is necessary to ensure an accident-free model in the presence of numerical errors arising from discretization.

[4] In contrast to the original publication, we assume the speed to be constant within the reaction time.

- If the current speed is greater than $v_{\text{safe}} - a\Delta t$ or $v_0 - a\Delta t$, the vehicle will reach the minimum of v_0 and v_{safe} during the next time step.[5]
- Otherwise the vehicle accelerates with constant acceleration a until either the safe speed or the desired speed is reached.

11.2.3 Steady-State Equilibrium

The homogeneous steady state implies $v(t + \Delta t) = v_l = v$, thus

$$v = \min(v_0, v_{\text{safe}}) = \min\left(v_0, -b\Delta t + \sqrt{b^2\Delta t^2 + v^2 + 2b(s - s_0)}\right),$$

which yields the steady-state speed-gap relation

$$v_e(s) = \max\left[0, \min\left(v_0, \frac{s - s_0}{\Delta t}\right)\right] \tag{11.12}$$

and, assuming constant vehicle lengths l, the familiar "triangular" fundamental diagram

$$Q_e(\rho) = \min\left(v_0\rho, \frac{1 - \rho l_{\text{eff}}}{\Delta t}\right), \tag{11.13}$$

where $l_{\text{eff}} = (l + s_0)$. As in the Newell model, the parameter Δt can be interpreted in four different ways: (i) As the reaction time introduced in the derivation of v_{safe}, (ii) as the numerical update time step of the actual model equation (11.11), (iii) as a speed adaption time in Eq. (11.11) (at least, if $v(t + \Delta t)$ is restricted by v_{safe} or v_0), or (iv) as the "safety time gap" $(s - s_0)/v_e$ in congested traffic as deduced from the fundamental diagram (11.12).

11.2.4 Model Characteristics

Unlike the minimal models described in the previous chapter, the Gipps' model is transparently derived from a few basic assumptions and uses parameters that are easy to interpret and assign realistic values (Table 11.1). Furthermore, Gipps' model is—again, in contrast to the minimal models—*robust* in the sense that meaningful results can be produced from a comparatively wide range of parameter values.

Highway traffic. The simulation of the highway scenario (Fig. 11.1, left) produces more realistic results than the OVM or the Newell model: The speed field in panel

[5] Strictly speaking, this means that deceleration $(v - v_{\text{safe}})/\Delta t$ is not restricted to b. In multi-lane simulations, it can be greater if another vehicle "cuts in" in front of the considered vehicle.

Table 11.1 Parameters of the simplified Gipps' model and typical values in different scenarios

Parameter	Typical value Highway	Typical value City traffic
Desired speed v_0	120 km/h	54 km/h
Adaption/reaction time Δt	1.1 s	1.1 s
Acceleration a	1.5 m/s^2	1.5 m/s^2
Deceleration b	1.0 m/s^2	1.0 m/s^2
Minimum distance s_0	3 m	2 m

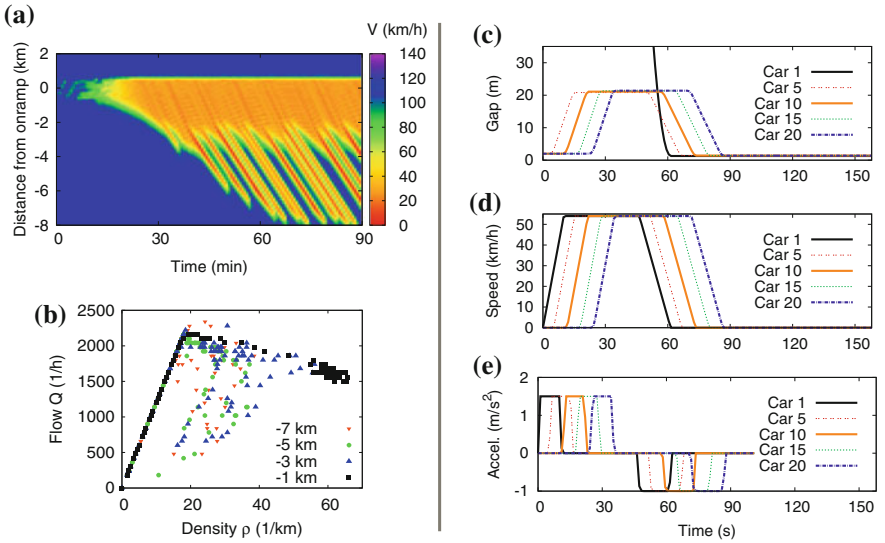

Fig. 11.1 Fact sheet of Gipps' model (11.11), (11.10). Simulation of the two standard scenarios "highway" (*left*) and "city traffic" (*right*) with the parameter values listed in Table 11.1. See Chap. 10.5 for a detailed description of the scenarios

(a) exhibits small perturbations which are caused by vehicles merging from the on-ramp and grow into stop-and-go waves while propagating upstream. The propagation velocity $c_{\text{cong}} = -l_{\text{eff}}/\Delta t$ is constant and of the order of the empirical value (≈ -15 km/h). Furthermore, the wave length (of the order of 1–1.5 km) is not too far away from the empirical values (1.5–3 km).

The flow-density diagram in Fig. 11.1b, obtained from virtual detectors, shows a strongly scattered cloud of data points in the region of congested traffic, i.e., everywhere to the right of the straight line indicating free traffic. Such a wide scattering is in agreement with empirical data (cf. Figs. 4.11 and 4.12). By looking at scatter plots of individual detectors, one observes that detectors that are closer to the bottleneck produce data points that are shifted towards greater densities and closer to the fundamental diagram of steady-state traffic. Moreover, the data points of virtual detectors positioned inside the region of stationary traffic immediately upstream

of the bottleneck (solid black squares) lie on the fundamental diagram itself. This apparent density increase near the outflow region of a congestion, also known as *pinch effect*, can be observed empirically. However, the systematic density underestimation, which conspicuously increases with the degree of the scattering of the data points, suggests that the *real* density increase is smaller, or even nonexistent. This means that the pinch effect is essentially a result of data misinterpretation, or, more specifically, by estimating the density with the time mean speed instead of the space mean speed (cf. Sect. 3.3.1). This interpretation is confirmed by simulation as will be shown in Fig. 11.5b. We draw an important conclusion that is not restricted to Gipps' model (and not even to traffic flow models):

> When using empirical data to assert the accuracy and predictive power of models, one has to simulate both the actual traffic dynamics *and* the process of data capture and analysis.

City traffic. Compared to the simple models of the previous chapter, the city-traffic scenario (Fig. 11.1, right column) is closer to reality as well. However, the acceleration time-series is unrealistic. By definition, there are only three values for the acceleration: Zero, a, and $-b$ (cf. Panel (e)). The resulting driving behavior is excessively "robotic" and the abrupt transitions are unrealistic.

Moreover, Gipps' model does not differentiate between comfortable and maximum deceleration: Assuming that b in Eq. (11.10) denotes the maximum deceleration, the model is accident-free but every braking maneuver is performed *very* uncomfortably with full brakes. On the other hand, when interpreting b as the comfortable deceleration and allowing for heterogeneous and/or multi-lane traffic the model possibly produces accidents if leading vehicles (which might be simulated using different parameters or even different models) brake harder than b.

In summary, Gipps' model produces good results in view of its simplicity. Modified versions of this model are used in several commercial traffic simulators. One example of such a modification is *Krauss' model* which essentially is a stochastic version of the Gipps model.

11.3 Intelligent Driver Model

The time-continuous *Intelligent Driver Model* (IDM) is probably the simplest complete and accident-free model producing realistic acceleration profiles and a plausible behavior in essentially all single-lane traffic situations.

11.3.1 Required Model Properties

As Gipps' model, the IDM is derived from a list of basic assumptions (*first-principles model*). It is characterized by the following requirements:

1. The acceleration fulfills the general conditions (11.1)–(11.5) for a complete model.
2. The equilibrium bumper-to-bumper distance to the leading vehicle is not less than a "safe distance" $s_0 + vT$ where s_0 is a minimum (bumper-to-bumper) gap, and T the (bumper-to-bumper) time gap to the leading vehicle.
3. An *braking strategy!intelligent* controls how slower vehicles (or obstacles or red traffic lights) are approached:
   - Under normal conditions, the braking maneuver is "soft", i.e., the deceleration increases gradually to a comfortable value b, and decreases smoothly to zero just before arriving at a steady-state car-following situation or coming to a complete stop.
   - In a critical situation, the deceleration exceeds the comfortable value until the danger is averted. The remaining braking maneuver (if applicable) will be continued with the regular comfortable deceleration b.
4. Transitions between different driving modes (e.g., from the acceleration to the car-following mode) are smooth. In other words, the time derivative of the acceleration function, i.e., the *jerk* J, is finite at all times.[6] This is equivalent to postulating that the acceleration function $a_{\text{mic}}(s, v, v_l)$ (or $\tilde{a}_{\text{mic}}(s, v, \Delta v)$) is continuously differentiable in all three variables. Notice that this postulate is in contrast to the action-point models such as the *Wiedemann Model* where acceleration changes are modeled as a series of discrete jumps.
5. The model should be as parsimonious as possible. Each model parameter should describe only one aspect of the driving behavior (which is favorable for model calibration). Furthermore, the parameters should correspond to an intuitive interpretation and assume plausible values.

11.3.2 Mathematical Description

The required properties are realized by the following acceleration equation:

$$\boxed{\dot{v} = a\left[1 - \left(\frac{v}{v_0}\right)^{\delta} - \left(\frac{s^*(v, \Delta v)}{s}\right)^2\right] \quad \text{IDM.}} \tag{11.14}$$

[6] Typical values of a "comfortable" jerk are $|J| \leq 1.5\,\text{m/s}^3$.

The acceleration of the Intelligent Driver Model is given in the form $\tilde{a}_{\text{mic}}(s, v, \Delta v)$ and consists of two parts, one comparing the current speed v to the desired speed v_0, and one comparing the current distance s to the desired distance s^*. The desired distance

$$s^*(v, \Delta v) = s_0 + \max\left(0, vT + \frac{v\Delta v}{2\sqrt{ab}}\right) \tag{11.15}$$

has an equilibrium term $s_0 + vT$ and a *dynamical term* $v\Delta v/(2\sqrt{ab})$ that implements the "intelligent" braking strategy (see Sect. 11.3.4).[7]

11.3.3 Parameters

We can easily interpret the model parameters by considering the following three standard situations:

- When *accelerating on a free road from a standstill*, the vehicle starts with the maximum acceleration a. The acceleration decreases with increasing speed and goes to zero as the speed approaches the desired speed v_0. The exponent δ controls this reduction: The greater its value, the later the reduction of the acceleration when approaching the desired speed. The limit $\delta \to \infty$ corresponds to the acceleration profile of Gipps' model while $\delta = 1$ reproduces the overly smooth acceleration behavior of the Optimal Velocity Model (10.19).
- When *following a leading vehicle*, the distance gap is approximatively given by the *safety distance* $s_0 + vT$ already introduced in Sect. 11.3.1. The safety distance is determined by the time gap T plus the minimum distance gap s_0.
- When *approaching slower or stopped vehicles*, the deceleration usually does not exceed the comfortable deceleration b. The acceleration function is smooth during transitions between these situations.

Each parameter describes a well-defined property (Fig. 11.2). For example, transitions between highway and city traffic, can be modeled by solely changing the desired speed (Table 11.2). All other parameters can be kept constant, modeling that somebody who drives aggressively (or defensively) on a highway presumably does so in city traffic as well.

Since the IDM has no explicit reaction time and its driving behavior is given in term of a continuously differentiable acceleration function, the IDM describes more closely the characteristics of semi-automated driving by adaptive cruise control

[7] The maximum condition in Eq. (11.15) ensures that the conditions (11.1)–(11.5) for model completeness hold for all situations. Strictly speaking, this condition violates the postulate of a smooth acceleration function. However, it comes into effect only in two situations: (i) For finite speeds if the leading car is much faster, (ii) for stopped queued vehicles when the queue starts to move. The first situation may arise after a cut-in maneuver of a faster vehicle. Since $s \gg s_0$ for this case, the resulting discontinuity is small. In the second case, the maximum condition prevents an overly sluggish start and the associated discontinuous acceleration profile may even be realistic.

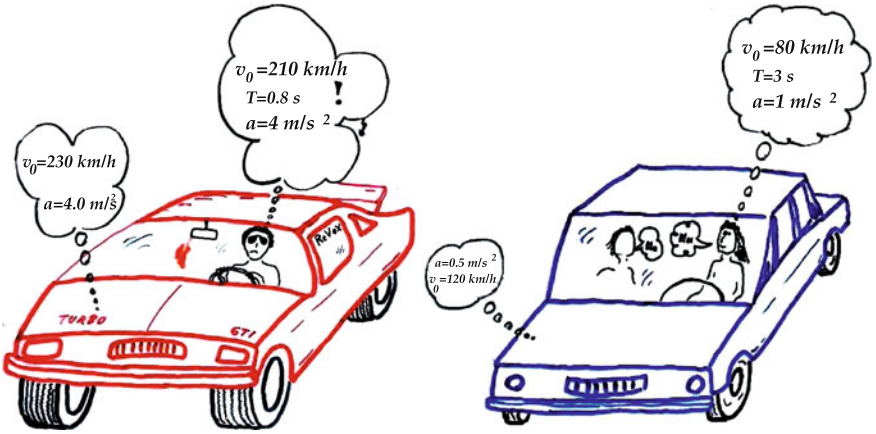

Fig. 11.2 By using intuitive model parameters like those of Gipps' model or the Intelligent Driver Model (IDM) we can easily model different aspects of the driving behavior (or physical limitations of the vehicle) with corresponding parameter values

Table 11.2 Model parameters of the Intelligent Driver Model (IDM) and typical values in different scenarios (vehicle length 5 m unless stated otherwise)

Parameter	Typical value Highway	Typical value City traffic
Desired speed v_0	120 km/h	54 km/h
Time gap T	1.0 s	1.0 s
Minimum gap s_0	2 m	2 m
Acceleration exponent δ	4	4
Acceleration a	1.0 m/s^2	1.0 m/s^2
Comfortable deceleration b	1.5 m/s^2	1.5 m/s^2

(ACC) than that of a human driver. However, it can easily be extended to capture human aspects like estimation errors, reaction times, or looking several vehicles ahead (see Chap. 12).

In contrast to the models discussed previously, the IDM explicitly distinguishes between the safe time gap T, the speed adaptation time $\tau = v_0/a$, and the reaction time T_r (zero in the IDM, nonzero in the extension described in Chap. 12). This allows us not only to reflect the conceptual difference between ACCs and human drivers in the model, but also to differentiate between more nuanced driving styles such as "sluggish, yet tailgating" (high value of $\tau = v_0/a$, low value for T) or "agile, yet safe driving" (low value of $\tau = v_0/a$, normal value for T, low value for b).[8] Furthermore, all these driving styles can be adopted independently by ACC systems (reaction time $T_r \approx 0$, original IDM), by attentive drivers (T_r

[8] Obviously, the first behavior promotes instabilities which will be confirmed by the stability analysis in Chap. 15.

comparatively small, extended IDM), and by sleepy drivers (T_r comparatively large, extended IDM).

11.3.4 Intelligent Braking Strategy

The term $v\Delta v/(2\sqrt{ab})$ in the desired distance s^* (11.15) of the IDM models the dynamical behavior when approaching the leading vehicle. The equilibrium terms $s_0 + vT$ always affect s^* due to the required continuous transitions from and to the equilibrium state. Nevertheless, to study the braking strategy itself, we will set these terms to zero, together with the free acceleration term $a[1 - (v/v_0)^\delta]$ of the IDM acceleration equation. When approaching a standing vehicle or a red traffic light ($\Delta v = v$), we then find

$$\dot{v} = -a\left(\frac{s^*}{s}\right)^2 = -\frac{av^2(\Delta v)^2}{4abs^2} = -\left(\frac{v^2}{2s}\right)^2 \frac{1}{b}. \tag{11.16}$$

With the *kinematic deceleration* defined as

$$b_{\text{kin}} = \frac{v^2}{2s}, \tag{11.17}$$

this part of the acceleration can be written as

$$\dot{v} = -\frac{b_{\text{kin}}^2}{b}. \tag{11.18}$$

When braking with deceleration b_{kin}, the braking distance is exactly the distance to the leading vehicle, thus b_{kin} is the minimum deceleration required for preventing a collision. With Eq. (11.18), we now understand the self-regulating braking strategy of the IDM:

- A "critical situation" is defined by b_{kin} being greater than the comfortable deceleration b. In such a situation, the actual deceleration is *even stronger* than necessary, $|\dot{v}| = b_{\text{kin}}^2/b > b_{\text{kin}}$. This overcompensation decreases b_{kin} and thus helps to "regain control" over the situation.
- In a non-critical situation ($b_{\text{kin}} < b$), the actual deceleration is less than the kinematic deceleration, $b_{\text{kin}}^2/b < b_{\text{kin}}$. Thus, b_{kin} increases in the course of time and approaches the comfortable deceleration.

Hence, the braking strategy is *dynamically self-regulating* towards a situation in which the kinematic deceleration equals the comfortable deceleration. One can show (see Problem 11.4) that this self-regulation is explicitly given by the differential equation

$$\frac{\mathrm{d}b_{\text{kin}}}{\mathrm{d}t} = \frac{v\, b_{\text{kin}}}{s\, b}\big(b - b_{\text{kin}}\big). \tag{11.19}$$

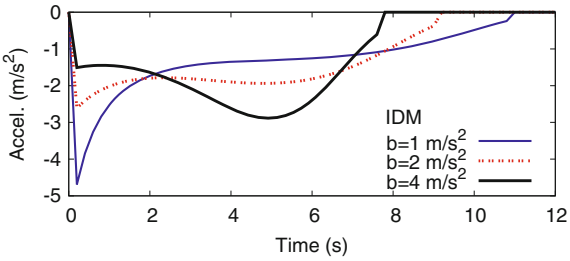

Fig. 11.3 Acceleration time-series of approaching the stop line of a *red* traffic light for different values of the comfortable deceleration. The initial speed is $v = 54$ km/h. The traffic light switches to *red* (at time $t = 0$) when the vehicle is 60 m away

Thus, the kinematic deceleration drifts towards the comfortable deceleration in *any* situation.

In the above considerations, we have ignored parts of the IDM acceleration function. To estimate their effects, the time series of Fig. 11.4e display the complete IDM dynamics when approaching an initially very distant, standing obstacle ($b_{\text{kin}} \ll b$): First, the deceleration increases towards the comfortable deceleration according to Eq. (11.19). However, due to the defensive nature of the neglected terms, the comfortable value is never realized, at least for the first vehicle. Eventually, the deceleration smoothly reduces until the vehicle stops with exactly the minimum gap s_0 left between itself and the obstacle. The following vehicles experience slightly larger decelerations than the comfortable ones, but without having to perform any emergency braking or being in danger of a collision.

Figure 11.3 shows the effects of the self-regulatory braking strategy in a situation where the vehicle is suddenly forced to stop. Drivers with $b = 1\,\text{m/s}^2$ will perceive this situation as "critical" ($b_{\text{kin}} = v^2/(2s) = 1.9\,\text{m/s}^2$) and overcompensate with even stronger deceleration. In contrast, if the comfortable deceleration is given by $b = 4\,\text{m/s}^2$, the comfortable deceleration is initially well above the kinematic deceleration and the simulated driver will brake only weakly, so that b_{kin} increases. Again, due to the other terms in the acceleration function, the actual deceleration will not reach the value of comfortable deceleration.

Why do "IDM drivers" act in a more anticipatory manner for smaller values of b? Yet why are very small values of b (less than about $1\,\text{m/s}^2$) not meaningful?

Consider the situation of approaching a standing obstacle as described above and convince yourself that the effect of the dynamical part of s^* on the acceleration prevails against all other terms. Furthermore, show that these other terms are negative in nearly all situations, thus making the driving behavior more defensive.

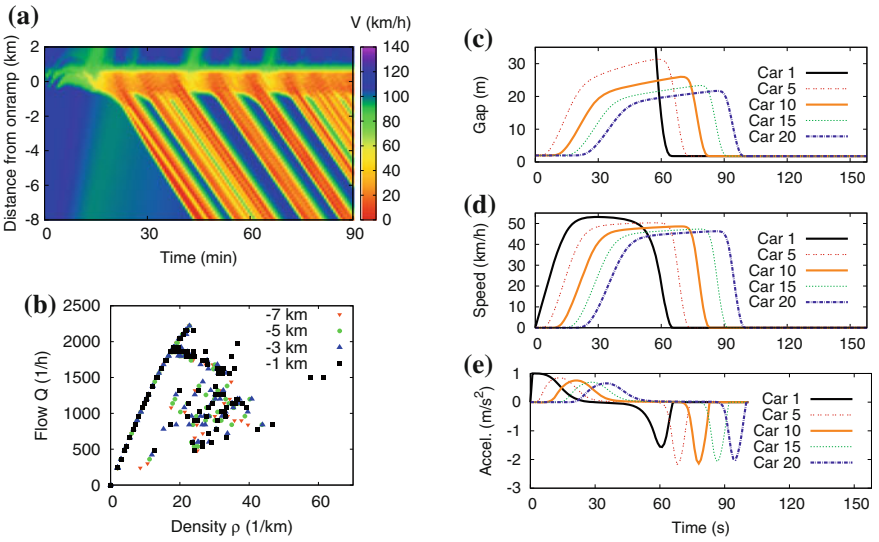

Fig. 11.4 Fact sheet of the Intelligent Driver Model (11.14). The two standard scenarios "highway" (*left*) and "city traffic" (*right*) are simulated with parameters as listed in Table 11.2. See Sect. 10.5 for a detailed description of the scenarios

11.3.5 Dynamical Properties

The *fact sheet* of the IDM, Fig. 11.4, shows IDM simulations of the two standard scenarios "traffic breakdown at a highway on-ramp" and "acceleration and stopping of a vehicle platoon in city traffic".

Highway traffic. The speed field in the highway scenario (Fig. 11.4a) exhibits dynamics similar to the one found in Gipps' model (cf. Fig. 11.1): Stationary congested traffic is found close to the bottleneck, while, further upstream, stop-and-go waves emerge and travel upstream with a velocity of approximately −15 km/h. The wavelength tends to be smaller than in real stop-and-go traffic, but the empirical spatiotemporal dynamics are otherwise reproduced very well. The growing stop-and-go waves in the simulations are caused by a collective instability called *string instability* which will be discussed in more detail in Chap. 15. As we will see in this chapter, the IDM is either unstable with respect to stop-and-go waves (string-unstable) or absolutely stable, depending on the parameters and traffic density. The model is free of accidents, however, except for very unrealistic parameters under specific circumstances.

The flow-density diagram of virtual loop detectors in Fig. 11.4b reproduces typical aspects of empirical flow-density data:

- Data points representing free traffic fall on a line, while data points from congested traffic are widely scattered.

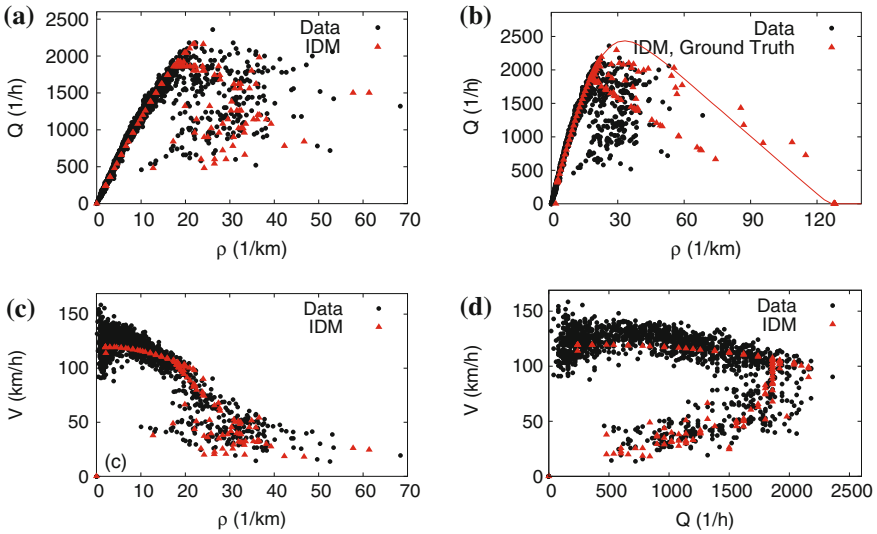

Fig. 11.5 **a** Fundamental diagram, **c** speed-density diagram, and **d** speed-flow diagram showing data from a virtual detector in the highway simulation shown in Fig. 11.4 (positioned 1 km upstream of the ramp). For comparison, empirical data from a real detector on the Autobahn A5 near Frankfurt, Germany, is shown. Velocities have been calculated using arithmetic means in both the real data and the simulation data. **b** Flow-density diagram with the same empirical data but using the real (local) density for the IDM simulation rather than the density derived from the virtual detectors

- The free-traffic branch is not a perfectly straight line but is slightly curved, especially towards the maximum flow.
- Near the maximum flow, the points are arranged in a pattern that looks like a mirror image of the Greek letter λ (*inverse-λ form*), meaning that for a range of densities (here $\approx 18-25$ veh/h), both free and congested traffic states are possible. Thus, the IDM reproduces the empirically observed bistability and the resulting hysteresis effects like the *capacity drop* (about 300 veh/h or 15 % in the present example).

Comparing the virtual detector data with the real data in Fig. 11.5a, c, and d, we find almost quantitative agreement of the flow-density, speed-density, and speed-flow diagrams. Contrary to Gipps' model, the IDM also reproduces the curvature of the free-traffic branch correctly. This agreement with the data allows us to scrutinize the nature of the observed strong scattering of flow-density data points corresponding to congested traffic. First, we compare the *estimated* density using the virtual stationary detector data with the *real* spatial density which, of course, is available in the simulation. The result displayed in Fig. 11.5b reminds us that one has to be very careful when interpreting flow-density data. Moreover, even the scattering of the data points itself is a matter of the way the data is plotted: While the congested traffic data is much more scattered than the free-flow data in the flow-density data in Fig. 11.5a, both branches show similar scattering in the speed-flow diagram 11.5d—in spite of the fact that both diagrams show the *same* data.

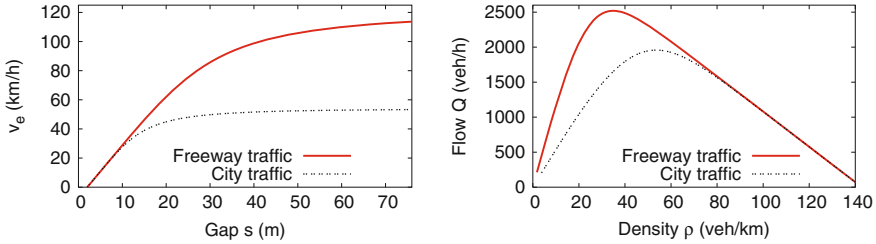

Fig. 11.6 Microscopic (*left*) and macroscopic (*right*) fundamental diagram of the IDM using the parameters shown in Table 11.2

City traffic. In the city traffic simulation (Fig. 11.4c–e) we see a smooth, realistic acceleration/deceleration profile, except in vehicle platoons with speed close to v_0 where followers do not accelerate up to the desired speed and thus the distance between the vehicles does not reach a constant value before the braking maneuver begins. This happens because, when approaching the desired speed, the free acceleration function decreases continuously to zero while the interaction (braking) term s^*/s remains finite (reaching zero only in the limit $s \to \infty$). Thus, for $v \lesssim v_0$, the actual steady-state equilibrium distance (where the free acceleration and the interaction terms cancel each other) is significantly larger than $s^*(v, 0)$. In the next section, we will investigate this more closely and propose a solution in Sect. 11.3.7.

11.3.6 Steady-State Equilibrium

By postulating $\dot{v} = \Delta v = 0$ we obtain the condition for the steady-state equilibrium of the IDM from the acceleration function (11.14):

$$1 - \left(\frac{v}{v_0}\right)^{\delta} - \left(\frac{s_0 + vT}{s}\right)^2 = 0. \tag{11.20}$$

For arbitrary values of δ we can solve this equation in closed form only for s (cf. Fig. 11.6),

$$s = s_e(v) = \frac{s_0 + vT}{\sqrt{1 - \left(\frac{v}{v_0}\right)^{\delta}}}. \tag{11.21}$$

This yields the equilibrium gap $s_e(v)$ with the speed being the independent variable (instead of the equilibrium speed $v_e(s)$ as a function of the gap). Using the micro-macro relation (10.16), $s_e = \frac{1}{\rho_e} - 1$, $v = V$, and $Q_e = \rho_e V$, we obtain the speed-density and the fundamental diagrams shown in Fig. 11.6.

Note that due to the continuous transition between free and congested traffic, the equilibrium gap $s_e(v)$ is *not* given by $s^*(v, 0) = s_0 + vT$. Instead, for $v \lesssim v_0$ it is much larger which can be seen by looking at the denominator of Eq. (11.21). Therefore the fundamental diagram is not a perfect triangle but rounded close to the maximum flow. This causes the curvature in the macroscopic speed-density and flow-density diagrams (Fig. 11.5), but also produces the mentioned unrealistic car-following behavior in platoons with identical driver-vehicle units.

11.3.7 Improved Acceleration Function

Using the IDM as example, this section shows the scientific modeling process, aiming at eliminating some deficiencies of a model while retaining the good and well-tested features and keeping the model parsimonious, i.e., adding as few model parameters as possible.[9] The IDM is unrealistic in following aspects:

- If the actual speed exceeds the desired speed (e.g., after entering a zone with a reduced speed limit), the deceleration is unrealistically large, particularly for large values of the acceleration exponent δ.
- Near the desired speed v_0, the steady-state gap (11.21) becomes much greater than $s^*(v, 0) = s_0 + vT$ so that the model parameter T loses its meaning as the desired time gap. This means that a platoon of identical drivers and vehicles disperses much more than observed. Moreover, not all cars will reach the desired speed (Fig. 11.4c, d).
- If the actual gap is considerably smaller than desired (which may happen if another vehicle cuts too close when changing lanes) the braking reaction to regain the desired gap is exaggerated as illustrated in Problem 11.3.

We will treat the first two aspects here while the third aspect (which is only relevant in multi-lane situations) will be deferred to Sect. 11.3.8.

To improve the behavior for $v > v_0$, we require that the maximum deceleration must not exceed the comfortable deceleration b if there are no interactions with other vehicles or obstacles. The parameter δ should retain its meaning also in the new regime, i.e., leading to smooth decelerations to the new desired speed for low values and decelerating more "robotically" for high values. Furthermore, the free acceleration function $a_{\text{free}}(v)$ should be continuously differentiable, and remain unchanged for $v \le v_0$, i.e., $a_{\text{free}}(v) = \lim_{s\to\infty} a_{\text{IDM}}(s, v, \Delta v)$ for $v \le v_0$. Probably the simplest free-acceleration function meeting these conditions is given by

$$a_{\text{free}}(v) = \begin{cases} a\left[1 - \left(\frac{v}{v_0}\right)^{\delta}\right] & \text{if } v \le v_0, \\ -b\left[1 - \left(\frac{v_0}{v}\right)^{a\delta/b}\right] & \text{if } v > v_0. \end{cases} \tag{11.22}$$

[9] Ideally, no parameters are added as in this example.

To improve the behavior near the desired speed, we tighten the second condition in Sect. 11.3.1 by requiring that the equilibrium gap $s_e(v) = s^*(v, 0)$ should be *strictly equal* to $s_0 + vT$ for $v < v_0$. However, we would like to implement any modification as conservatively as possible in order to preserve all the other meaningful properties of the IDM (especially the "intelligent" braking strategy). Thus, changes should only have an effect

- near the steady-state equilibrium, i.e., if $z(s, v, \Delta v) = s^*(v, \Delta v)/s \approx 1$,[10]
- and when driving with $v \approx v_0$ and $v > v_0$.

We can accomplish this by distinguishing between the cases $z = s^*(v, \Delta v)/s < 1$ (the actual gap is greater than the desired gap) and $z \geq 1$. The new condition requires $\tilde{a}_{\text{mic}} = 0$ for all input values that satisfy $z(s, v, \Delta v) = 1$ and $v < v_0$. The other conditions in Sect. 11.3.1 and the conditions (11.1)–(11.5) are automatically satisfied if $\partial \tilde{a}_{\text{mic}}/\partial z < 0$, and if $\tilde{a}_{\text{mic}}(z)$ is continuously differentiable at the transition point $z = 1$. Probably the simplest acceleration function that fulfills all these conditions for $v \leq v_0$ is given by

$$\left.\frac{\mathrm{d}v}{\mathrm{d}t}\right|_{v \leq v_0} = \begin{cases} a\,(1 - z^2) & z = \frac{s^*(v, \Delta v)}{s} \geq 1, \\ a_{\text{free}}\left(1 - z^{(2a)/a_{\text{free}}}\right) & \text{otherwise.} \end{cases} \tag{11.23}$$

For $v > v_0$, there is no steady-state following distance, and we simply combine the free acceleration a_{free} and the interaction acceleration $a(1 - z^2)$ such that the interaction vanishes for $z \leq 1$ and the resulting acceleration function is continuously differentiable:[11]

$$\left.\frac{\mathrm{d}v}{\mathrm{d}t}\right|_{v > v_0} = \begin{cases} a_{\text{free}} + a(1 - z^2) & z(v, \Delta v) \geq 1, \\ a_{\text{free}} & \text{otherwise.} \end{cases} \tag{11.24}$$

This *Improved Intelligent Driver Model* (IIDM) uses the same set of model parameters as the IDM and produces essentially the same behavior except when vehicles follow each other near the desired speed or when the vehicle is faster than the desired speed. Simulating the standard city traffic scenario with the IIDM shows that all vehicles in the platoon now accelerate up to the desired speed (Fig. 11.7, left) while the self-stabilizing braking strategy and the observance of a comfortable deceleration are still in effect (Fig. 11.7, right).

However, the fundamental diagram is an exact triangle now. Thus, simulating highway traffic will no longer produce curved free-traffic branches in the flow-density, speed-flow, and speed-density diagrams (contrary to the unmodified IDM, cf. Fig. 11.5). Problem 11.6 discusses an alternative cause of this curvature.

---

[10] In fact, this condition is more general since it also includes continuations of the steady state to nonstationary situations.

[11] At $v = v_0$ and $z > 1$, the full acceleration function (11.23), (11.24) is only continuous, but not differentiable with respect to v. It would require a disproportionate amount of complication to resolve this special case of little relevance.

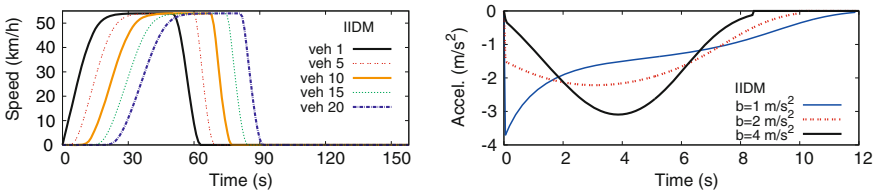

Fig. 11.7 Simulation of the city traffic scenario (*left*) and the situation shown in Fig. 11.3 (*right*) using the Improved Intelligent Driver Model (IIDM) with the parameters listed in Table 11.2

11.3.8 Model for Adaptive Cruise Control

While ACC systems only automate the longitudinal driving task, they must also react reasonably if the sensor input variables—the gap s and approaching rate Δv—change discontinuously as a consequence of "passive" lane changes (another lane-changing vehicle becomes the new leader), and also "active" lane changes (the ACC driver changes lanes manually). This means, the third of the IDM deficiencies mentioned in the previous Sect. 11.3.7—overreactions when the gap decreases discontinuously by external actions—must be taken care of.

The reason for the overreactions is the intention of the IDM (and IIDM) development to be accident-free even in the *worst case*, in which the driver of the leading vehicle suddenly brakes to a complete standstill. However, there are situations characterized by low speed differences and small gaps where human drivers rely on the fact that the drivers of preceding vehicles will *not* suddenly initiate full-stop emergency brakings. In fact, they consider such situations only as mildly critical. As a consequence, a more plausible and realistic driving behavior will result when drivers act according to the *constant-acceleration heuristic* (CAH) rather than considering the worst-case scenario. The CAH is based on the following assumptions:

- The accelerations of the considered and leading vehicle will not change in the near future (generally a few seconds).
- No safe time gap or minimum distance is required at any given moment.
- Drivers (or ACC systems) react without delay, i.e., with zero reaction time.

For actual values of the gap s, speed v, speed v_l of the leading vehicle, and constant accelerations $\dot{v}$ and $\dot{v}_l$ of both vehicles, the maximum acceleration $\max(\dot{v}) = a_{\mathrm{CAH}}$ that does not lead to an accident under the CAH assumption is given by

$$a_{\mathrm{CAH}}(s, v, v_l, \dot{v}_l) = \begin{cases} \dfrac{v^2 \tilde{a}_l}{v_l^2 - 2s\tilde{a}_l} & \text{if } v_l(v - v_l) \le -2s\tilde{a}_l, \\ \tilde{a}_l - \dfrac{(v - v_l)^2 \Theta(v - v_l)}{2s} & \text{otherwise.} \end{cases} \tag{11.25}$$

The effective acceleration $\tilde{a}_l(\dot{v}_l) = \min(\dot{v}_l, a)$ (with the maximum acceleration parameter a) has been used to avoid the situation where leading vehicles with higher acceleration capabilities may cause "drag-along effects" of the form (11.6), or other

artefacts violating the general plausibility conditions (11.1)–(11.5). The condition $v_l(v - v_l) = v_l \Delta v \leq -2s\dot{v}_l$ is true if the vehicles have stopped at the time the minimum gap $s = 0$ is reached. The Heaviside step function $\Theta(x)$ (with $\Theta(x) = 1$ if $x \geq 0$, and zero, otherwise) eliminates negative approaching rates Δv for the case that both vehicles are moving at the time t^* of least distance. Otherwise, t^* would lie in the past.

In order to retain all the "good" properties of the IDM, we will use the CAH acceleration (11.25) only as an *indicator* to determine whether the IDM will lead to unrealistically high decelerations, and modify the acceleration function of a model for ACC vehicles only in this case. Specifically, the proposed ACC model is based on following assumptions:

- The ACC acceleration is never lower than that of the IIDM. This is motivated by the circumstance that the IDM and the IIDM are accident-free, i.e., sufficiently defensive.
- If both, the IIDM and the CAH, produce the same acceleration, the ACC acceleration is the same as well.
- If the IIDM produces extreme decelerations, while the CAH yields accelerations in the comfortable range (greater than $-b$), the situation is considered to be mildly critical, and the resulting acceleration should be between $a_{\mathrm{CAH}} - b$ and a_{CAH}. Only for *very* small gaps, the decelerations should be somewhat higher to avoid an overly reckless driving style.
- If both, the IIDM and the CAH, result in accelerations significantly below $-b$, the situation is seriously critical and the ACC acceleration is given by the maximum of the IIDM and CAH accelerations.
- The ACC acceleration should be a continuous and differentiable function of the IIDM and CAH accelerations. Furthermore, it should meet the consistency requirements (11.1)–(11.5).

Probably the most simple functional form satisfying these criteria is given by

$$a_{\mathrm{ACC}} = \begin{cases} a_{\mathrm{IIDM}} & a_{\mathrm{IIDM}} \geq a_{\mathrm{CAH}}, \\ (1-c)\, a_{\mathrm{IIDM}} + c \left[a_{\mathrm{CAH}} + b \tanh\left(\frac{a_{\mathrm{IIDM}} - a_{\mathrm{CAH}}}{b} \right) \right] & \text{otherwise.} \end{cases} \tag{11.26}$$

This *ACC model* has only one additional parameter compared to the IDM/IIDM, the "coolness factor" c. For $c = 0$ one recovers the IIDM while $c = 1$ corresponds to the "pure" ACC model. Since the pure ACC model would produce a reckless driving behavior for very small gaps, a small fraction $1 - c$ of the IIDM is added. It turns out that a contribution of 1 % (corresponding to $c = 0.99$) gives a good compromise between reckless and overly timid behavior in this situation while it is essentially irrelevant, otherwise.

In contrast to the other models of this section, the ACC model has the *acceleration* $\dot{v}_l$ of the leading vehicle as additional exogenous factor (besides the speed, the

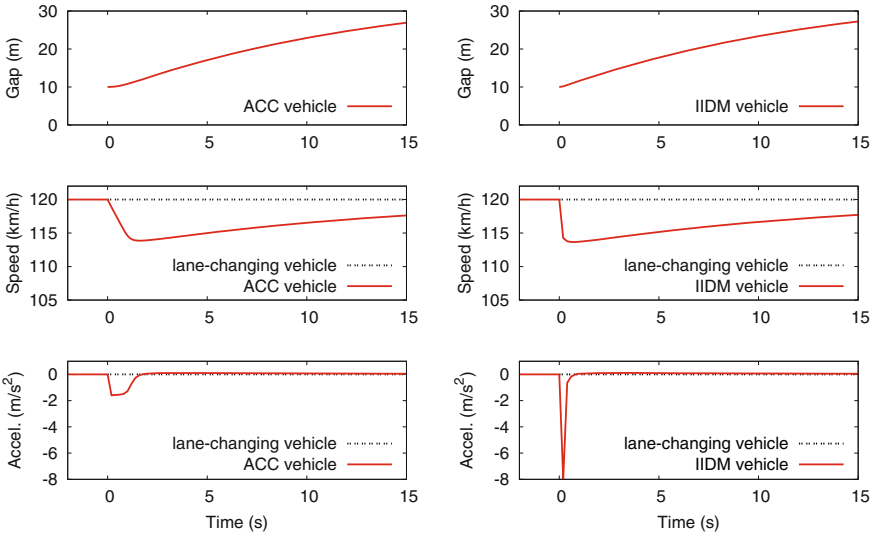

Fig. 11.8 Response of an ACC and an IIDM vehicle (parameters of Table 11.2 and coolness factor $c = 0.99$) to the lane-changing maneuver of another vehicle immediately in front of the considered vehicle. The initial speed of both vehicles is 120 km/h (equal to the desired speed), and the initial gap is 10 m which is about 30 % of the desired gap. This can be considered as a "mildly critical" situation

speed difference, and the gap). This models a behavior similar to the human reactions to brake lights, but in a continuous rather than in an off-on way.[12]

The Figs. 11.8 and 11.9 show the effect of this model improvement: In the mildly critical situation of Fig. 11.8, a lane-changing car driving at the same speed as the considered car cuts in front leaving a gap of only 10 m which is less than one third of the "safe" gap $s_0 + vT = 35.3$ m. While the IIDM (and IDM) will initiate a short emergency braking maneuver in this situation, the ACC reflects a relaxed reaction by braking at about the comfortable deceleration. In contrast, if the situation becomes really critical (Fig. 11.9), both the (I)IDM and the ACC model will initiate an emergency braking.

When implementing all these modifications, one needs to bear in mind that, in most situations, the ACC model should behave very similarly to the IDM so as to retain its well-tested good properties. To verify this, Fig. 11.10 shows the familiar *fact sheet* for the two standard situations. As expected, there is little difference compared to the IDM (and the IIDM) since the modified behavior kicks in only in the highway scenario, and only at the merging region of the on-ramp.

In summary, the ACC model can be considered as a minimal fully operative control model for ACC systems. With minor modifications, it has been implemented in real cars and tested on test tracks as well as on public roads and highways.

[12] Since the acceleration $\dot{v}_l$ cannot be measured directly, it is obtained by numerical differentiation of the approaching rate and the speed-changing rate. Care has to be taken to control the resulting discretization errors.

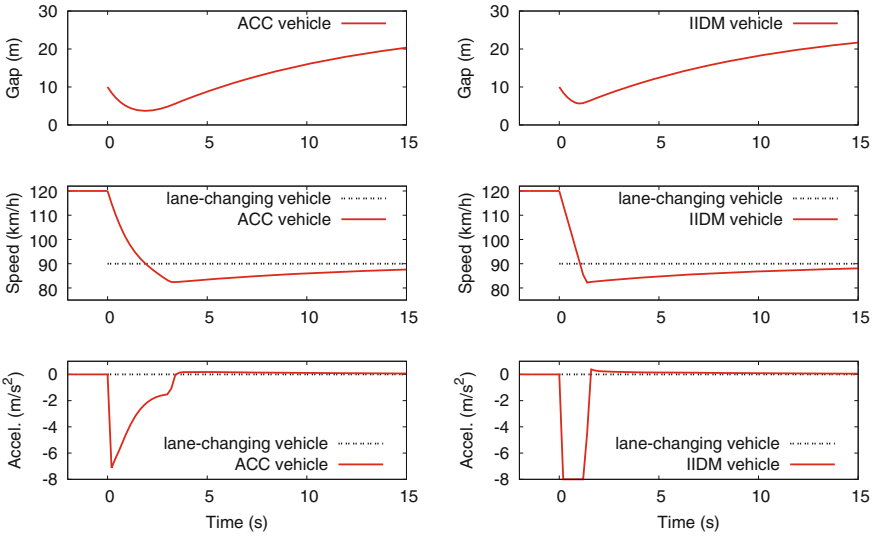

Fig. 11.9 Response of an ACC and an IIDM vehicle to a dangerous lane-changing maneuver of a slower vehicle (speed 90 km/h) immediately in front of the considered vehicle driving initially at $v_0 = 120$ km/h. The decelerations are restricted to 8 m/s^2. The parameters are according to Table 11.2 and a coolness factor of $c = 0.99$ for the ACC vehicles. The desired speed of the lane-changing vehicle is reduced to 90 km/h

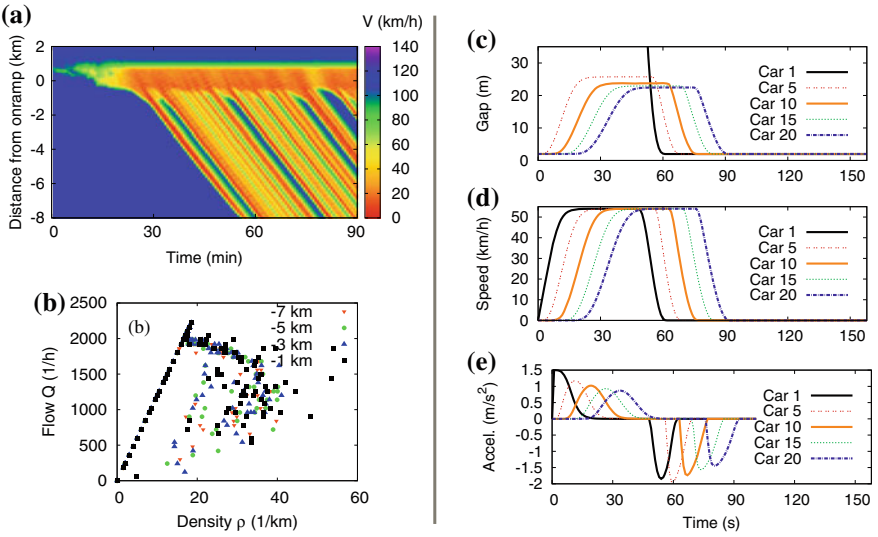

Fig. 11.10 Fact sheet of the ACC-model. The two standard scenarios "highway" (*left*) and "city traffic" (*right*) are simulated with the parameter values listed in Table 11.2 and the "coolness factor" $c = 0.99$. See Sect. 10.5 for a detailed description of the simulation scenarios

Problems

11.1 Conditions for the microscopic fundamental diagram
Use the consistency conditions (11.1)–(11.5) to derive the conditions (11.7) that have to be fulfilled by the steady-state speed-distance relation $v_e(s)$ (microscopic fundamental diagram).

11.2 Rules of thumb for the safe gap and braking distance

1. A common US rule for the safe gap is the following: "Leave one car length for every ten miles per hour of speed". Another rule says "Leave a time gap of two seconds". Compare these two rules assuming a typical car length of 15 ft. For which car length are both rules equivalent?
2. In Continental European countries, one learns in driving schools the following rule: "The safe gap should be at least half the reading of the speedometer". Translate this rule into a safe time gap rule and compare it with the US rule stated above. Take into account that, in Continental Europe, speed is commonly expressed in terms of km per hour.
3. A rule of thumb for the braking distance says "Speed squared and divided by 100". If speed is measured in km/h, what braking deceleration is assumed by this rule?

11.3 Reaction to vehicles merging into the lane
A vehicle enters the lane of the considered car causing the gap s to fall short of the equilibrium gap s_e by 50 %. Both vehicles drive at the same speed. Find the resulting (negative) accelerations produced by the simplified Gipps' model and the IDM, assuming the parameter values $\Delta t = 1\,\mathrm{s}$, $b = 2\,\mathrm{m/s^2}$, $a = 1\,\mathrm{m/s^2}$, $\delta = 4$, and $v = v_0/2 = 72\,\mathrm{km/h}$ for all vehicles. (No other parameter values are needed for this problem.)

11.4 The IDM braking strategy
Derive Eq. (11.19) for the explicit description of the self-regulating braking strategy when approaching a standing obstacle ($\Delta v = v$). Assume that the IDM acceleration can be reduced to the braking term $\dot{v} = -b_{\mathrm{kin}}^2/b$ for this case. *Hint*: Keep in mind that $\dot{s} = -\Delta v$.

11.5 Analysis of a microscopic model
Assume a car-following model that is given by the following acceleration equation:

$$\frac{\mathrm{d}v}{\mathrm{d}t} = \begin{cases} a & \text{if } v < \min(v_0, v_{\mathrm{safe}}), \\ 0 & \text{if } v = \min(v_0, v_{\mathrm{safe}}), \\ -a & \text{otherwise,} \end{cases} \qquad v_{\mathrm{safe}} = -aT + \sqrt{a^2T^2 + v_l^2 + 2a(s - s_0)}.$$

As usual, v_l is the speed of the leading vehicle, and s the corresponding bumper-to-bumper gap.

1. Explain the meaning of the parameters a, s_0, v_0, and T by examining (i) the acceleration on a free road segment, (ii) the driving behavior when following another vehicle with constant speed and gap, and (iii) the braking maneuver performed when approaching a standing vehicle.
2. Find the steady-state speed $v_e(s)$ as a function of the distance assuming $v_0 = 20\,\text{m/s}$, $a = 1\,\text{m/s}^2$, $T = 1.6\,\text{s}$, and $s_0 = 3\,\text{m}$. Also, sketch the fundamental diagram for vehicles of length 5 m.
3. Assume that a vehicle standing at position $x = 0$ for $t \leq 0$ accelerates for $t > 0$ and then stops at a red traffic light at $x = 603\,\text{m}$. Derive the speed function $v(t)$ for this scenario, assuming the parameter values $v_0 = 20\,\text{m/s}$, $a = 1\,\text{m/s}^2$, $T = 0$, and $s_0 = 3\,\text{m}$. (Hints: The traffic light is modeled by a standing "virtual" vehicle; the vehicle will reach its desired speed in this scenario.)

11.6 Heterogeneous traffic

For identical vehicles and drivers, the modified IDM with its strictly triangular fundamental diagram (IIDM) does not produce the pre-breakdown speed drop observed in Fig. 11.5. Is it possible to produce the speed drop by introducing a combination of different desired speeds or the possibility of passing maneuvers?

11.7 City traffic in the modified IDM (IIDM)

On a road segment with two traffic lights, a number of vehicles is standing in front of the first traffic light. When the light turns green, the vehicles accelerate but have to stop again at the second traffic light. The upper panel shows trajectories of all 15 vehicles and the red lights (horizontal lines). The lower panel shows the corresponding speeds of the two bold trajectories.

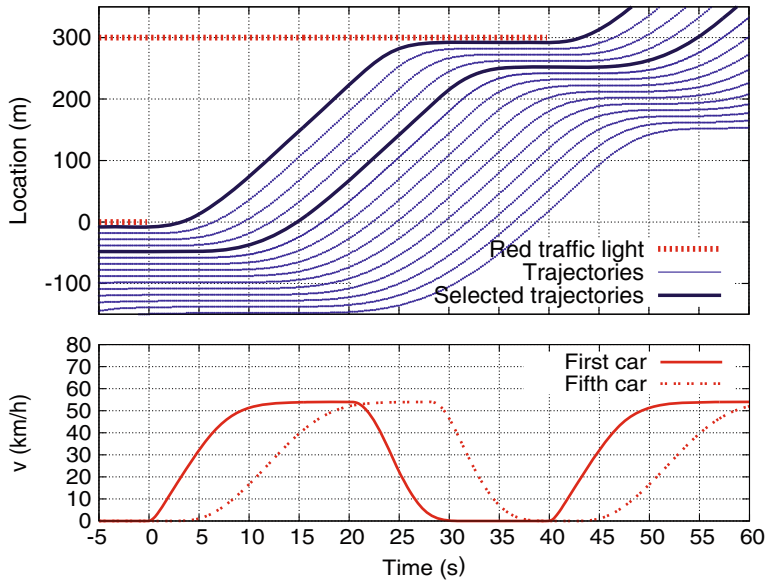

1. Estimate the capacity C of the free road segment (without traffic lights) by finding the maximum possible flow.
2. How many vehicles are able to pass the traffic light at $x = 0$ if the green light is on for (i) 5 s, (ii) 15 s, or (iii) 40 s? Find appropriate τ_0 and β such that $\tau(n) = \tau_0 + \beta n$ is the time the light has to be green to let n vehicles pass.
3. Estimate the velocity c_{cong} of the transition "standing traffic" $\rightarrow$ "starting to move" from the shown trajectories.
4. Estimate the IDM parameters v_0, $l_{\text{eff}} = l + s_0$, $T = 1/(\rho_{\max} c_{\text{cong}})$, a, and b used in the simulation. Add appropriate tangents to the speed diagram to find the accelerations.

Further Reading

- Gipps, P.G.: A behavioural car-following model for computer simulation. Transportation Research Part B: Methodological **15** (1981) 105–111
- Krauss, S.: Microscopic Modeling of Traffic Flow: Investigation of Collision Free Vehicle Dynamics. Ph.D. Thesis, University of Cologne, Cologne, Germany (1997)
- Treiber, M., Hennecke, A., Helbing, D.: Congested traffic states in empirical observations and microscopic simulations. Physical Review E **62** (2000) 1805–1824
- Kesting, A., Treiber, M., Helbing, D.: Enhanced Intelligent Driver Model to access the impact of driving strategies on traffic capacity simulations. Philosophical Transactions of the Royal Society A **368** (2010) 4585–4605

Chapter 12
Modeling Human Aspects of Driving Behavior

It takes 8460 bolts to assemble an automobile, and one nut to scatter it all over the road.

Author unknown

Abstract The driving characteristics described by the microscopic models of the previous chapters correspond, from a formal perspective, to semi-automated driving as realized by *adaptive cruise control* (ACC). On the one hand, human drivers are less efficient than ACC systems since reaction times, attention time spans, and estimation errors play a significant role. On the other hand, humans can take into account more input stimuli than acceleration controllers, for example: brake lights, turning signals, next-nearest neighbors, and external conditions. Moreover, in contrast to the present-day ACC systems reflected by the previous models, they can *anticipate* the situation for the next few seconds. All these specific human aspects will be formulated in terms of psycho-physiological extensions to the previous car-following models, in particular Gipps' model and the Intelligent Driver Model. Another class of psycho-physiological models explicitly take into account finite perception thresholds leading to sudden changes in accelerations whenever the difference from the ideal acceleration becomes significant. We present the Wiedemann model as a representative of this model class.

12.1 Man Versus Machine

The exogenous (input) variables of the models presented in Chaps. 10 and 11 are the own speed v, the (bumper-to-bumper) gap s to the leading vehicle, and its speed v_l (For the ACC model (11.26), the acceleration $\dot{v}_l$ is an additional input). The model output is the acceleration $a_{\mathrm{mic}}(s, v, v_l)$ or the targeted speed $v_{\mathrm{mic}}(s, v, v_l)$ for time-continuous or discrete models, respectively. Remarkably, both the input and the output are essentially the same as that required by the acceleration controllers for

M. Treiber and A. Kesting, *Traffic Flow Dynamics*,
DOI: 10.1007/978-3-642-32460-4_12, © Springer-Verlag Berlin Heidelberg 2013

semi-automated driving. Such driver-assistance systems, often called *adaptive cruise control* (ACC), are already available for many makes of cars. ACC systems obtain their input directly from the rotation rate of the tires (v), and by forward-looking radar or infrared-laser range finders (s and v_l). The acceleration $\dot{v}_l$ can be calculated from the speed v_l by taking the numerical time derivative (and smoothing the result).[1] The acceleration output of the car-following models corresponds to the signals the ACC system sends to the controllers for the engine and the brakes. The car-following model itself corresponds to the core control logic of the ACC system.[2]

In summary, the ACC-like driving styles generated by the models of the previous chapters are characterized by negligible estimation errors and response times, and an unshakeable attention. However, the restriction to the three input variables v, s, and v_l corresponds to a certain shortsightedness (only the immediate leader is considered but no vehicles driving further ahead), a tunnel vision (external circumstances as well as vehicles driving on neighboring lanes or behind are ignored), and ignorance brake lights, turning signals, horns, or headlight flashes are not taken into account).

In the following sections, we describe and model human driving characteristics that have not been captured in the models of the previous chapters:

- *Finite reaction time*. For attentive drivers, it is about $T_r = 1$ s. Depending on the driver and the situation, it can be significantly greater.
- *Estimation errors*. Gaps and speeds can only estimated with limited accuracy.
- *Temporal anticipation*. Experienced drivers can predict the traffic situation for the next few seconds.
- *Multi-vehicle anticipation* or *spatial anticipation*. The driver takes into consideration next-nearest and further vehicles ahead. Sometimes, vehicles on other lanes (particularly when driving through highway work zones) or the vehicle behind (when tailgating) play a role as well.
- *More input signals* like brake lights, direction indicators, horns.
- *Context sensitivity*. The driving style depends on the present and past overall traffic situation (*memory effect*). For example, after driving for some time in congested traffic, the time gap to the leading vehicle becomes greater and the driver's alertness wears down. In contrast, when approaching a lane closure and driving on one of the through lanes, drivers react to vehicles squeezing into their lane in a more relaxed manner, and drivers temporarily accept a smaller time gap than normal.
- *Finite perception threshold*. Humans cannot perceive small changes in exogenous factors but only respond to significant changes.
- *Courtesy and cooperation*. This aspect of human drivers is particularly relevant in situations with mandatory lane changes: Human drivers move out of the inside lane to allow the vehicle from the on-ramp to enter, or they brake (or accelerate) to

[1] In future, it may also be possible to directly measure accelerations with inertial sensors fused with gyroscopic sensors and others.

[2] This can be taken literally: During one of the authors' projects with a car manufacturer, the ACC model in Eq. (11.26) was implemented (with some modifications) as kernel of an ACC system of a mid-range car, and was tested on public city streets and highways.

make space for other drivers. This will be discussed in Sect. 14.3.3 in the context of modeling lane changes.

Because human driver models combine physiological restrictions (reaction times, estimation errors, perception thresholds) and psychological aspects (anticipation heuristic, context sensitivity, driving strategy in general), they are also referred to as *psycho-physiological car-following models*.

Remarkably, it turns out that the destabilizing effects caused by human imperfections are essentially compensated for by the stabilizing effects of anticipation and context sensitivity. In many situations this allows us to describe the traffic flow of human drivers by "machine-like" acceleration models of the type (10.3).

On the other hand, when investigating the strengths and weaknesses of human drivers and their influence on the efficiency and stability of traffic flow, the psycho-physiological models to be described below become necessary tools. Similarly to the lane-changing and decision models to be described in Chap. 14, we will formulate the above aspects (with the exception of finite perception thresholds) in terms of *extensions* to the ACC-like car-following models such as the IDM or the simplified Gipps' model. Another class of psycho-physiological model explicitly takes into account finite perception thresholds. We will briefly describe the Wiedemann model as most prominent representative of this model class.

12.2 Reaction Times

From the traffic flow modeler's point of view the reaction time T_r is composed of the following contributions:

- The *mental processing time* which, in turn, is composed of the sensation time ("there is a moving object on the road"), the perception or recognition time ("the object is a pedestrian"), the "situation awareness time" needed to recognize and interpret the scene ("I am moving towards the pedestrian possibly resulting in a crash"), and the decision time ("I will brake instead of do nothing or steering to the left").
- The *movement* or *action time*, e.g., to lift the foot from the throttle pedal, move it to the brake pedal, and apply pressure.
- And the *technical response time* of the respective vehicle components (about 100 ms for the brakes, several 100 ms for the accelerator).[3]

The reaction time depends on many factors such as the age and experience of the driver, visibility conditions, degree of surprise, and urgency of action. Nevertheless, nearly all models and simulators assume a constant common value of the order of 1 s for all drivers in all situations.

In time-continuous models, the driver's response is directly given by the acceleration function a_{mic}. So it is straightforward to introduce a reaction time: One simply

[3] The technical response time also applies to ACC systems.

calculates the acceleration function with time delayed input stimuli (gap, own speed,[4] and speed difference),

$$\dot{v}(t) = a_{\text{mic}}\big[s(t - T_r), v(t - T_r), v_l(t - T_r)\big]. \tag{12.1}$$

From the mathematical point of view, the differential equations of the time-continuous models become *delay-differential equations*. It is known from control theory that systems become more unstable with increased *dead times*. In the traffic context this means that traffic flow becomes more unstable with increased reaction times; this is intuitively plausible.

Equation (12.1) cannot be integrated analytically, but it is straightforward to approximatively solve it numerically. This is true even if the reaction time T_r is not a multiple of the update time Δt of the numerical scheme (10.9), (10.10). One simply approximates the quantity $u(t - T_r)$ (where u may stand for s, v, Δv, or v_l) in the update step $i = t/\Delta t$ by linear interpolation:

$$u(t - T_r) = r u_{i-j-1} + (1 - r)u_{i-j}, \quad j = \text{int}\left(\frac{T_r}{\Delta t}\right), \quad r = \frac{T_r}{\Delta t} - j. \tag{12.2}$$

Here $\text{int}(x)$ and r denote the integer and fractional parts of x, respectively. In order to implement this formula, it is necessary to temporarily save the past $j + 1$ values $u_{i-j-1}, \ldots, u_i$ of the dynamical variables u in a buffer. With this approach, it is possible to model variations of the reaction time over the drivers and circumstances, as discussed above.

When modeling traffic flow by time-discrete iterated coupled maps or cellular automata (Chap. 13), the reaction time is often identified with the update time. However, this corresponds to another concept of the driver's reaction: While Eq. (12.1) represents a permanently attentive driver who (together with his or her vehicle) always needs the same reaction time to put the input stimuli into action, the speed function v_{mic} together with the update rules (10.7) and (10.8) of the iterated maps corresponds to a vehicle with zero response time and an instantly reacting driver who, however, looks at the traffic situation only at fixed time instances which are an *attention span* Δt apart. At all other times, the drivers are inattentive and do nothing, i.e., do not change the acceleration.[5]

Both the proper reaction time T_r and the attention span Δt contribute to the *effective reaction time* T_{eff}. In order to compare the relative effects of these factors, we reinterpret the numerical update time of time-continuous models as a model parameter in its own right (instead of an auxiliary numerical quantity) which has the same meaning as in the discrete-time models.

---

[4] One can argue that the own speed is known a priori without delay, so the associated sensation and recognition times are zero. However, as discussed above, these times make up only a fraction of the reaction time, so the speed argument of the acceleration function should be given by $v(t - T_r')$ with $T_r' < T_r$. Some models nevertheless assume $T_r' = 0$. In Eq. (12.1), we have assumed $T_r' = T_r$.

[5] This interpretation assumes that the acceleration is directly given by the pressure on the throttle or brake pedals. For time intervals within Δt this is a good approximation.

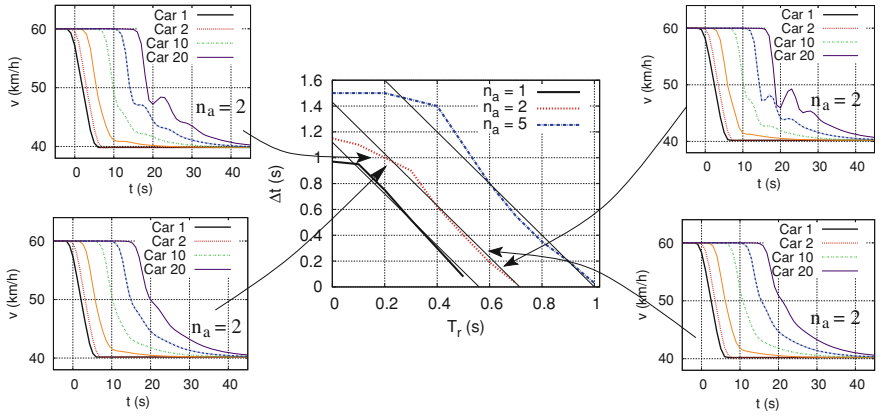

Fig. 12.1 Influence of the reaction time T_r, the update time interval Δt, and the number n_a of anticipated leading vehicles on the string stability (stability against the formation of traffic waves) of a vehicle platoon. The thick *solid lines* of the central diagram show the limits of string stability for $n_a = 1$, 2, and 5 anticipated vehicles. The curve for $n_a = 1$ corresponds to the IDM (see Sect. 11.3) with time delay. Traffic is string stable in the region below the corresponding line, and string unstable, otherwise. The diagrams at the *four corners* show the speed profiles of selected vehicles responding to a braking maneuver of the leading vehicle (Car 1) for $n_a = 2$ anticipated vehicles and values of T_r and Δt indicated by the *arrows* pointing to the central diagram

Figure 12.1 shows the reaction of a platoon of vehicles to a braking maneuver of a leading vehicle (Car 1) that cannot be overtaken. The solid thick lines of the central diagram of this figure shows the limits of string stability as a function of the reaction time T_r and the attention span Δt. In a wide range, this limit is approximatively given by the linear relation (thin solid lines)

$$T_r + \frac{\Delta t}{2} = T_{\text{eff}} = \text{const.} \tag{12.3}$$

We conclude that the destabilizing effect of T_r is *twice* as large as that of Δt. This can be understood by averaging the varying effective delaying effect $T_a(t)$ of the finite attention span over time: Immediately after an update, i.e., at times $t = i\,\Delta t,\ i = 1, 2, \ldots$, the acceleration response is instantaneous ($T_a = 0$). In contrast, the unchanged acceleration just before an update corresponds to a maximum delay $T_a = \Delta t$, so the average delay $\langle T_a \rangle = \Delta t/2$. Adding the reaction time T_r and assuming that the destabilizing effect grows linearly with the average total response time $T_r + \langle T_a \rangle = T_r + \Delta t/2 = T_{\text{eff}}$ leads to the relation (12.3). The central diagram in Fig. 12.1 shows that this relation is not satisfied for very large values of Δt where the assumption of linearly growing destabilization effects breaks down.

We conclude that the update time of iterated maps (or of the numerical integration method of time-continuous models) acts as an effective reaction time when considering its global effects. However, the value $\langle T_a \rangle = \Delta t/2$ of the effective reaction time is only *half* the numerical value of the update time.

12.3 Estimation Errors and Imperfect Driving Capabilities

Apart from the delay by reaction times, human driving behavior deviates from the machine-like driving style modeled by the acceleration function a_{mic} in two further ways: Firstly, humans make errors when estimating the input stimuli s, v, and v_l of the acceleration function. Secondly, the driving behavior is not completely rational, i.e., even if the same input stimuli are estimated for different times, drivers will behave differently.

Here and in the following, we formulate the specific human driving elements in terms of modifications of the acceleration function. This does not restrict the analysis to time-continuous models: The considerations carry over to the speed function $v_{\text{mic}}(s, v, v_l)$ of time-discrete models by means of Eq. (10.11) mapping the acceleration function to the speed function *via* the relation $v_{\text{mic}}(s, v, v_l) = v + \Delta t\, a_{\text{mic}}(s, v, v_l)$.

12.3.1 Modeling Estimation Errors

When exclusively considering estimation errors, the acceleration function a_{mic} itself remains unchanged while the true values of its independent variables s and v_l are replaced by the estimated values s^{est} and v_l^{est}, respectively. Since the driver's own speed v can be estimated with sufficient accuracy by looking at the speedometer, we will neglect the associated errors.[6] The magnitude of the estimating errors $s^{\text{est}} - s$ and $v_l^{\text{est}} - v_l$ depends on the driving situation, on the driver, and on external circumstances such as illumination and visibility. It can be determined by traffic psychological experiments in a driving simulator.[7] In the following, we will consider how the driving situation influences the errors when estimating the gap to and the speed of the leader.

Estimation error of the gap. In most driving situations, the *relative* estimation error for the gap, or, equivalently, the error of the logarithm of the gap, turns out to be essentially constant:

$$\ln s^{\text{est}} - \ln s = V_s w_s(t). \tag{12.4}$$

The model parameter V_s describes the relative standard deviation of s_{est} from the true value s, also known as statistical *variation coefficient*. Typical values are of the order of 10 %. The error is assumed to have no bias. The (0,1)-normally distributed stochastic variable $w_s(t)$ describing the temporal evolution of the error will be discussed below.

---

[6] In fact, the speed indicated by the speedometer can be greater than the true speed by up to 5 %. Due to its systematic nature, this error will be taken care of automatically at model calibration time, so there is no need to consider it explicitly in the model development.

[7] Notice that generating and modeling surrounding traffic for driving simulators is one of the applications of microscopic traffic flow models; the effects of the driver's actions themselves (such as steering or braking) are described by sub-microscopic models, cf. Table 1.1.

Estimation error of the speed of the leading vehicle. The driver estimates the speed v_l of the leader relative to his or her own speed (whose true value is assumed to be known) by the change of the apparent optical angle $\phi \approx w_{\text{veh}}/s$ under which the leading vehicle of width w_{veh} is seen. Based on experiments, we assume the error of the *rate of relative angular change* to be constant,

$$r = \frac{\mathrm{d}\phi/\mathrm{d}t}{\phi} = \frac{\frac{w_{\text{veh}}}{s^2}\Delta v}{w_{\text{veh}}/s} = \frac{\Delta v}{s} = \frac{1}{\tau_{\text{TTC}}}. \tag{12.5}$$

Interestingly, the rate r of relative change is the inverse of the *time-to-collision* $\tau_{\text{TTC}} = s/\Delta v$ which is an important safety indicator.

> The safety indicator *time-to-collision* (TTC) $\tau_{\text{TTC}} = s/\Delta v$ is defined by the hypothetic time interval to a collision if neither vehicle accelerates or brakes. Values in the range $0 < \tau_{\text{TTC}} \leq 4\,\text{s}$ are generally considered as critical. TTC is only meaningful for positive approach rates.

Assuming a constant standard deviation σ_{r} of the relative approach rate (of the order of $r = 0.01\,\text{s}^{-1}$) we obtain

$$v_l^{\text{est}} - v_l = -\left(\Delta v^{\text{est}} - \Delta v\right) = -s\left(\frac{1}{\tau_{\text{TTC}}^{\text{est}}} - \frac{1}{\tau_{\text{TTC}}}\right) = -s\,\sigma_{\text{r}}\,w_l(t). \tag{12.6}$$

In analogy to the quantity $w_s(t)$, the stochastic quantity $w_l(t)$ describes the distribution of the error and its change in time. In the following, we will look more closely how to model $w_l(t)$ and $w_s(t)$.

A model for the time dependence of estimation errors. The Eqs. (12.4) and (12.6) reduce the estimation errors for the gap and the speed difference to the time-dependent stochastic quantities $w_s(t)$ and $w_l(t)$. Each driver has his or her own set of stochastic variables $\{w_s(t), w_l(t)\}$, which all are independent from each other.

Generally, time-dependent stochastic variables are defined by a *stochastic process*. In the following, we will assume that both $w_s(t)$ and $w_l(t)$ are instances of a stationary process $w(t)$ which is defined by (i) the distribution function at a given time (which is time independent), (ii) the *autocorrelation* function describing the correlation of the stochastic process at different times as a function of the time difference. As distribution function, we assume a standardized Gaussian

$$w(t) \sim N(0,1), \quad \langle w(t)\rangle = 0, \quad \left\langle w^2(t)\right\rangle = 1. \tag{12.7}$$

On average, the estimation errors are zero. This is no restriction since systematic errors can be mapped to changes of the model parameters which will be taken care of when calibrating the model.

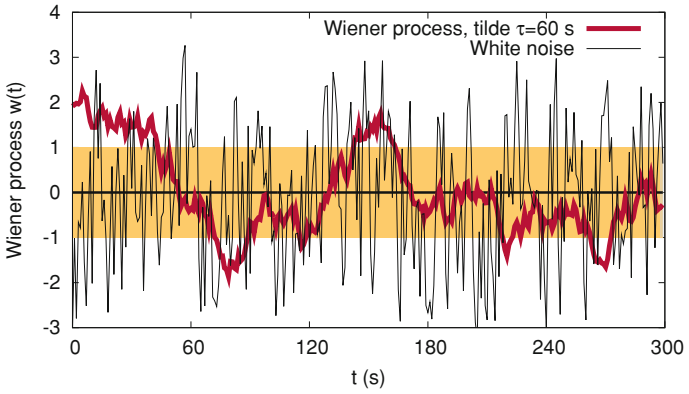

Fig. 12.2 Time series of a Wiener process ($\tilde{\tau} = 60\,\mathrm{s}$) generated by Eq. (12.11). Also shown is the range of one standard deviation around the mean $\langle w \rangle(t) = 0$ and white noise

When describing the autocorrelation function, we take into account that human errors are characterized by a certain *persistence*: If a driver, say, underestimates the gap at a given time, he or she is likely to underestimate it in the next second as well. In mathematical terms, the errors at two times are positively correlated for small time differences of a few seconds up to one minute. This can be described by following autocorrelation function:

$$\left\langle w(t)w(t') \right\rangle = \exp\left(-\frac{|t - t'|}{\tilde{\tau}} \right), \tag{12.8}$$

where the persistence time $\tilde{\tau}$ is a model parameter of the order of several seconds (cf. Table 12.1 and Fig. 12.2). In Problem 12.1, we show that a stochastic process $\{w(t)\}$ satisfying the conditions (12.7) and (12.8) can be generated by following stochastic differential equation also known as *Wiener process*:

$$\frac{\mathrm{d}w}{\mathrm{d}t} = -\frac{w}{\tilde{\tau}} + \sqrt{\frac{2}{\tilde{\tau}}}\xi(t). \tag{12.9}$$

The "standardized white noise" $\xi(t)$ is characterized by

$$\langle \xi(t) \rangle = 0, \quad \left\langle \xi(t)\xi(t') \right\rangle = \delta(t - t'). \tag{12.10}$$

Here, Dirac's δ-function $\delta(t)$ is equal to zero for all $t \neq 0$. For $t = 0$, the function diverges in a way that any integral $\int_a^b \delta(t)\mathrm{d}t = 1$ as long as the integration range includes zero, $a < 0 < b$.[8]

[8] Strictly speaking, $\delta[\cdot]$ is a *functional*, i.e., a mapping of a function $f(x)$ to a number: $\delta[f(x)] = f(0)$. This functional can be represented by a definite integral: $\delta[f(x)] = \int_{-\infty}^{\infty} \delta(x) f(x)\mathrm{d}x = f(0)$. Consequently, the δ-function does only make sense inside an integral.

The stochastic differential equation (12.9), (12.10) for the Wiener process allows for a simple and efficient numerical integration scheme. The update rule to generate the quantity $w_i = w(i\,\Delta t)$ of the ith step is given by

$$w_i = \mathrm{e}^{-\Delta t/\tilde{\tau}} w_{i-1} + \sqrt{\frac{2\Delta t}{\tilde{\tau}}}\,\eta_i, \tag{12.11}$$

where η_i are instances of computer-generated i.i.d. pseudo-random numbers with expectation zero and unit variance.[9] Since the prefactors $\exp(-\Delta t/\tilde{\tau})$ and $\sqrt{2\Delta t/\tilde{\tau}}$ can be calculated in advance at the beginning of the simulation, this is a very efficient numerical scheme. There are two independent Wiener processes $w_s(t)$ and $w_l(t)$ for each driver which are initialized using the pseudo-random number generator as well, $w_0 = \eta_0$.

Get yourself the idea that a persistence time going to infinity, $\tilde{\tau} \to \infty$, corresponds to simulating heterogeneous traffic of deterministically behaving drivers instead of homogeneous traffic of stochastically behaving drivers: Each driver has his or her individual acceleration function which is defined by the initialization of the two respective Wiener processes.

12.3.2 Modeling Imperfect Driving

Driving errors and irregularities in driving style result in erratic components of the driver's action, i.e., acceleration. This can be modeled by adding to the acceleration function a_{mic} itself some *acceleration noise* of standard deviation σ_a whose time dependence is modeled by a third Wiener process. Including the estimation errors, the resulting acceleration is given by

$$\dot{v}(t) = a_{\mathrm{mic}}(s^{\mathrm{est}}, v, v_l^{\mathrm{est}}) + \sigma_a w_a(t). \tag{12.12}$$

Besides modeling imperfections of the drivers, acceleration noise can also represent corrections due to factors that are not explicitly considered, or due to deficiencies of the model itself.[10]

In most stochastic models, the persistence of the acceleration noise is ignored and its time dependence is modeled by white noise $\delta(t)$ (or a time-discrete version $\{\eta_i\}$ of it) rather than by a correlated Wiener process $w_a(t)$. Particularly, this ansatz is

[9] The numbers may be normally distributed but it is not required. For $\tilde{\tau} \gg \Delta t$, the central limit theorem guarantees that w_i is Gaussian for any distribution of η_i satisfying $\langle \eta_i \rangle = 0$ and $\langle \eta_i^2 \rangle = 1$, for example, a uniform distribution.

[10] In this sense, this random term represents an admission that not everything can be modeled precisely. It has the same meaning as the additive stochastic term of econometric models.

adopted for essentially all cellular automaton models (see Chap. 13) but also for some stochastic variants of Gipps' model such as Krauss' model. However, since driving errors have a certain persistence as well, this is unrealistic. For each application, one has to decide whether the increased simplicity of using white noise compensates for the deficiencies in describing the phenomena.

12.4 Temporal Anticipation

Figure 12.1 shows that simulating time-continuous ACC-like car-following models with reaction-time delays of the order of the normal time gap, or even less, generally leads to crashes. This is true even if none of the human imperfections described above (Sect. 12.3) are applied. From this point of view, it is remarkable that humans drive essentially accident-free in spite of reaction times of this order, and additional estimation errors, and driving imperfections. Moreover, in dense but not yet congested traffic, traffic is free of instabilities (traffic oscillations) even if the average time gap s/v is *smaller* than the reaction time T_r (cf. Fig. 4.8). Simulations and the analytical analysis of Chap. 15 show that this is only possible when considering several leading vehicles (multi-anticipation, see Sect. 12.5) and when anticipating the traffic situation for the next few seconds as described in the following. We can model the anticipation ability of experienced drivers by assuming that they adopt following simple *heuristic*:[11]

1. The own speed and acceleration is known. Furthermore, the acceleration will not change during the anticipation time horizon assumed to be equal the reaction time T_r to bridge the delay caused by the reaction time.[12] This *constant-acceleration heuristic* for the movement of the own vehicle corresponding to a linear forward projection of the speed:

$$v^{\mathrm{prog}}(t) = v^{\mathrm{est}}(t - T_r) + T_r\, \dot{v}(t - T_r). \tag{12.13}$$

   Here, $\dot{v}(t - T_r)$ is the acceleration realized at time $t - T_r$.

2. The acceleration of the leading vehicle is difficult to estimate since only the binary information "brake lights on or off" is available.[13] Most models do not consider brake lights as an exogenous factor at all (see Sect. 12.6 for an exception).

[11] Heuristic refers to experience-based assumptions and strategies for finding a sufficiently good solution to a problem with limited knowledge in a short time. Generally, a heuristic cannot be justified or "proven" in any precise sense.

[12] Regarding the driver's actions, this essentially corresponds to the "do nothing" assumption: The pressure on the throttle or the brake pedal remains unchanged.

[13] In some cases, further information on the acceleration may be available from the situational context ("truck approaching a hill", "vehicle approaching an exit", "roadworks ahead"), or from multi-anticipation ("red brake lights several vehicle ahead", "jam ahead"). These factors are described in the Sects. 12.5 and 12.7.

Therefore, we adopt the *constant-speed heuristic* for the preceding vehicle (and for all further vehicles if multi-anticipation is considered). To first order in the reaction time, this also corresponds to a linear forward projection of the gap:

$$v_l^{\text{prog}}(t) = v_l^{\text{est}}(t - T_r), \quad s^{\text{prog}}(t) = s^{\text{est}} - T_r\, \Delta v^{\text{est}}(t - T_r). \tag{12.14}$$

12.5 Multi-Vehicle Anticipation

Human drivers do not only form hypotheses about the traffic state in the near future (temporal anticipation) but they take into account several vehicles ahead whenever this is possible.[14] This anticipation is also denoted as spatial anticipation or *multi-anticipation*.

To express this in mathematical terms by a generalization of the existing model, we divide the acceleration function $a_{\text{mic}}(s, v, v_l)$ of time-continuous models into a *free-flow acceleration* a_{free} and an *interaction acceleration* a_{int} representing the obstructions caused by other vehicles:

$$a_{\text{mic}}(s, v, v_l) = a_{\text{free}}(v) + a_{\text{int}}(s, v, v_l), \quad a_{\text{free}}(v) = \lim_{s\to\infty} a_{\text{mic}}(s, v, v_l). \tag{12.15}$$

By means of the relation $v_{\text{mic}}(s, v, v_l) = v + \Delta t\, a_{\text{mic}}(s, v, v_l)$, multi-anticipation can be defined for time-discrete models in analogy. The general plausibility conditions (11.1)–(11.5) imply that a_{int} is non-positive. In this sense, the acceleration function (and the speed function of time-discrete models) can be considered as a composition of two *social forces*: The free-flow acceleration reflects the driver's desire to drive at a certain speed. The decelerating interaction a_{int} exerted on the driver of the subject vehicle by the leading vehicle reflects the necessity to avoid crashes and keep a minimum time gap.

When considering $n_a \geq 1$ leading vehicles $\alpha - 1, \ldots, \alpha - n_a$, it is most straightforward to add the decelerating social forces caused by these vehicles as though the vehicles in between do not exist.[15] For vehicle α, this results into the acceleration function[16]

---

[14] Often, one can recognize vehicles further ahead through the windows of the immediate leader, or by looking past the sides of vehicles when the road is curved. If this is not possible (e.g., when driving behind trucks or SUVs), driving is perceived as less comfortable and the gap will be increased measurably.

[15] In physics, this corresponds to a linear superposition of all forces without shielding effects. Examples include gravitational forces or electrostatic forces for non-polarizable particles.

[16] In this context, the vehicle indices are relevant, so they will no longer be omitted as has been done previously for readability. Notice that, when modeling heterogeneous traffic the acceleration functions of each driver-vehicle unit (not only the function arguments) are different, so each functions should have an index on its own. This index will still be omitted.

$$\dot{v}_\alpha = a_{\text{free}}(v_\alpha) + \sum_{\beta=\alpha-n_a}^{\alpha-1} a_{\text{int}}(s_{\alpha\beta}, v_\alpha, v_\beta), \quad s_{\alpha\beta} = \sum_{j=0}^{\alpha-\beta-1} s_{\alpha-j}. \tag{12.16}$$

Since the vehicle lengths play no role in the dynamics, the total gap $s_{\alpha\beta}$ is calculated by summing only over the individual gaps $s_{\alpha-j}$, i.e., the lengths of all vehicles in between are excluded.

One should realize that, for accelerations satisfying the general plausibility criteria of Sect. 11.1, the immediate leader exerts the largest decelerating social force, in agreement with experience.

Directly implementing this ansatz, however, leads to unwanted consequences: The total social force appearing in Eq. (12.16) becomes more negative when increasing the number of considered vehicles for a given configuration of the vehicle positions and speeds. As a consequence, the fundamental diagram changes and the modeled road capacity decreases. In order to directly compare the behavior with and without multi-anticipation, we require that the fundamental diagram does not change. This can be realized by multiplying all social forces with a common prefactor $c \leq 1$ (which possibly depends on the speed) such that following condition for the steady-state equilibrium $v_\alpha = v_\beta = v$, $s_\alpha = s_{\alpha-j} = s_e(v)$ is satisfied:

$$c(v) \sum_{j=1}^{n_a} a_{\text{int}}(j s_e(v), v, v) = a_{\text{int}}(s_e(v), v, v). \tag{12.17}$$

For the IDM, this leads to the speed independent reduction factor (see Problem 12.3)

$$c_{\text{IDM}} = \left(\sum_{j=1}^{n_a} \frac{1}{j^2} \right)^{-1}. \tag{12.18}$$

Even when considering infinitely many leading vehicles, $c_\infty = 6/\pi^2 \approx 0.61$ is nonzero reflecting the fact that the infinite sum of all social forces converges. In this case, the immediate leader is responsible for 61 % of the total interactions, and all other vehicles for the remaining 39 %.

In summary, the multi-anticipative acceleration function is given by

$$a_{\text{multi}}(s_\alpha, v_\alpha, \{s_\beta\}, \{v_\beta\}) = a_{\text{free}}(v_\alpha) + c \sum_{\beta=\alpha-n_a}^{\alpha-1} a_{\text{int}}(s_{\alpha\beta}, v_\alpha, v_\beta). \tag{12.19}$$

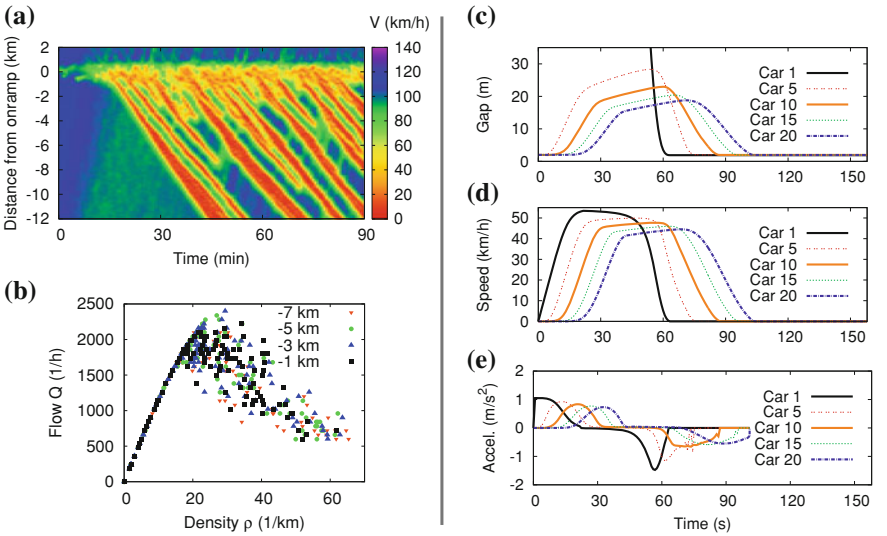

Fig. 12.3 Fact sheet of the Human Driver Model (12.20). The reaction time T_r, the number of considered vehicles, and error standard deviations and persistence times are given in Table 12.1. The IDM parameters are that of Table 11.2. The simulation scenarios are discussed in detail in Sect. 10.5

When simultaneously considering estimation errors, temporal anticipation, and reaction times, one inserts into the acceleration function the estimated arguments $s_\alpha^{\text{prog}}(t)$, $v_\alpha^{\text{prog}}(t)$, and $v_\beta^{\text{prog}}(t)$. The human-driver extensions (12.19), (12.13), and (12.14) can be applied to the acceleration and speed functions of any time-continuous and time-discrete model, respectively.

When applying the extensions to the IDM, we obtain the Human Driver Model (HDM):

$$\dot{v} = a_{\text{free}}^{\text{IDM}}(v_\alpha) + c_{\text{IDM}} \sum_{\beta=\alpha-n_a}^{\alpha-1} a_{\text{int}}^{\text{IDM}}(s_{\alpha\beta}^{\text{prog}}, v_\alpha^{\text{prog}}, v_\beta^{\text{prog}}) \quad \text{HDM}. \tag{12.20}$$

The speed estimate v_α^{prog} is evaluated using Eq. (12.13), and the gap and leading speed estimates $s_{\alpha\beta}^{\text{prog}}$ and v_β^{prog} by Eq. (12.14), respectively. The free-flow and interaction accelerations are given by

$$a_{\text{free}}^{\text{IDM}}(v) = a\left[1 - \left(\frac{v}{v_0}\right)^\delta\right], \quad a_{\text{int}}^{\text{IDM}}(s, v, v_l) = -a\left(\frac{s^*(v, v - v_l)}{s}\right)^2 \tag{12.21}$$

with s^* from Eq. (11.15).

Figure 12.3 shows simulations of the HDM for the two standard scenarios discussed in detail in Sect. 10.5. The most notable change with respect to the original

Table 12.1 Parameters of the human driver extensions to the acceleration function

Parameter	Typical value
Reaction time T_r	0.6 s
Number of anticipated vehicles n_a	5
Variation coefficient of gap estimation error V_s	10 %
Estimation error for the inverse TTC σ_r	0.01 s^{-1}
Magnitude of acceleration noise σ_a	0.1 m/s^2
Persistence time of the estimation errors $\tilde{\tau}$	20 s
Persistence time of the acceleration noise $\tilde{\tau}_a$	1 s

IDM (cf. Fig. 11.4) is the increased wavelength of the traffic waves in the freeway scenario, and the decrease of the maximum braking decelerations for the vehicles further behind in the queue. Both are essentially caused by multi-anticipation. The finite reaction time and the temporal anticipation essentially cancel each other while the estimation errors (10 % for the gap and 0.01 s^{-1} for the relative approaching rate, see Table 12.1) have little influence. Increasing the errors, however, will eventually lead to drastic effects or even accidents.

Figure 12.1 demonstrates that the limit of string stability of a platoon of vehicles as a function of the reaction time T_r and the attention span Δt depends strongly on the number of considered vehicles. When considering $n_a = 5$ leaders, the critical effective reaction time $T_r + \Delta t/2$ at the stability limit is about twice as large as the corresponding critical value without multi-anticipation ($n_a = 1$). Particularly, traffic can be stable even if the reaction time exceeds the average time headway. This agrees with everyday observations but cannot be realized in simulations without multi-anticipation. There are limits, however: Anticipating more than five vehicles ahead will change the dynamics insignificantly.

We emphasize that, in accordance with the design principles presented in Sect. 11.3.7, the model extensions have been formulated with as few additional parameters as possible. Apart from the specification of the estimation errors, there are only two additional parameters which both have an intuitive meaning and plausible values: reaction time and the number of anticipated vehicles.

12.6 Brake Lights and Further Exogenous Factors

Several cellular automata (see Chap. 13) and a few continuous models include *brake lights* as a further binary input variable: Brake lights on or off:

$$z_b = \begin{cases} 1 & \dot{v}_l < a_c, \\ 0 & \text{otherwise.} \end{cases} \tag{12.22}$$

The parameter a_c (typical values are around $-0.2\,m/s^2$) corresponds to the deceleration if neither the throttle nor the brake pedal are touched. If the lights are on ($z_b = 1$), the drivers adapt their driving style or their anticipation heuristic to a

Table 12.2 Implementing changes of the driving mode for some simple models in response to brake lights of the leader ($z_b = 1$) or flashing headlights of the follower ($z_t = 1$)

Parameter	Reference	Brake lights ($z_b = 1$)	Tailgating ($z_t = 1$)
Desired speed v_0 (all models)	120 km/h	120 km/h	140 km/h
Time gap T (OVM, FVDM, IDM)	1.0 s	1.5 s	1.0 s
Acceleration a (Gipps, IDM)	1.0 m/s^2	1.0 m/s^2	2.0 m/s^2
Comfortable deceleration b (Gipps, IDM)	1.5 m/s^2	1.0 m/s^2	1.5 m/s^2

more defensive mode compared to the situation with "brake lights off" ($z_b = 0$). Table 12.2 shows a possible implementation of this behavioral change for some elementary models.[17] Notice that z_b can be considered as a discrete version of the acceleration $\dot{v}_l$ of the leading vehicle which is already an exogenous variable of the ACC model (cf. Sect. 11.3.8).

Analogously, including direction indicators in the model allows one to simulate cooperative and anticipative lane changing strategies (see Chap. 14). Extending multi-anticipation to include the rear vehicle allows one to simulate forward social forces caused by tailgating drivers, e.g., by parameter changes as given in Table 12.2. Tailgating can be characterized by the binary exogenous variable

$$z_t = \begin{cases} 1 & s_{\alpha+1}/v_{\alpha+1} < T_c \text{ or follower flashes headlamps,} \\ 0 & \text{otherwise.} \end{cases} \tag{12.23}$$

This means a driver is subject to tailgating if the time gap $s_{\alpha+1}/v_{\alpha+1} < T_c$ of the follower is below some critical value T_c or if the follower flashes headlamps. Beside forward social forces, one can also include social forces urging a lane change if the subject vehicle is on the faster lane.[18]

12.7 Local Traffic Context

After driving for some time in congested or jammed traffic, most drivers become less alert, the accelerations decrease, and the time gaps increase. This *resignation effect* implies a less efficient driving style which reduces the flow downstream of the bottleneck compared to the situation before the breakdown. This so-called *capacity drop* leads to a positive feedback of jam formation that is often observed in reality (cf. Sects. 4.3 and 4.4). Figure 12.4 shows the result of modeling the resignation effect with the IDM by gradually reducing its acceleration parameter a and increasing the

[17] In Gipps' model, the time gap is "hardwired" to the update time step and therefore is not available to model a behavioral change of some vehicles.

[18] In some countries and in some situations, it may be useful to include using the horn or displaying rude gestures as further exogenous binary variables.

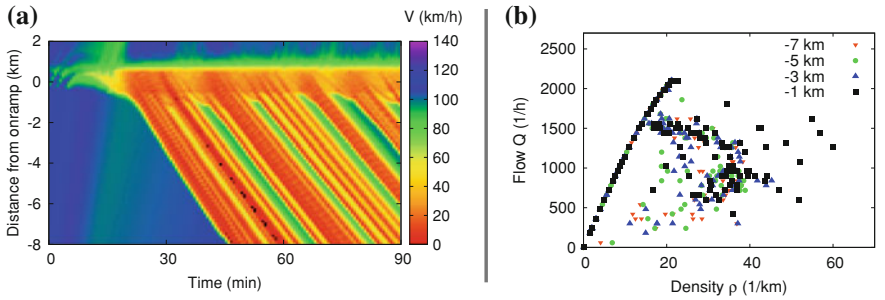

Fig. 12.4 Simulations of the standardized highway scenario using the IDM with *memory effect*. When driving in a jam, the time gap parameter T is increased up to 140 %, and the IDM acceleration parameter a decreased down to 50 % of the corresponding reference values on a time scale of 10 min. The reference parameters are given by Table 11.2. See Sect. 10.5 for a detailed description of the highway scenario

time gap parameter T over time scales of several minutes. When comparing this figure with the IDM simulation of Fig. 11.4a, one observes that the inverse-λ shape of the flow-density data of the virtual detectors indicating the capacity drop is more pronounced. The plot of the spatiotemporal local speed (Fig. 12.4a) shows more congestions (red areas) than that for the IDM. This indicates that resignation effects aggravate the congestion.

On the flip side, if it were possible to locally invert the sign of this effect near bottlenecks, this would open the possibility to dynamically "fill" the local "capacity holes" constituting the bottleneck. In Sect. 21.5, we will present simulations of a future driver assistance system that makes use of this possibility by increasing the agility near bottlenecks or when leaving a congested zone, and adopting a more defensive driving style when approaching roadworks or jams.

More generally, one can interpret the influencing regions of variable speed limits and other control measures as a local traffic context, or simply the distinction between city and freeway traffic. By changing the model parameters, it is straightforward to model or simulate a change of the driving mode caused by a new context. This can be done gradually on time scales of several minutes as in the memory effect discussed above or when lightning or weather conditions change. Other situations require an instantaneous change such as passing a new speed limit sign, entering/leaving a tunnel, approaching a zone of roadworks, or entering/leaving the city limits.

12.8 Action Points

In the previous models, drivers are assumed to react to the exogenous stimuli of the traffic environment in a continuous way, no matter how small their changes. However, it is well known from physio-psychological investigations that humans have finite *perception thresholds* in discriminating different gaps, speeds, or speed differences.

Perception thresholds can be modeled by the concept of *action-point models*: drivers react actively (by changing the pressure on the throttle or brake pedals or switching the pedals) only if the current action deviates significantly from the action considered as ideal for the given situation. For car-following models described by an acceleration function this essentially amounts to a constant acceleration most of the time until the actual acceleration differs significantly from the "ideal" acceleration given by the acceleration function a_{mic}. Alternatively, one can describe the event triggering a conscious action in terms of perceptible changes of the exogenous variables s, v, or Δv.[19] Once the threshold is exceeded, the driver reverts his or her acceleration to the value of the acceleration function a_{mic} for the present situation and keeps the new acceleration until the perception threshold is again exceeded. The thresholds and the associated acceleration or behavioral changes at irregular time instances define the *action points*. Trajectory data show that not only the time intervals between two action points but also the thresholds and the actions itself (i.e., the acceleration changes) are stochastic quantities. Generally, acceleration changes caused by action points are hard to distinguish from the effects of correlated acceleration noise. To date, the existence of action points in the data remains controversial.

12.9 The Wiedemann Car-Following Model

A model that considers both the local traffic context and action points is the time continuous *Wiedemann-Model*. It serves as basis for some commercial traffic flow simulators.[20] This model describes the psycho-physiological aspects of the driving behavior in terms of four discrete driving regimes: (i) free flow, (ii) approaching slower vehicles, (iii) car-following near the steady-state equilibrium, and (iv) critical situations requiring stronger braking actions. In each of these regimes k, different acceleration functions $a_{\text{mic}}^{(k)}(s, v, \Delta v)$ apply. The boundaries between the regimes are given by nonlinear equations of the form $f_{k'}(s, v, \Delta v) = 0$ defining curved areas in three-dimensional state space $(s, v, \Delta v)$ spanned by the exogenous variables (see Fig. 12.5). Additionally, acceleration noise of the type described in Sect. 12.3.2 is superimposed. In accordance with the philosophy of action points, the acceleration changes abruptly at the boundaries of the regimes to the new acceleration function representing the driving mode in the new regime. Nevertheless, the Wiedemann model does not implement the concept of action points in its pure form: Firstly, the regime boundaries, i.e., the conditions for action points, are deterministically fixed by the conditions $f_{k'}(s, v, \Delta v) = 0$ rather than stochastic. Secondly, the "do nothing" philosophy between the action points is replaced by the acceleration

[19] If the model includes binary exogenous factors, their changes (e.g., brake lights on or off) would trigger a conscious action as well, see Sect. 12.6.

[20] The actual acceleration functions of these simulators strongly deviate from the original formulation of the Wiedemann model.

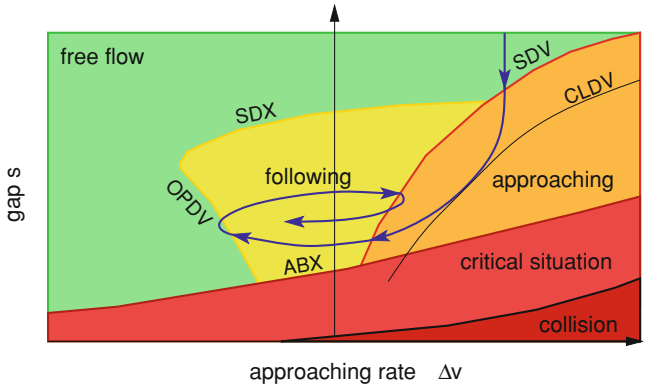

Fig. 12.5 Schematic and simplified representation of the regimes of the Wiedemann model in the three-dimensional state space spanned by s, v, and Δv. Shown are the intersections of the regimes and their boundaries with the plane $v_l = v - \Delta v = \text{constant}$ (the leader drives at constant speed v_l). The *blue line* shows the trajectory of a vehicle approaching a slower vehicle in the projected state space. The speed-difference thresholds CLDV ("closing in"), OPDV ("opening"), SDV ("sensitivity threshold"), and the gap-related thresholds ABX and SDX (minimum and maximum gap in car-following regime) are denoted as in the literature

functions $a_{\text{mic}}^{(k)}(s, v, \Delta v)$ of the different driving modes.[21] In spite of its psycho-physiological nature, the Wiedemann model does not contain explicit reaction times. The model is complex since four acceleration functions, several nonlinear equations for defining the boundaries of each regime, and the acceleration noise have to be specified.

Simulating the Wiedemann model typically leads to oscillations in state space with quasi-periodic transitions between different regimes as illustrated by the blue trajectory of Fig. 12.5.[22] This trajectory represents a car approaching a slower vehicle that cannot be overtaken. Initially, the driver of the car is in the free-flow regime (acceleration function $a_{\text{free}}(v)$) cruising at his or her desired speed. This corresponds to a constant approaching rate $\Delta v > 0$. Once the perception threshold of recognizing the leading vehicle is crossed, the driver enters the approaching regime. The driving mode in this regime reflects the strategy to simultaneously reach the speed of the leader and the desired gap by braking accordingly. Here, this strategy is successful and the driver enters the car-following regime. Once in this regime, the trajectory oscillates around the ideal state $\Delta v = 0$ and $s = s_e(v_l)$. Depending on the model variant, the boundaries of this regime may be reached or slightly exceeded (as in the schematic Fig. 12.5).

For comparison, Fig. 12.6 shows the trajectory in state space $(s, \Delta v)$ of a vehicle approaching a slower vehicle as simulated with the original IDM and for an IDM

[21] Notice that this implies a response to infinitesimal changes which is at variance to the pure idea of action points.

[22] In order to reflect basic kinematic constraints, the qualitative shape of the regime boundaries and the vehicle trajectory have been modified with respect to the figure in the original publication.

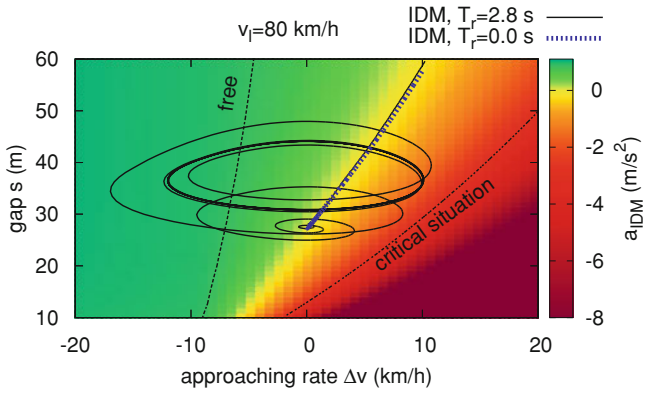

Fig. 12.6 Changes of the state space coordinates s and Δv of a simulated vehicle (desired speed 120 km/h) approaching a slower vehicle driving at constant speed $v_l = 80$ km/h. The *solid curve* is for the IDM with the parameters of Table 11.2 and a reaction time $T_r = 2.8$ s (no other HDM elements added). The *dotted line* is for the reference IDM with no delay. The color-coded surfaces depicts the IDM acceleration function. The critical approaching regime is defined by IDM accelerations below $-2b = -3$ m/s^2

variant with finite reaction time (all other aspects of the HDM have been omitted). The IDM trajectory shows two qualitative differences:

- There is no vertical part of the trajectory since the leader exerts a nonzero social force on the follower even if the gap is significantly larger than the safety gap,
- There are no oscillations.[23]

When introducing instabilities by adding a large reaction time to the (otherwise unchanged) IDM, the resulting trajectories in state space are qualitatively similar to that of the Wiedemann model. Similar trajectories can also be observed for any car-following model when simulating string unstable traffic flow (stop-and-go waves). Again, this shows that it is hard to empirically determine whether action points and discrete driving modes play a significant role in describing human-driven traffic flow.

Problems

12.1 Statistical properties of the Wiener process

Verify that the stochastic differential equation (12.9) for the stochastic process $w(t)$ leads to the autocorrelation function (12.8) once stationary conditions are reached. In order to show this, use the formal solution

[23] In Chap. 15, we will show that traffic flow is strongly string unstable if even the slightest (and strongly over-damped) oscillations appear in this situation.

$$w(t) = \sqrt{\frac{2}{\tilde{\tau}}} \int_{-\infty}^{t} \mathrm{e}^{-(t-t')/\tilde{\tau}} \xi(t') \mathrm{d}t'$$

and evaluate $\langle w(t)w(t') \rangle$ for $t' \leq t$ making use of the relation $\langle \xi(t_1)\xi(t_2) \rangle = \delta(t_1 - t_2)$.

12.2 Consequences of estimation errors
Consider a platoon of several identical cars α (desired speed $v_0 = 120$ km/h) driving in steady-state equilibrium behind a truck at $v_\alpha = 80$ km/h. Assume that the cars drive according to the Optimal Velocity Model with triangular fundamental diagram with the parameters $s_0 = 0$, $T = 1.4$ s, $v_0 = 120$ km/h, and $\tau = 0.65$ s. What are the effects on the actual steady-state gap when all drivers constantly overestimate the gap by $V_s\, w_s = 10\,\%$? To illustrate this, calculate the steady-state gap with and without this estimation error. What are the effects on the steady-state gap when there are no estimation errors but a constant additional acceleration of 0.4 m/s^2 (acceleration noise for $\tilde{\tau} \to \infty$)?

12.3 Multi-anticipation for the IDM
Derive Eq. (12.18) for the reduction factor c of the interaction part of the IDM acceleration. Furthermore, show that, instead of multiplying the interaction acceleration by the reduction factor, one could multiply the model parameters s_0 and T by a factor of $\sqrt{c}$.

Further Reading

- Green, M.: "How long does it take to stop?" Methodological analysis of driver perception-brake times. Transportation Human Factors **2** (2000) 195–216
- Treiber, M., Kesting, A., Helbing, D.: Delays, inaccuracies and anticipation in microscopic traffic models. Physica A **360** (2006) 71–88
- Kesting, A., Treiber, M.: How reaction time, update time and adaptation time influence the stability of traffic flow. Computer-Aided Civil and Infrastructure Engineering **23** (2008) 125-137
- Treiber, M., Helbing, D.: Memory effects in microscopic traffic models and wide scattering in flow-density data. Physical Review E **68** (2003) 046119
- Treiber, M., Kesting, A., Helbing, D.: Understanding widely scattered traffic flows, the capacity drop, and platoons as effects of variance-driven time gaps. Physical Review E **74** (2006) 016123
- Barceló, Jaume (Ed.): Fundamentals of Traffic Simulation. Springer, ISBN 978-1-4419-6141-9 (2010)
- Wiedemann, R.: Simulation des Straßenverkehrsflusses. In: Heft 8 der Schriftenreihe des IfV. Institut für Verkehrswesen, Universität Karlsruhe (1974)

Chapter 14
Lane-Changing and Other Discrete-Choice Situations

Imagination is more important than knowledge.
Albert Einstein

Abstract Simulating any nontrivial traffic situation requires describing not only acceleration and braking but also lane changes. When modeling traffic flow on entire road networks, additional discrete-choice situations arise such as deciding if it is safe to enter a priority road, or if cruising or stopping is the appropriate driver's reaction when approaching a traffic light which is about to change to red. This chapter presents a unified utility-based modeling framework for such decisions at the most basic operative level.

14.1 Overview

From the driver's point of view, there are three main actions that directly influence traffic flow dynamics: Accelerating, braking, and steering.[1] The dynamics of steering is part of the vehicle dynamics and therefore the domain of *sub-microscopic models* (cf. Table 1.1). Traffic flow dynamics describes the dynamics one level higher by directly modeling lane-changing decisions and the associated actions. At this level, the set of possible actions is discrete, i.e., performing a lane change, or not. Details of the lane-changing maneuver such as duration or lateral accelerations are not resolved, and the lane-changing itself is assumed to take place instantaneously.[2]

[1] Further actions such as using direction indicators, flashing headlights, or applying the horn, are only considered in very detailed models.

[2] In reality, the duration of a lane-changing maneuver is of the order of a few seconds. In many microscopic traffic flow simulators, lane changes are *represented* graphically as a smooth process but *simulated* as an instantaneous jump to the target lane. For the other drivers, the car is already on the target lane when the visualized lane change begins.

M. Treiber and A. Kesting, *Traffic Flow Dynamics*,
DOI: 10.1007/978-3-642-32460-4_14, © Springer-Verlag Berlin Heidelberg 2013

Discrete decisions and actions can also pertain to the longitudinal dynamics, in parallel to the continuous actions modeled by the acceleration function $a_{\mathrm{mic}}(s, v, v_l)$: When approaching a yellow traffic light which is about to turn red, the driver has to decide whether it is safe to pass this traffic light without changing speed, or if it is necessary to stop. Furthermore, lane changes generally influence the longitudinal acceleration of the decision maker (e.g., preparing for a lane change) or that of the other affected drivers (e.g., cooperatively making a gap to enable a change, or restoring the safety gap afterwards). Discrete choices in the traffic-flow context involve several levels:

1. The *strategic level* (destination choice, mode choice, and route choice) is modeled within the domain of transportation planning (cf. Table 1.1).
2. The *tactical level* includes anticipatory measures to enable or facilitate operative actions such as changing lanes or entering a priority road. This includes cooperative behavior such as allowing another vehicle to merge at a point of lane closure (*zipper mode* merging). Modeling the tactical level is notoriously difficult and is only attempted in the most elaborate commercial simulators.
3. On the *operative level*, the actual decision is made.
4. Finally, in the *post-decision phase*, the actions pertaining to this decision are simulated, e.g. performing the lane change or keeping to one's lane, waiting or entering a priority road, or cruising versus stopping at the traffic light.

In this chapter, we restrict the description to the operative level and the post-decision phase. We model the different discrete-choice situations consistently in terms of maximizing *utility functions* associated with each alternative. The utility of a given alternative increases with the (hypothetical) longitudinal acceleration that would be possible once this alternative had been adopted.

Using accelerations as utility ensures the compatibility between the acceleration and discrete-choice models. Furthermore, this ansatz is parsimonious since it minimizes the number of parameters and assumptions. For example, when the acceleration model is parameterized to simulate aggressive drivers, the lane-changing style of these drivers becomes aggressive as well, without introducing further parameters. Generally, any aspect considered in the longitudinal model carries over to the decision model. Specifically, the lane-changing considerations take into account speed differences, brake lights, or anticipative elements if, and only if, these exogenous factors are included in the acceleration model.

The approach reaches its limits when tactical and cooperative measures are crucial. One example of such a situation is zipper-like merging, or, more generally, merges to a congested target lane.

14.2 General Decision Model

We assume that, at a given moment, the driver can chose from a discrete set K of alternatives k. In the context of lane changes, the alternatives would be the (active) decisions to change to the left or right, and the (passive) decision not to change.

When about to enter a priority road, the alternatives would be to initiate the merging, or stopping and waiting for a sufficient gap between the main-road vehicles. We assume that the drivers are aware of the consequences of their decisions, i.e., they can anticipate, for each alternative, the speeds and gaps of all involved vehicles. This allows us to calculate all relevant accelerations (i.e., the utilities) using the normal acceleration functions of these vehicles. If the acceleration model is formulated as an iterated map or cellular automaton, the acceleration is calculated using Eq. (10.11).

In the decision process, the driver maximizes his or her utility (incentive criterion) subject to the condition that the action is safe (safety criterion). Both criteria are based on the acceleration function as follows:

Safety criterion. None of the drivers β affected by the consequences of opting for alternative k (including the decision maker α) should be forced to perform a critical maneuver as a consequence of a decision for alternative k. A maneuver is deemed to be critical, if it entails braking decelerations exceeding the *safe deceleration* b_{safe}:

$$a_{\text{mic}}^{(\beta,k)} > -b_{\text{safe}}. \tag{14.1}$$

The value of the model parameter b_{safe} (of the order of $2\,\text{m/s}^2$) is comparable to the comfortable deceleration b of the IDM or Gipps' model. For reason of parsimony, the safe deceleration can be inherited from these models ($b_{\text{safe}} = b$), if applicable.

Incentive criterion. Choosing among all safe alternatives k', the driver α selects the option of maximum utility U:

$$k_{\text{selected}} = \arg \max_{k'} U^{(\alpha,k')}. \tag{14.2}$$

As in most other discrete-choice models, the incentive criterion is based on a rational decision maker (also called *homo oeconomicus*) who maximizes his or her utility. In the simplest case, the utility is directly given by the acceleration function,

$$U^{(\alpha,k)} = a_{\text{mic}}^{(\alpha,k)}. \tag{14.3}$$

In contrast to the standard framework for discrete decisions (multinomial Logit and Probit models and their variants) we do not assume explicit stochastic utilities unless the acceleration model itself contains stochastic terms.[3]

For some discrete-choice situations such as discretionary lane changes, one needs an additional threshold preventing all active decisions (e.g., a decision to change lanes rather than to stay put) when the associated advantage is only marginal. Such a threshold prevents unrealistically frequent withdrawals of an active decision taken in the last time step which could, for example, lead to frantic lane-changing actions.

[3] The rationale behind stochastic utilities is to include in a global way all uncertainties of the decision process and contingencies in evaluating the utilities. In microscopic traffic flow simulations, there are so many *directly considered* contingencies in form of the positions and types of the involved vehicles influencing the decision process that further stochastic elements are superfluous.

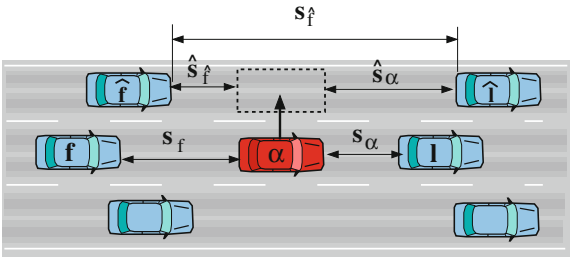

Fig. 14.1 Notation for a lane change of the *center* vehicle α to the *left*. All quantities with a hat pertain to the new situation after the (possibly hypothetical) lane change

Traffic rules (such as a "keep right" directive) may also enter the utility. Finally, one can include all consequences of a decision to other drivers by introducing a *politeness factor* (Sect. 14.3.3).

14.3 Lane Changes

Figure 14.1 depicts the general situation. The vehicle α of the decision maker (speed v_α) is located in the center. There are three alternatives: Change to the right, change to the left, and no change. Without loss of generality, we compare only the last two alternatives. Here, and in the following, we denote the vehicle of the decision maker with α, the leading vehicle with l, and the following vehicle with f. All accelerations, gaps, or vehicle indices with a hat refer to the new situation after the lane change has been completed while quantities without a hat denote the old situation.[4]

14.3.1 Safety Criterion

Assuming that the present situation (i.e., the alternative "no change") is safe, the safety criterion (14.1) refers to the acceleration $\hat{a}_{\hat{f}}$ of the new follower ($\beta = \hat{f}$) after a possible change, and also to the new acceleration $\hat{a}_\alpha$ of the decision maker him or herself ($\beta = \alpha$). For the follower, this criterion becomes

$$\boxed{\hat{a}_{\hat{f}} = a_{\text{mic}}(\hat{s}_{\hat{f}}, v_{\hat{f}}, v_\alpha) > -b_{\text{safe}} \qquad \text{safety criterion.}} \tag{14.4}$$

In order that this condition also prevents lane changes whenever there are following vehicles on the target lane at nearly the same longitudinal position (the gap $\hat{s}_{\hat{f}}$ is

[4] Examples: $a_{\hat{f}}$ denotes the acceleration of the new follower in the old situation, $\hat{a}_f$ the acceleration of the old follower in the new situation, and $\hat{s}_\alpha$ the gap of the decision maker's vehicle in the new situation. Notice that $\hat{\alpha} = \alpha$ (the decision maker is the same before and after the lane change), and $\hat{v} = v$ (lane changes are modeled as instantaneous jumps without changes of the speed).

negative, i.e., a change would result in an immediate accident), the acceleration function $a_{\text{mic}}(s, v, v_l)$ should return prohibitively negative values if $s < 0$. The parameter b_{safe} indicates the maximum deceleration imposed on the new follower which is considered to be safe (cf. Problem 14.2). If one simulates heterogeneous traffic with individual acceleration functions, the acceleration function $\hat{a}_{\hat{f}}$ of the new follower $\hat{f}$ is calculated with the function and parameters of *this* driver-vehicle unit.[5]

Regarding the safety of the decision maker him- or herself ($\beta = \alpha$), condition (14.4) prevents changes if the new gap $\hat{s}_\alpha$ is dangerously low such that $\hat{a}_\alpha = a_{\text{mic}}(\hat{s}_\alpha, v_\alpha, v_{\hat{f}}) < -b_{\text{safe}}$. Since this condition is less restrictive than the incentive criterion to be discussed below, there is no need to explicitly check this condition. In any case, the condition on the acceleration function to return prohibitively negative values for negative gaps guarantees that changes are prohibited if the leader on the target lane is essentially at the same longitudinal position ($\hat{s}_\alpha < 0$) which would result in an immediate crash.

14.3.2 Incentive Criterion for Egoistic Drivers

Most lane-changing models formulate the incentive criterion exclusively from the perspective of the decision maker ignoring the advantages and disadvantages to the other drivers. Furthermore, the lane-changing behavior depends on the legislative regulations of the considered countries. For example, a *right-overtaking ban* is in effect on most European highways.[6] Here, we will restrict to the simpler situations of lane changes on highways in the United States, or more generally to lane changes in city traffic, where lane usage is only mildly asymmetric.[7] Then, the incentive criterion for the egoistic driver reads

$$\hat{a}_\alpha - a_\alpha > \Delta a + a_{\text{bias}}, \tag{14.5}$$

where

$$a_\alpha = a_{\text{mic}}(s_\alpha, v_\alpha, v_l) \quad \hat{a}_\alpha = a_{\text{mic}}(\hat{s}_\alpha, v_\alpha, v_{\hat{f}}). \tag{14.6}$$

The lane-changing threshold Δa prevents lane changes when the associated advantage is only marginal (cf. Table 14.1). Furthermore, the constant weight a_{bias} introduces a simple form of asymmetric behavior. If a keep-right directive is to be modeled,

[5] One may object that—lacking mind-reading abilities—drivers do not know the acceleration function of others. However, the evidence allows for a coarse judgement. At the least, one can distinguish between cars and trucks, and between normal and evidently very sluggish or agile drivers.

[6] For asymmetric "European" lane-changing rules we refer to the literature (Kesting, A., Treiber, M., Helbing, D.: General lane-changing model MOBIL for car-following models).

[7] Often, a "keep to the right" directive is in effect in countries with right-hand traffic. Furthermore, in the United States, one should preferably overtake on the left lanes. However, this is not enforced and, *de facto*, overtaking takes place to the left and to the right.

Table 14.1 Parameters of the lane-changing models 14.4–14.7

Parameter	Typical value
Limit for safe deceleration b_{safe}	$2\,\text{m/s}^2$
Changing threshold Δa	$0.1\,\text{m/s}^2$
Asymmetry term (keep-right directive) a_{bias}	$0.3\,\text{m/s}^2$
Politeness factor p (MOBIL lane-changing model)	0.0–1.0

The parameters b_{safe} and Δa apply to any changing model, $a_{\text{bias}} \neq 0$ only if asymmetric driving rules are to be modeled, and $p \neq 0$ if the drivers are not purely egoistic

a_{bias} would be positive for changes to the left, and reverses its sign for changes to the right. This contribution should be relatively small ($|a_{\text{bias}}| \ll b_{\text{safe}}$) but greater than Δa. Otherwise, vehicles would not change to the right lanes if the highway was essentially empty (see Table 14.1).

Jamming paradox: **The grass is always greener on the other side**. A motivation to change lanes in jammed situations is the observation that the other lanes are faster, most of the time, suggesting that these lanes are "better". In Problem 14.1 we show that this is a fallacy: Even if the travel times on all lanes are the same, the fraction of the time one finds oneself on the slower lane is greater than 50 % *on any lane*. The fallacy is resolved by observing that, when the other lanes are slower, the active overtaking rate (overtaken vehicles per time unit) is greater than the passive overtaking rate in the periods where the other lanes are faster. Since the models presented here do not include tactical components, the simulated drivers also succumb to this fallacy and tend to change lanes unnecessarily often.

14.3.3 Lane Changes with Courtesy: MOBIL Model

The changing conditions (14.4) and (14.5) characterize purely egoistic drivers who consider other drivers only via the safety criterion. If the lane change is mandatory as in lane-closure or merging situations, this behavior is plausible (and, additionally, the changing threshold $\Delta p = 0$). On the other hand, if the lane change is not necessary (also termed a *discretionary* lane change), most drivers refrain from changing lanes if their own advantage is disproportionally small compared to the disadvantage imposed on others, even if the safety criterion is satisfied. This can be modeled by augmenting the balance of the incentive criterion with the utilities of the affected drivers, weighted with a *politeness factor* p,

$$\boxed{\hat{a}_\alpha - a_\alpha + p\left(\hat{a}_{\hat{f}} - a_{\hat{f}} + \hat{a}_f - a_f\right) > \Delta a + a_{\text{bias}} \quad \text{MOBIL incentive.}} \tag{14.7}$$

For the special case when politeness $p = 1$ (corresponding to a rather altruistic driver), no bias ($a_{\text{bias}} = 0$), and negligible threshold ($\Delta a = 0$), a lane change takes place if the

sum of the accelerations of all affected vehicles increases by this maneuver.[8] Hence the acronym for this model:

MOBIL—**M**inimizing **o**verall **b**raking deceleration **i**nduced by **l**ane changes.

The central component of the MOBIL criterion is the politeness factor indicating the degree of consideration of other drivers if there are no safety restraints. Since a degree of consideration amounting to $p = 1$ is rare (which would correspond to "Love thy neighbor as thyself"), sensible values are of the order 0.2.[9]

What is your estimate for the politeness factor p of the two drivers sketched in Fig. 11.2? Is it possible to describe by appropriate, possibly event-driven values of the politeness p following situations: (i) purely altruistic drivers (exclusively caring for the well-being of others), (ii) malign drivers (accepting own disadvantages to obstruct others), (iii) self-righteous drivers (obstructing other speeding drivers to "teach" them the traffic rules), (iv) timid drivers quickly making way when tailgated by others?

14.3.4 Application to Car-Following Models

The general lane-changing criteria presented above return explicit rules only when combined with a longitudinal acceleration model. In principle, the safety criterion (14.4) and the incentive criteria (14.5) or (14.7) are compatible with any longitudinal model providing the acceleration function a_{mic} either directly (time-continuous car-following models) or indirectly via Eq. (10.11) (time-discrete iterated coupled maps, see Sect. 10.2, or cellular automata, see Chap. 13).

When applying the safety criterion (14.4) to any acceleration model satisfying the general plausibility conditions discussed in Sect. 11.1, we obtain a minimum condition for the *lag gap* $\hat{s}_{\hat{f}}$ of the new follower behind the changing vehicle on the new lane,

$$\hat{s}_{\hat{f}} > s_{\text{safe}}(v_{\hat{f}}, v_\alpha). \tag{14.8}$$

The *safe gap function* $s_{\text{safe}}(v_f, v)$ is obtained by solving the equation defining marginal safety of the follower,

[8] As always, the safety criterion must be satisfied unconditionally. However, safety is nearly always given if the incentive criterion for $p = 1$ is satisfied.

[9] On the interactive simulation website www.traffic-simulation.de, one can simulate traffic flow with variable degree of politeness (altruism) which can be controlled by the user. The underlying acceleration model is the IDM (see Sect. 14.3.4).

$$a_{\text{mic}}\left(s_{\text{safe}}, v_f, v\right) = -b_{\text{safe}}, \tag{14.9}$$

for the gap s_{safe}. Notice that a unique solution s_{safe} exists by virtue of the plausibility condition (11.2) stating that, in the interaction range, the function a_{mic} increases strictly monotonically with respect to s. This means, the safety criterion allows changes if the following gap (lag gap) on the target lane is greater than some minimum value depending on the speeds of the changing vehicle and the new follower $\hat{f}$, i.e., the safety criterion becomes a generalized *gap-acceptance* rule for the lag gap.

Similarly, the general incentive criterion (14.5) of egoistic drivers can be written as a generalized gap-acceptance rule for the *lead gap* of the changing vehicle on the new lane,

$$\hat{s}_{\text{lead}} = \hat{s}_\alpha > s_{\text{adv}}(s_\alpha, v_\alpha, v_l, v_{\hat{l}}). \tag{14.10}$$

The *advantageous gap function* $s_{\text{adv}}(s, v, v_l, v_{\hat{l}})$ is obtained by solving the equation

$$a_{\text{mic}}\left(s_{\text{adv}}, v, v_{\hat{l}}\right) - a_{\text{mic}}(s, v, v_l) = \Delta a + a_{\text{bias}} \tag{14.11}$$

defining a marginal change of utility, for s_{adv}. Again, condition (11.2) ensures that a unique solution s_{adv} exists if $a_{\text{mic}}(s, v, v_l) + \Delta a + a_{\text{bias}} < a_{\text{free}}(v)$ where $a_{\text{free}}(v) = a_{\text{mic}}(\infty, v, v_l)$ is the free-flow acceleration function (11.3). In contrast to the safety condition, however, this is not always satisfied. Then, s_{adv} is not unique or even does not exist. Obviously, this corresponds to an infinite advantageous gap reflecting the fact that there is no need to change lanes because one can either drive freely on the old lane, or there is an obstruction but it is so small that the finite threshold $\Delta a + a_{\text{bias}}$ prevents lane changing for marginal utility improvements, even if the target lane is free. In the following, we discuss the application to three specific longitudinal models.

Rules for the Optimal Velocity Model. Introducing the OVM acceleration $\dot{v} = (v_{\text{opt}}(s) - v)/\tau$ into the safety criterion (14.8) with Eq. (14.9), we obtain the condition

$$\hat{s}_{\hat{f}} > s_{\text{safe}}^{\text{OVM}}(v_{\hat{f}}) = s_e\left(v_{\hat{f}} - \tau b_{\text{safe}}\right) \tag{14.12}$$

for the minimum safe lag gap of the OVM driver. Here,

$$s_e(v) = v_{\text{opt}^{-1}}(s) \tag{14.13}$$

is the inverse function of the optimal-velocity function indicating the steady-state gap for a given speed, i.e., $v_{\text{opt}}(s_e(v)) = v$ (see the paragraph below Eq. (10.13) for details). This means that, after the (yet hypothetical) change, the optimal velocity of the follower on the target lane must not be smaller than the actual speed of this follower minus the safe deceleration multiplied by the speed adaptation time, $v_{\text{opt}}(\hat{s}_{\hat{f}}) > v_{\hat{f}} - \tau b_{\text{safe}}$.

In analogy, the incentive criterion (14.10) for egoistic drivers with Eq. (14.11) leads to a further gap-acceptance rule for the lead gap between the changed vehicle

and its new leader:

$$\hat{s}_{\text{lead}} > s_{\text{adv}}^{\text{OVM}}(s_\alpha) = s_e\left[v_{\text{opt}}(s_\alpha) + \tau(\Delta a + a_{\text{bias}})\right]. \tag{14.14}$$

For the special case of the optimal velocity function (10.22) corresponding to a triangular fundamental diagram, and its inverse function $s_e(v) = s_0 + vT$ for $v < v_0$, we obtain the three conditions[10]

$$\begin{aligned} \hat{s}_{\hat{f}} &> s_0 + T\,\left(v_{\hat{f}} - b_{\text{safe}}\tau\right), \\ \hat{s}_{\text{lead}} &> s_\alpha + T\,\tau\,\left(\Delta a + a_{\text{bias}}\right), \\ s_\alpha &< s_0 + T\,\left[v_0 - \tau\,\left(\Delta a + a_{\text{bias}}\right)\right]. \end{aligned} \tag{14.15}$$

Notice that the parameters T and τ are both of the order of 1 s (cf. Table 10.1, and the accelerations b_{safe} and Δa are of the order of 1 m/s^2 or less, respectively (cf. Table 14.1). Consequently, all contributions in the conditions (14.15) containing products of τT are of the order of 1 m or less, i.e., negligible compared to the gaps s_α, $\hat{s}_\alpha$, and $\hat{s}_{\hat{f}}$. Effectively, this results in

$$\hat{s}_{\hat{f}} > s_e(v_{\hat{f}}), \quad \hat{s}_{\text{lead}} > s_\alpha, \quad v_{\text{opt}}(s_\alpha) < v_0. \tag{14.16}$$

This means, there are three conditions for a lane change to be safe and desirable: (i) the new lag gap is greater than the safe gap, (ii) the lead gap on the target lane is larger than the actual lead gap, and (iii) an obstruction exists. We emphasize that, for $b_{\text{safe}} = \Delta a = 0$, rules that are identical to the gap acceptance rules (14.16) can be derived for any longitudinal model with a unique steady-state speed function if the speed difference does not enter as an exogenous factor. This includes Newell's model (Sect. 10.8), and even some cellular automata such as the Nagel-Schreckenberg Model (Sect. 13.2).

However, the gap-acceptance rules (14.16) are unrealistic since, in real situations, the minimum lead and lag gaps depend crucially on speed differences: Given a certain lag gap, it makes a big safety difference whether the new follower drives at about the same speed or approaches quickly. Therefore, we now apply the general safety and incentive gap-acceptance rules (14.8) and (14.10) to acceleration models taking into account the speed difference. We expect that this new exogenous factor carries over to the resulting lane-changing rules in a consistent way.

Rules for the Full Velocity Difference Model. The acceleration of the Full Velocity Difference Model (FVDM) is that of the OVM plus a contribution depending linearly on the speed difference, $a_{\text{FVDM}}(s, v, v_l) = a_{\text{OVM}}(s, v) - \gamma(v - v_l)$ (cf. Sect. 10.7). Applying the safety condition (14.8) and the incentive criterion (14.10) to this acceleration function gives

[10] The third condition ensures that s_{adv} is defined. Otherwise, there is never an incentive for changing, see the text below (14.11) for details.

$$\hat{s}_{\hat{f}} > s_{\text{safe}}^{\text{FVDM}}(v_{\hat{f}}, v_\alpha) = s_e\left[v_{\hat{f}} - \tau b_{\text{safe}} + \tau\gamma(v_{\hat{f}} - v_\alpha)\right], \tag{14.17}$$

$$\hat{s}_{\text{lead}} > s_{\text{adv}}^{\text{FVDM}}(s_\alpha, v_l, v_{\hat{l}}) = s_e\left[v_{\text{opt}}(s_\alpha) + \tau\ \left(\Delta a + a_{\text{bias}} + \gamma(v_l - v_{\hat{l}})\right)\right]. \tag{14.18}$$

As a result, the minimum lead and lag gaps on the target lane allowing a change depend on the speed difference, i.e., they are consistent with the acceleration law.

We emphasize that the speed difference contributions are significant as illustrated by following example: With typical value of the FVDM speed adaptation time $\tau = 5\,s$ and the sensitivity $\gamma = 0.6\,\text{s}^{-1}$ for speed differences (cf. the caption of Fig. 10.6),[11] we have $\gamma\tau = 3$, i.e., the speed differences in the arguments of the equilibrium gap function $s_e(v)$ are weighted thrice with respect to the respective speeds themselves. Assuming furthermore a linear steady-state gap function $s_e(v) = s_0 + vT$ (corresponding to the congested branch of the triangular fundamental diagram) and bound traffic on either lane (no gap is larger than $s_0 + v_0 T$), the above conditions become

$$\hat{s}_{\hat{f}} > s_{\text{safe}}^{\text{FVDM}}(v_{\hat{f}}, v_\alpha) = s_0 + T\left[v_{\hat{f}} - \tau b_{\text{safe}} + \gamma\tau(v_{\hat{f}} - v_\alpha)\right] \quad \text{safety,} \tag{14.19}$$

$$\hat{s}_{\text{lead}} > s_{\text{adv}}^{\text{FVDM}}(s_\alpha, v_l, v_{\hat{l}}) = s_\alpha + T\tau\left[\Delta a + a_{\text{bias}} + \gamma(v_l - v_{\hat{l}})\right] \quad \text{incentive.} \tag{14.20}$$

With the steady-state time gap $T = 1.4\,\text{s}$, the lane-changing threshold $\Delta a = 0.1\,\text{m/s}^2$, and asymmetry $a_{\text{bias}} = [0.3]m/s^2$ (cf. Tables 10.1 and 14.1), this leads to following relations:

- The minimum lag gap implied by the safety rule increases by 1.4 m when all affected drivers drive faster by 1 m/s. Furthermore, it increases by 4.2 m if only the new follower drives faster by 1 m/s.
- If the old and new leaders drive at the same speed, the incentive criterion implies that a lane change to the left is desirable if the new lead gap is larger than the old one by at least 2.8 m while the asymmetry term makes changes to the right desirable even if there is a smaller lead gap provided it is smaller by at most 1.4 m. Furthermore, every 1 m/s speed advantage on the new lane compensates for a decrease of the new lead gap by 4.2 m.

Rules for the Intelligent Driver Model. In contrast to most versions of the OVM or FVDM, the IDM safe gap function $s_{\text{safe}}(v_{\hat{f}}, v_\alpha)$ defining the gap-acceptance rule (14.8) for the lag gap can be analytically calculated,

$$\hat{s}_{\hat{f}} > s_{\text{safe}}^{\text{IDM}}(v_{\hat{f}}, v_\alpha) = \frac{s^*(v_{\hat{f}}, v_{\hat{f}} - v_\alpha)}{\sqrt{\frac{1}{a}\left(a_{\text{free}}(v_{\hat{f}}) + b_{\text{safe}}\right)}}. \tag{14.21}$$

[11] Because of the additional anticipation introduced by the speed difference term, larger and more realistic values of the speed adaptation time τ can be assumed for the FVDM compared to the OVM which would lead to crashes if τ exceeds the order of 1 s.

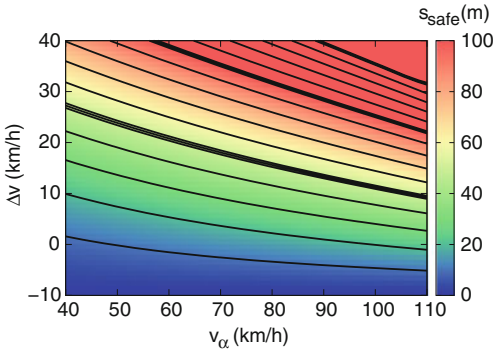

Fig. 14.2 Minimum lag gap (14.21) of the IDM as a function of the speed v_α of the changing vehicle, and the speed difference $\Delta v = v_{\hat{f}} - v_\alpha$ of the new follower with respect to this vehicle. The distance between two *thin* and *thick lines* correspond to a change of the minimum gap by 10 and 50 m, respectively

In the improved IDM (IIDM, Sect. 11.3.7), the condition becomes even simpler and does not depend on the desired speed parameter,

$$\hat{s}_{\hat{f}} > s_{\text{safe}}^{\text{IIDM}}(v_{\hat{f}}, v_\alpha) = \frac{s^*(v_{\hat{f}}, v_{\hat{f}} - v_\alpha)}{\sqrt{1 + \frac{b_{\text{safe}}}{a}}}. \tag{14.22}$$

In any case, the denominators are of the order unity, so the minimum lag gap is essentially given by the dynamical desired IDM gap s^*, Eq. (11.15), evaluated for the new follower.

Figure 14.2 shows the minimum lag gap (14.21) for the highway IDM parameters of Table 11.2 and $b_{\text{safe}} = b = 1.5\,\text{m/s}^2$. If, for example, both the changing vehicle and the following vehicle on the target lane drive at 50 km/h, the minimum lag gap according to the safety criterion is about 10 m. At this gap, the new follower would have to brake with a deceleration b_{safe} in order to regain his or her safe gap which is of the order of 17 m.[12]

If, however, the new follower drives at 70 km/h, i.e., approaches by a rate of $\Delta v = 20$ km/h, the safety criterion displayed in Fig. 14.2 gives a minimum acceptable gap of about 40 m amounting to an increase of about 6 m for every 1 m/s the follower drives faster. As in the FVDM, the IDM minimum gap depends crucially on the speed *difference*. In contrast to the former, the dependence is a nonlinear one and takes into account kinematic facts such as the quadratic dependence of the braking distance on the speed.

[12] In fact, investigations on trajectory data show that drivers temporarily accept shorter gaps after a change and only brake minimally such that the gap increases only gradually to the normal gap. This is part of the tactical behavior which is not considered here.

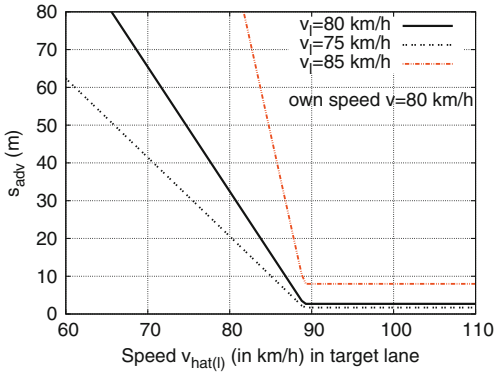

Fig. 14.3 Minimum lead gap on the target lane where a lane change is considered as advantageous as a function of the speeds of the leaders on the old and new lanes. The own speed is fixed to $v_\alpha = 80$ km/h, and the actual gap $s_\alpha = 30$ m

The minimum gap $s_{\text{adv}}(s_\alpha, v_\alpha, v_l, v_{\hat{l}})$ for an advantageous lane change appearing in the incentive criterion (14.10) is also accessible to analytical treatment resulting in

$$\hat{s}_{\text{lead}} = \hat{s}_{\text{adv}}^{\text{IDM}}(s, v, v_l, v_{\hat{l}}) = \frac{s^*(v, v - v_{\hat{l}})}{\sqrt{\left(\frac{s^*(v, v-v_l)}{s}\right)^2 - \frac{\Delta a + a_{\text{bias}}}{a}}}. \tag{14.23}$$

In agreement with intuition, the minimum advantageous gap depends strongly on the speed difference between the actual and the new leader, i.e., essentially on the speed difference driven on the new and old lanes: The higher the speed on the new lane, the smaller the accepted gaps for a change to this lane (cf. Fig. 14.3). Notice that the IDM gap-acceptance criterion accepts very small gaps if the leading vehicles are significantly faster. Nevertheless, the situation remains safe: After all, it is certain that the gaps will increase in the following seconds.[13]

14.4 Approaching a Traffic Light

When approaching a signalized intersection and the traffic light switches from green to yellow, it is necessary to decide whether it is better to cruise over the intersection with unchanged speed, or to stop (Fig. 14.4). This can be modeled within the general discrete-choice framework of Sect. 14.2. Since incentives are not relevant for this

[13] Such "close shaves" may not feel comfortable to most drivers, however. In order to suppress such a behavior, it is most straightforward to modify the minimum condition of Eq. (11.15) for the dynamical desired IDM gap $s^*(v, \Delta v)$, e.g., by not allowing the dynamical IDM gap s^* to be below $s_0 + \frac{1}{2}vT$.

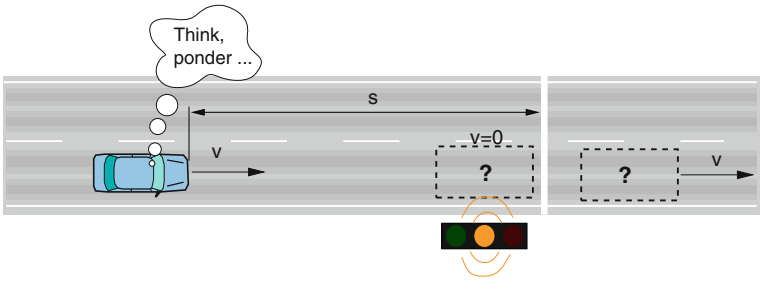

Fig. 14.4 Illustration of the decision to stop or to cruise at a traffic signal about to go *red*

situation,[14] the decisions are determined by the safety criterion alone: "Stop if it is safe to do so". In our general framework, the decision to stop is considered as safe if the anticipated braking deceleration will not exceed the safe deceleration b_{safe} at any time of the braking maneuver. For models with a plausible braking strategy, it is sufficient to consider the braking deceleration for this option *at decision time*.[15]

To calculate this deceleration, we model the traffic light as a standing virtual vehicle ($v_l = 0$, $\Delta v = v$, desired speed $v_0 = 0$) of zero extension such that s denotes the distance of the front bumpers to the stopping line. This results in the simple rule

$$\begin{array}{ll} \text{cruise} & \text{if } \ a_{\text{mic}}(s, v, v) < -b_{\text{safe}} \Leftrightarrow s < s_{\text{crit}}(v), \\ \text{stop} & \text{otherwise.} \end{array} \tag{14.24}$$

Obviously, the critical distance s_{crit} where the decision changes is a special case of the safe gap function (14.8) of the safety criterion,

$$s_{\text{crit}}(v) = s_{\text{safe}}(v, 0). \tag{14.25}$$

It is particularly instructive to apply this rule to the IDM safe gap (14.21) for the common situation when the driver approaches the signalized intersection at his or her desired speed, and the IDM parameters satisfy approximatively $a = b = b_{\text{safe}}$. In this case, $s_{\text{crit}}(v) = s^*(v, v)$ is equal to the dynamic desired IDM gap for $\Delta v = v$, and condition (14.24) becomes

$$\begin{array}{ll} \text{cruise} & \text{if } s < s^* = s_0 + v_0 T + \frac{v_0^2}{2b}, \\ \text{stop} & \text{otherwise.} \end{array} \tag{14.26}$$

[14] Sometimes, one observes that drivers pass yellow traffic lights, or even accelerate, if they could safely stop. Obviously, there *are* incentives at work. We will not attempt to model this behavior.

[15] If larger decelerations are unavoidable for kinematic reasons, the drivers described by such models will attempt to bring the situation under control as soon as possible, i.e., they will brake hardest at the beginning. The IDM belongs to this model class.

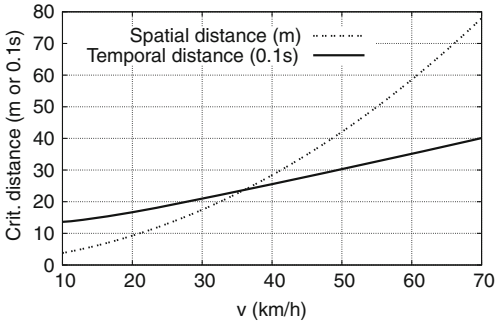

Fig. 14.5 Critical distance to the stopping line of a traffic light at decision time as a function of the speed for the IDM with $b = 2\,\mathrm{m/s^2}$, $b_{\mathrm{safe}} = 3\,\mathrm{m/s^2}$, and further IDM parameters taken from Table 11.2. Also shown is the associated TTC value

When setting the desired time gap T equal to the driver's reaction time, this means that one stops if, at decision time, the distance to the stopping line is greater than the *stopping distance* (11.8). This is perfectly consistent since this distance (which we have already introduced when formulating Gipps' model) is necessary to stop in a controlled way taking into account reaction time.

Figure 14.5 shows that, also for more general parameter settings, the critical distance increases quadratically with the speed, while the critical *time-to-collision* (TTC) (here defined as the time to reach the stopping line at unchanged speed) increases essentially linearly. We emphasize that the critical TTC of 3 s for 50 km/h, and 4 s for 70 km/h is consistent with European legislative regulations for the minimum duration of yellow phases of traffic lights at streets with the respective speed limits (Problem 14.2).

14.5 Entering a Priority Road

This situation can be considered as a special case of mandatory lane-changing decisions:

- The (nearest lane of the) main-road corresponds to the target lane of the lane-changing situation.
- The merging action to enter the road corresponds to the lane-changing maneuver.
- The speed of the merging/lane-changing vehicle is very low or zero (the latter is true if there are stop signs, or the entering vehicle is already waiting).
- And the incentive criterion is always satisfied.[16]

In contrast to normal (discretionary) lane-changing decisions, entering a priority road implies *two* safety criteria, one for the new follower and one for the merging vehicle

[16] After all, a driver wants to enter the main-road as soon as it can be done safely.

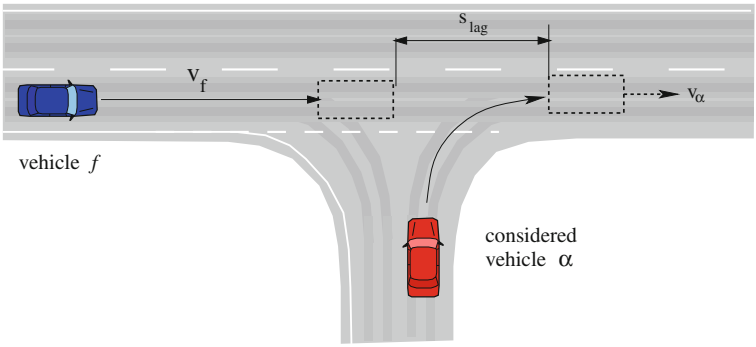

Fig. 14.6 Illustration of the safety criterion for the decision "stopping/waiting or merging" when entering a priority road

itself. The latter was not necessary for discretionary lane changes since, there, a fulfilled incentive criterion automatically implies safety for the decision maker him or herself (cf. the last paragraph of Sect. 14.3). When formulating the criteria, we assume that the driver of the merging vehicle can anticipate his or her speed v_α, the speeds v_f and v_l of the follower and leader, and the corresponding gaps s_f and s_l, respectively, at merging time (Fig. 14.6)[17]

$$\begin{array}{ll} \text{merge} & \text{if } s_f > s_{\text{safe}}(v_f, v_\alpha) \text{ AND } s_{\text{lead}} > s_{\text{safe}}(v_\alpha, v_l), \\ \text{stop or wait} & \text{otherwise.} \end{array} \tag{14.27}$$

Problems

14.1. Why the grass is always greener on the other side?
Give the reason why, when driving in congested conditions, one generally spends more time in the slower lanes and that a lane change does not help. Consider following situation:

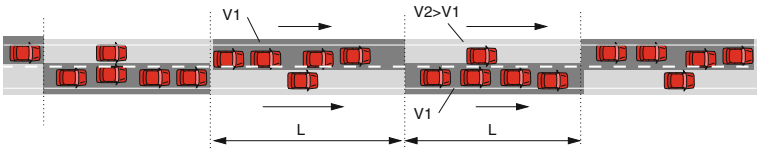

The figure shows two-lane traffic with staggered traffic waves of length L containing jammed traffic creeping at average speed V_1, and the regions in between (of length L as well) where traffic flows more quickly ($V_2 > V_1$) but yet not freely (the

[17] Since there are no relevant cars to consider for the alternative "stop or wait", we have dropped all hats denoting the new situation, for simplicity.

congested branch of the fundamental diagram remains relevant). Assume a triangular fundamental diagram and negligible speed adaptation times (which is a good approximation for the OVM or Newell's model). Calculate the fraction p_{slow} of the time one drives inside a wave, i.e., the other lane is faster, as a function of V_1, V_2, and the model parameters T and l_{eff}. Be astounded by the result!

Hint: You can solve this problem by calculating the relative velocity between the driven speed and the wave velocity. Or simply count the vehicles.

14.2. Stop or cruise?
A decision strategy abiding traffic regulation and restricting braking decelerations to minimal values while taking into account reaction times is the following [cf. the IDM condition (14.26)]: Anticipate if you can pass the traffic light at unchanged speed before it turns red. If so, cruise. Otherwise, brake smoothly with constant deceleration so as to stop just before the stopping line. When the speed limit is 50 km/h, the minimum duration of the yellow phase prescribed by law is $\tau_y = 3$ s. What is the maximum deceleration the legislative authority expects you to use, assuming a complex reaction time of 1 s?

14.3. Entering a highway with roadworks
Assume a highway on-ramp whose merging section, due to roadworks, is nearly nonexistent, i.e., one has to merge at essentially zero speed. The relevant safety criterion is defined by the OVM with a triangular fundamental diagram ($s_0 = 0$ s, $T = 1$ s) assuming a safe deceleration threshold $b_{\text{safe}} = 0\,\text{m/s}^2$. The driver of the considered car waits at the merging position while another car approaches on the main-road at 72 km/h. At decision time, the safety condition is just satisfied (the lag gap is only marginally greater than s_{safe}), so the driver begins to merge. Calculate the minimum deceleration at which the driver of the main-road vehicle has to brake in order to avoid a collision. Assume that the entering car accelerates with $2\,\text{m/s}^2$ for the first few seconds. Furthermore, assume that the driver on the main-road reacts instantaneously and is able to anticipate the situation perfectly. Discuss whether the OVM safe gap-acceptance criterion is really "safe", particularly, when assuming finite reaction times.

14.4. An IDM vehicle entering a priority road
Formulate the IDM safety criterion for merging into a priority road with a stop sign (the initial speed of the merging vehicle is zero). Calculate the safe lead and lag gaps for the IDM parameters $a = b = b_{\text{safe}} = 2\,\text{m/s}^2$, $T = 1$ s, $v_0 = 50$ km/h, and $s_0 = 0$ m if the speed on the main road is 50 km/h.

Further Reading

- Ben-Akiva, M., Lerman, S.: Discrete choice analysis: Theory and application to travel demand. MIT press (1993)
- Gipps, P.G.: A model for the structure of lane-changing decisions. Transportation Research Part B: Methodological **20** (1986) 403–414

- Kesting, A., Treiber, M., Helbing, D.: General lane-changing model MOBIL for car-following models. Transportation Research Record: Journal of the Transportation Research Board **1999** (2007) 86–94
- Nagel, K., Wolf, D., Wagner, P., Simon, P.: Two-lane traffic rules for cellular automata: A systematic approach. Physical Review E **58** (1998) 1425–1437
- Thiemann, C., Treiber, M., Kesting, A.: Estimating acceleration and lane-changing dynamics from next generation simulation trajectory data. Transportation Research Record: Journal of the Transportation Research Board **2088** (2008) 90–101
- Redelmeier, D., Tibshirani, R.: Why cars in the next lane seem to go faster. Nature **401** (1999) 35.